S

Hanford Double-Shell Tank Thermal and Seismic Project - Sensitivity of Double-Shell Dynamic Response to the Waste Elastic Properties

Author: TC Mackey
WRPS
Richland, WA 99352
U.S. Department of Energy Contract DE-AC27-08RV14800

EDT/ECN: EDT-822929 UC:
Cost Center: Charge Code:
B&R Code: Total Pages: 93

Key Words: DST, Double-Shell Tanks, dynamic response, waste elastic properties, increased fluid level, sludge level, DST comments

Abstract: This analysis evaluates the dynamic response of the tank due to various waste elastic properties.

LE Bratton 1/14/2009
Release Approval Date

Release Stamp

Approved For Public Release

RPP-RPT-38511, Rev. 0
M&D-2036-003-RPT-01, Rev. 1

U.S. DEPARTMENT OF ENERGY

PNNL-17720, Rev. 1
Limited Distribution

Prepared for the U.S. Department of Energy
Under Contract DE-AC05-76RL01830

Hanford Double-Shell Tank Thermal and Seismic Project – Sensitivity of Double-Shell Tank Dynamic Response to the Waste Elastic Properties

F. G. Abatt
K. I. Johnson

September 2008

Prepared for
CH2M HILL Hanford Group, Inc.
in Support of the
Double-Shell Tank Integrity Program

Pacific Northwest
NATIONAL LABORATORY

PACIFIC NORTHWEST NATIONAL LABORATORY
operated by
BATTELLE
for the
UNITED STATES DEPARTMENT OF ENERGY
under Contract DE-AC05-76RL01830

RPP-RPT-38511, Rev. 0
M&D-2036-003-RPT-01, Rev. 1

PNNL-17720, Rev. 1
Limited Distribution

Hanford Double-Shell Tank Thermal and Seismic Project – Sensitivity of Double-Shell Tank Dynamic Response to the Waste Elastic Properties

F. G. Abatt[(a)]
K. I. Johnson

September 2008

Prepared for
CH2M HILL Hanford Group, Inc.
in Support of the
Double-Shell Tank Integrity Program

Pacific Northwest National Laboratory
Richland, Washington 99352

(a) M&D Professional Services, Richland, Washington

Intentionally left blank.

Sensitivity of Double-Shell Tank Dynamic Response to the Waste Elastic Properties

F.G. Abatt
K.I. Johnson

September 2008

Prepared by
M&D Professional Services, Inc.
and
Pacific Northwest National Laboratory

Prepared by F.G. Abatt 9/26/08

K.I. Johnson 9/26/08

Intentionally left blank.

Executive Summary

The purpose of this study was to determine the sensitivity of the dynamic response of the Hanford double-shell tanks (DSTs) to the assumptions regarding the constitutive properties of the contained waste. In all cases, the waste was modeled as a uniform linearly elastic material. The focus of the study was on the changes in the modal response of the tank and waste system as the extensional modulus (elastic modulus in tension and compression) and shear modulus of the waste were varied through six orders of magnitude. Time-history analyses were also performed for selected cases and peak horizontal reaction forces and axial stresses at the bottom of the primary tank were evaluated. Because the analysis focused on the differences in the responses between solid-filled and liquid-filled tanks, it is a comparative analysis rather than an analysis of record for a specific tank or set of tanks.

The shear modulus was varied between 4×10^3 Pa and 4.135×10^9 Pa. The lowest value of shear modulus was sufficient to simulate the modal response of a liquid-containing tank, while *the higher values are several orders of magnitude greater than the upper limit of expected properties for tank contents*. The range of elastic properties used was sufficient to show liquid-like response at the lower values, followed by a transition range of semi-solid-like response to a clearly identifiable solid-like response. It was assumed that the mechanical properties of the tank contents were spatially uniform. Because sludge-like materials are expected only to exist in the lower part of the tanks, this assumption leads to an exaggeration of the effects of sludge-like materials in the tanks.

The results of the study show that up to a waste shear modulus of at least 40,000 Pa, the modal properties of the tank and waste system are very nearly the same as for the equivalent liquid-containing tank. This suggests that the differences in critical tank responses between liquid-containing tanks and tanks containing sludge-like materials having a shear modulus not exceeding 40,000 Pa are unlikely to be greater than those due to the uncertainties involved in the definition of the design ground motion or in the properties of the tank-waste system. This is the fundamental conclusion of the study.

The study also shows that increasing the waste extensional modulus and shear modulus does not lead to increased mass participation at the impulsive frequency of the liquid-containing system. Instead, increasing the waste stiffness eventually leads to fundamental changes in the modal properties including an increase in the fundamental system frequency.

The final comments from A.S. Veletsos (RPP-40036) were incorporated in this document for final closure.

Intentionally left blank.

Contents

Figures

Tables

1.0 Introduction

The purpose of this study was to determine the sensitivity of the critical dynamic responses of the Hanford double-shell tanks (DSTs) to changes in the constitutive properties of the contained material. The focus of the study was on the changes in the modal properties of the tank and waste system as the extensional modulus (elastic modulus in tension and compression) and shear modulus of the waste were varied through six orders of magnitude. This broad range was selected because it shows the transition of the system from a "fluid-like" response through a "semi-solid-like" response to a "solid-like" response. The expected upper end of elastic properties for sludge-like materials in the DSTs is expected to be several orders of magnitude less than the highest value used in this study, but the values were included to show the transitional behavior described above. The likely range of actual DST sludge properties is discussed in the report. Time- history analyses were also performed for selected cases, and peak horizontal reaction forces and axial stresses in the primary tank lower wall were reported.

In all cases, the tank waste was assumed to be a homogeneous linear elastic material – that is, the response of layered waste media was not investigated. In this sense, the study is expected to exaggerate the effects of sludge in the DSTs since the actual sludge levels are not expected to exceed approximately 50% of the tank capacity. The study was based on a sub-model of an AP tank with a waste level of 460 inches and a bulk specific gravity of 1.83. Because the analysis focused on the differences in the responses between solid-filled and liquid-filled tanks, it is a comparative analysis rather than an analysis of record for a specific tank or set of tanks.

1.1 Background

The seismic models of the DSTs reported in Deibler et al. (2008a; 2008b) and Rinker and Abatt (2008a, b) assumed that the tank waste responds as a homogeneous, inviscid, nearly incompressible liquid. These assumptions have been questioned by external reviewers (Kennedy and Veletsos 2005, 2006, 2007). The following is excerpted from Kennedy and Veletsos (2007) and also appears in Appendix A of Deibler et al. (2008a).

In the seismic analyses of the Hanford DSTs conducted so far – as in all previous analyses of waste-containing tanks that we are aware of – the waste was effectively modeled as a homogeneous, incompressible, practically inviscid liquid. There are fundamental uncertainties in this idealization, and it would be highly desirable to assess their effect on critical responses.

We recommend that at least a qualitative discussion be provided as to why it is considered to be acceptable to model the waste as a homogeneous liquid. From discussions on this issue during the June 7 [2007] meetings, we understand that the waste generally consists of:

1. *Liquid with a Specific Gravity (SG) of 1.3 to 1.5 over at least the upper 2/3 of the waste depth*
2. *Sludge with the consistency of over-saturated soil with a low angle of repose and a SG of 1.5 to 1.83 over the bottom portion of the tank.*

Based upon this description, we concur that it is probably reasonable as a first approximation to model the waste as a liquid with a SG of at least 1.7. However, we recommend that a seismic evaluation be conducted in the future with the waste characteristics more realistically modeled.

In defense of criticism that may legitimately be voiced on this issue, it is recommended that the critical responses of a simplified model of the tank-waste system (for example, one that does not provide for the effects of soil-structure interaction or the impact effects of the sloshing surface of the waste with the superimposed dome) be evaluated by representing the waste as a uniform, deformable solid with the properties of the lower portion of the waste. The computed responses must then be compared with those obtained for the liquid-like idealization of the waste.

A more realistic modeling of the waste and of the tank itself would be warranted only if the differences in the critical responses computed for the liquid-like and proposed representations of the waste are shown to be of practical significance.

Similar comments appear in Kennedy and Veletsos (2005, 2006).

1.2 Technical Approach

The fundamental question investigated is how the critical tank responses compare for a tank full of a sludge-like substance and a tank full of a liquid with the same mass density. As described in Veletsos and Younan (1998), for solid-containing flexible tank systems, the system response may be higher than, equal to, or lower than that of a liquid-only system of the same mass density owing to the opposing effects of the system effective mass and the amplification factor.

The evaluation was conducted by varying the shear modulus of the tank contents between 4×10^3 Pa and 4.135×10^9 Pa. The lowest value of shear modulus was sufficient to simulate the properties of a liquid, *while the higher values are several orders of magnitude greater than the upper limit of expected properties of the tank contents*. The mechanical properties of the tank contents were kept spatially uniform throughout the analysis.

The primary tank and waste system was modeled using a simplified ANSYS® sub-model similar to that reported in Rinker and Abatt (2008b). The sub-model consists of a flexible primary tank and the contained waste, which are supported at the top and base in a rigid concrete vault. The model was based on the AP tank configuration with a 460-inch waste level and a waste specific gravity of 1.83. The waste in the sub-model was simulated as a uniform elastic solid. Details of the sub-model are described in Chapter 2.0.

A change in the properties of the contained waste affects the effective modal masses and, hence, the associated frequencies and critical responses of the system. The latter responses are, of course, also affected by the characteristics of the exciting motion and of the associated response spectrum. The primary emphasis of the present study has been on the sensitivity of the critical modal properties of the system to changes in the characteristics of the waste. The relevant solutions are presented in Chapter 3.0.

Chapters 5.0 and 6.0 present solutions for the peak total horizontal wall force and the peak axial stress induced at the bottom of the tank wall by two different input motions. These motions are defined in Chapter 4.0. The first time history was extracted from the foundation of the global DST model described

in Chapter 2 of Rinker and Abatt (2008a), and the second time history represents free-field surface motion for the Hanford Waste Treatment Plant (WTP).

1.2.1 A Note on Units

The literature on the properties of tank waste on the Hanford Site is typically written in SI units. In keeping with that precedent, the elastic constants of the waste are typically expressed in SI units in this report. However, the ANSYS® model uses kips, feet, and seconds as the basic units. Consequently, even though the elastic properties for the waste are expressed in SI units in the report for clarity, they are, of course, input to the ANSYS® sub-model using the appropriate units.

1.3 Assumptions and Limitations of the Comparative Study

The study of the tank response using a sub-model with a fixed configuration (except for waste elastic properties) has several advantages. It is a relatively simple model that allows modal analyses to be performed quickly and it provides valuable insight into how the waste elastic properties influence the tank response. Time-history analyses can also be performed more quickly on a sub-model than on a more complete model. Given the nature of the review question and the goals of the comparative study, it was judged that the sub-model best served the stated purpose of the comparative study. However, the use of a sub-model does not replace an analysis of record of the tank using a more complete model.

Important assumptions and limitations of this study are listed below. The assumptions are, for the most part, a byproduct of the simplicity of the model and the project constraints. In this case, the objective of the comparative analysis was well-served by a fairly simple model. Removing the assumptions below would require either a significant increase in the model complexity, or a significant increase in the time required for the analysis. Neither of these options was considered compatible with the goals of the study and the project constraints.

1. Modal results for vertical motion were reported only for a few cases, and in the time-history analyses, only a single-component of horizontal excitation was considered.
2. The waste was assumed to be spatially uniform. No combinations of layered waste properties were considered. As already noted, this assumption is expected to exaggerate the effects of the sludge, which in reality is only present in the lower portions of DSTs.
3. The only configuration considered was an AP tank with a waste level of 460 inches and a bulk specific gravity of 1.83.
4. Although it is likely that tank waste will deform into its nonlinear yielding range during an earthquake, the waste was modeled as a linearly elastic material.
5. Poisson's ratio was fixed at 0.49999, a value that is appropriate for a liquid-like waste, but may be too high for a solid-like waste.

1.4 Summary of Modal Results

Table 1.1 presents a summary of the modal properties in the lateral direction for the tank configurations analyzed in Chapter 3.0.

Table 1.1. Summary of Modal Properties in the Lateral Direction

Case Name	Contact Condition	Waste Extensional Modulus (Pa)	Waste Shear Modulus (Pa)	Convective Frequency (Hz)	Impulsive Frequency (Hz)
Bonded_0839	Bonded	124,000[(a)]	4,000	0.21	5.86
Bonded_464	Bonded	124,000	22,000	0.27	5.8
Bonded_839	Bonded	124,000	40,000	0.3	5.7
Bonded_E10x	Bonded	1.24×10^6	413,500	0.96	6.0
Bonded_E1000x	Bonded	1.24×10^8	4.135×10^7	Dominant frequency of 6.9 Hz	
Bonded_E10000x	Bonded	1.24×10^9	4.135×10^8	Dominant frequency at 15.3 Hz	
Bonded_E100000x	Bonded	1.24×10^{10}	(4.135×10^9)[(b)]	Dominant frequency at 37.2 Hz	
Sliding_0839	Sliding	124,000	4,000	0.19	5.85
Sliding_464	Sliding	124,000	22,000	0.22	5.85
Sliding_839	Sliding	124,000	40,000	0.24	5.9
Sliding_E10x	Sliding	1.24×10^6	413,500	0.76	5.95
Sliding_E100x	Sliding	1.24×10^7	4.135×10^6	Multiple modes between 2.4 and 8 Hz	
Sliding_E500x	Sliding	6.21×10^7	2.07×10^7	Four significant modes between 4.9 and 8.2 Hz	
Sliding_E1000x	Sliding	1.24×10^8	4.135×10^7	Dominant frequency at 6.1 Hz	
Sliding_E10000x	Sliding	1.24×10^9	4.135×10^8	Dominant frequency at 12.1 Hz	
Capped Bonded_464	Bonded	124,000	22,000	Dominant frequency at 4.7 Hz	

(a) Based on the bulk modulus of water.
(b) Largest shear modulus considered is 70% of the stiffness of lead, and is four to five orders of magnitude higher than the expected upper limit for the waste shear modulus.

1.5 Discussion

The objective of this study was to determine the sensitivity of the DST critical responses to changes in waste properties. The waste was modeled as a uniform linearly elastic material and the shear and extensional moduli of the waste were varied. The lower bound for the waste shear modulus considered in the study was 4,000 Pa and the upper bound was 4.135×10^9 Pa. The lower bound, which is representative of the value of peanut butter at room temperature, effectively reproduced the critical responses of a liquid-containing tank, so there was no reason to consider lower values.

The upper bound value used on this evaluation was selected because it was sufficiently high to illustrate the complete transition from fluid-like through semi-solid-like to solid-like behavior. However, the upper bound value for the shear modulus of actual DST waste is much lower. Although an upper bound for the shear modulus of all DST waste is difficult to define, 40,000 Pa is expected to represent an upper bound for much of the DST waste.

The study of the modal properties of the system showed that if the waste shear modulus is no greater than 40,000 Pa, clearly identifiable convective and impulsive modes exist and the modal mass fractions are similar to those predicted in from Table 4.2 of BNL (1995). The impulsive frequency for such systems is within approximately 0.1 Hz of the equivalent liquid-containing system as shown in Table 1.1 above and in Table 7-1 of Rinker and Abatt (2008a). That is, *the critical modal properties for systems having a waste shear modulus up to at least 40,000 Pa are not significantly different than those for the equivalent liquid-containing tank.*

Changes in DST critical responses can be due to changes in seismic input as well as changes in modal properties. Changes in modal properties can be characterized independently of the seismic input, but ultimately, the seismic input must be known to draw conclusions about critical responses. The seismic excitations used in this study are approximations of the input to the primary tanks of the DSTs. A more complete time-history evaluation using the global model is required to support an analysis of record for the DSTs, but meaningful conclusions that include the effect of the seismic input can be drawn from this comparative study. To this end, it may be noted that:

1. It is reasonable to expect that the seismic excitation to a DST primary tank will consist of contributions from the tank foundation (basemat) motion and the dome motion. This expectation is confirmed by the fact (demonstrated in Chapter 5.0) that the maximum horizontal reaction force predicted from a global model of a DST is between the estimates based on the foundation motion and an approximate average of the foundation and dome apex motion.
2. When the waste shear modulus is less than 40,000 Pa, the impulsive frequency is within approximately 0.1 Hz of that predicted for the equivalent liquid-containing tank.
3. The steepest slope shown for any ground motion response spectra considered in this study (presented in Figure 4.11 and Figure 4.15) is approximately 0.75*g*/Hz, so that in the worst case, a change of 0.1 Hz in the dominant impulsive natural frequency would lead a spectral acceleration change of approximately 0.075*g*.
4. This study is based on the assumption that the waste properties do not vary with height. In reality, sludge levels in the tank are not expected to exceed 50% of the waste height. Thus, the effect of the sludge is expected to be overestimated by this study. If the effect of the sludge is overestimated by a factor of two (a likely value for a tank half full of sludge), the maximum variation in the dominant spectral acceleration would be $(0.075/2)g = 0.0375g$, or roughly 10% of the impulsive spectral acceleration of the liquid-containing tank. If the change in the dominant modal mass is practically negligible, the indicated change in spectral acceleration will lead to 10% changes in the critical responses of the system.

The above arguments support the conclusion that the if the waste shear modulus is less than 40,000 Pa, the difference in the critical tank responses between a tank containing sludge-like material and an equivalent liquid-containing tank is expected to be of the order of 10% or less. This is within the range of uncertainty involved in the definition of the design ground motion or in the properties of the tank-waste system.

Before this study was performed, it was thought that increased waste stiffness associated with a sludge-like material might cause a significant increase in the mass participation in the impulsive mode. The potential for this phenomenon was investigated by comparing modal properties of systems with high waste stiffness to those of systems with low waste stiffness.

It turned out that in order to achieve an essentially single-mode response by increasing the waste stiffness, the shear stiffness had to be in the 4×10^7 Pa to 4×10^8 Pa range. This range is two to three orders of magnitude higher than is believed to be representative of the DST waste. That is, for realistic values of the waste shear modulus, increasing the waste stiffness does not lead to noticeably higher mass participation in the impulsive mode.

As a benchmark, a case was run where the vertical displacement of the waste upper surface was constrained to be zero (capped). This case forces a pure impulsive response independent of the waste shear stiffness. The nearly 100% impulsive mass participation caused a drop in the dominant structural frequency from 5.8 Hz to 4.7 Hz. Forcing a pure impulsive response by prohibiting vertical movement of the waste free surface when the waste has fluid-like properties is very different than increasing the waste stiffness. In the former case, fluid-like waste responds in a single mode at an impulsive frequency consistent with nearly 100% mass participation. In the latter case, the response may be multi-modal with the frequencies and modal mass fractions dependent on the waste stiffness. In a practical sense, a pure impulsive response describes a tank that is full or nearly full of a liquid, but this description is less appropriate for a tank partially full of a semi-solid or solid-like material.

As the material stiffness began to increase, the two convective and impulsive modes tended to disperse into numerous modes grouped near the original two frequencies, and the convective frequency began to increase. In this range of waste stiffness, the response was multi-modal. As the stiffness of the material increased even more, the convective and impulsive modes disappeared and the multiple modes eventually coalesced into a single dominant structural mode at a frequency higher than the original impulsive frequency.

The yield strength in shear for the much of the tank waste is expected to be less than 2,000 Pa. At this level, it is reasonable to expect at least some of the waste to yield during an earthquake. The degree to which this will affect the results of this study has not been investigated other than by introducing sliding contact between the waste and the primary tank to provide a "yield mechanism." Additional study would involve determining the stress in the waste as a function of the input acceleration to determine if yielding is significant, and then employing yielding models of the waste as required. Use of nonlinear material models is incompatible with modal analysis, so further work would focus on static or time-domain analysis. Another option is to idealize the waste as a viscous liquid and determine the changes in the tank response as the viscosity is increased.

The modal analysis in the vertical direction showed a clearly recognizable fundamental vertical frequency at 5 Hz when the waste shear modulus was varied between 4,000 Pa and 40,000 Pa. At 413,500 Pa, the frequency increased and tended to disperse into multiple closely-spaced frequencies. Again, this demonstrates the transition to multi-modal response when the shear modulus is increased from 40,000 Pa to 413,500 Pa.

1.6 Conclusions

1. The modal properties of the tank system are insensitive to the waste shear modulus in the range of 4,000 to 40,000 Pa.

2. Up to a waste shear modulus of at least 40,000 Pa, the difference in the critical tank responses between a tank containing sludge-like material and an equivalent liquid-containing tank is expected to be of the order of 10% or less. This is within the range of uncertainty involved in the definition of the design ground motion or in the properties of the tank-waste system.

Intentionally left blank.

2.0 Model Description

The global ANSYS® model described in Section 2.0 of Rinker and Abatt (2008b) was used as the starting point for the development of the primary tank sub-model. The resulting sub-model consists of the flexible primary tank, the contained waste, and a rigid concrete vault that provides support at the base and top of the primary tank. The key modifications required to reduce the full model to the sub-model are described below.

All elements related to the modeling of the soil were unselected for the sub-model. This includes the soil and contact elements between the native and excavated soil (element types 8, 9, 90 and 91), contact elements between the soil and the concrete shell (element types, 60 through 63), spring elements between the concrete basemat and the underlying soil (element types 21, 22 and 23), the links used at the exterior surface of the soil (element type 30), and the mass elements used for applying the surface load (element type 10).

For the concrete shell elements, the modulus of elasticity was increased by a factor of 10,000 relative to the nominal values in the global model to obtain "rigid" behavior. The same increase in stiffness was also applied to the insulating concrete elements. This will ensure that the full sub-model is excited uniformly top and bottom. The geometry and properties for the majority of the primary tank were not changed in the sub-model. The only changes were to the elements in the primary tank dome region, where the modulus of elasticity was increased by a factor of 10,000 above the nominal values. Similarly, the elastic modulus of the secondary liner and the spring constants for the anchor bolts were increased by a factor of 10,000 above the nominal values in the global model.

The node-to-node contact elements (CONTA178) connecting the bottom of the concrete tank wall to the basemat were removed. In place of this contact condition, all the concrete tank nodes including the basemat nodes were coupled in three degrees of translation. This serves to tie the concrete tank and basemat together and ensures rigid body response.

2.1 Model Geometry

A plot of the ANSYS® primary tank sub-model is shown in Figure 2.1. Although the concrete portion of the DST is shown in the plot, the concrete was effectively rigid as stated in the previous section. A slice plot of the rigid regions of the model is shown in Figure 2.2. Flexible portions of the primary tank are shown in Figure 2.3, though the portion of the primary tank bottom in contact with the underlying insulation concrete is effectively rigid.

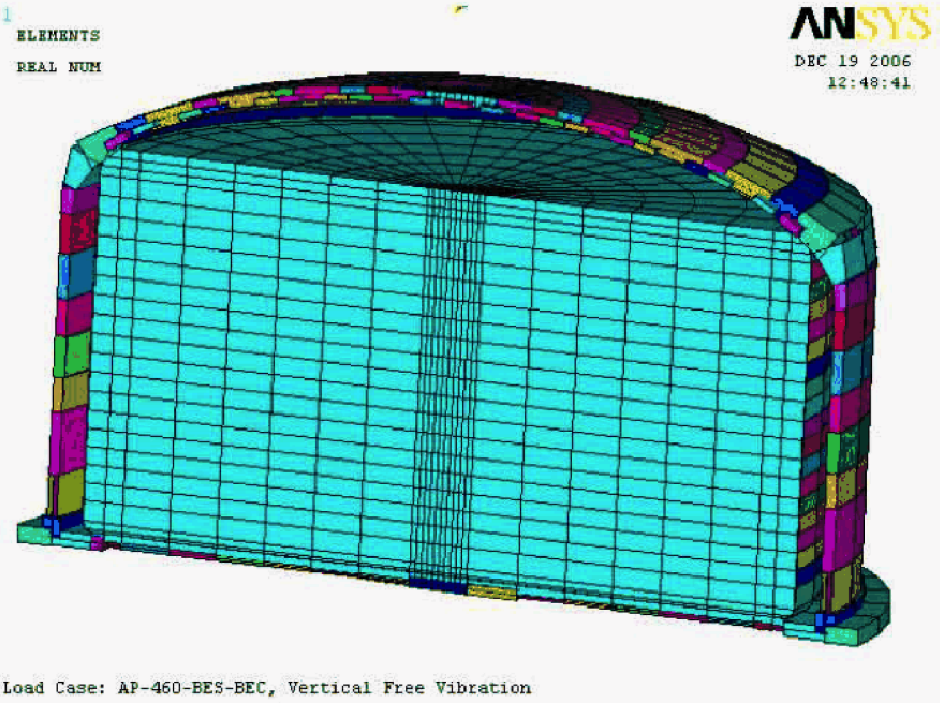

Figure 2.1. Plot of ANSYS® Primary Tank Sub-Model

Figure 2.2. Slice Plot Showing Rigid Regions of the ANSYS® Primary Tank Sub-Model

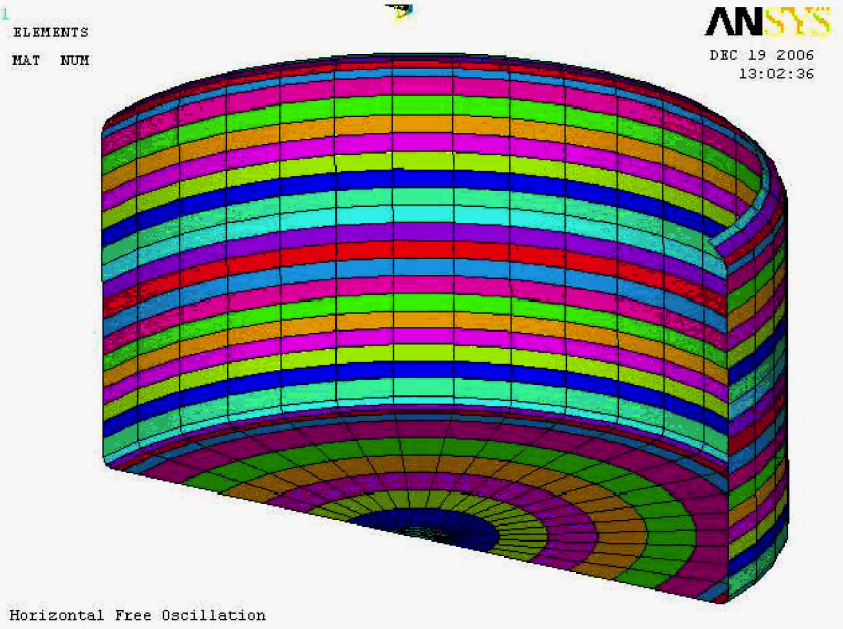

Figure 2.3. Plot of Flexible Primary Tank of ANSYS® Sub-Model

2.1.1 Model Mass Distribution

The waste mass for the half model is 298.4 kip-s^2/ft, according to the ANSYS® output. The primary tank mass for the half model is approximately 4.5 kip-s^2/ft, so the total mass of flexible portion of system (waste plus primary tank) is approximately 303 kip-s^2/ft, and the waste mass is more than 98% of the mass of the flexible portion of the system.

2.2 Contact Conditions

Modal analyses were performed with the boundary condition between the waste and the primary tank set to both sliding and bonded contact conditions. The sliding condition is judged to be the more realistic condition because is provides a "yield line" for the tank waste. However, modal analyses were run with bonded contact to assess the sensitivity of the modal properties of the system to this boundary condition.

The following contact surfaces are present in the sub-model:

1. The interface between the primary tank dome and the concrete dome (element type number 35).
2. The interface between the waste and the primary tank (element type numbers 45 and 46).
3. The interface between the bottom of the primary tank and the top of the insulating concrete (element type number 66).
4. The interface between the bottom of the insulating concrete and the top of the secondary liner (element type number 68).

Of interest was the effect of the second contact condition above on the results of the modal analyses. Contact surfaces using CONTA173 elements can be deactivated by setting key option 12 equal to 5 for

that element. That option ensures that the mating surfaces are always bonded (no separation or sliding). The intent was to determine the effect of the waste primary tank contact interface by activating or deactivating the key option for element types 45 and 46. When contact is not deactivated in the modal analysis, the condition is treated as sliding contact by ANSYS®. That is, sliding is permitted, but separation normal to the tank wall is not allowed.

In the modal analyses, the sliding vs. bonded contact analyses were, for the most part, run with either all of the contact surfaces allowed to slide or all contact surfaces bonded. The desired configuration for sliding contact was for all contact surfaces to be bonded except for element types 45 and 46 at the waste/primary tank interface. However, this discrepancy was shown to be insignificant to the results by a single benchmarking case (Modified Sliding_E_1000x). Thus, it is appropriate to talk about the effect of sliding vs. bonded contact along the waste/primary tank interface without re-running any other cases. Results of modal analyses for both sliding and bonded contact are reported in Section 3.1.

2.3 Waste Material Properties

The literature on testing of Hanford tank wastes was reviewed to estimate the range of elastic moduli for input to dynamic finite element models. Although significant research has been conducted to estimate the shear strengths of in situ waste (Gauglitz and Aikin 1997) there is little information regarding the elastic stiffness that precludes shear failure. Figure 2.4 shows two plots from Meyer et al. (1997) of shear-vane test results for a bentonite sludge simulant.

The figure on the left shows a shear yield of about 200 Pa at a shear failure strain of approximately 0.05. The elastic shear modulus can be approximated as G = 200/0.05 =4,000 Pa. Elastic perfectly plastic yielding may also be a good assumption since the shear resistance curve is flat after yielding. Gauglitz and Aiken (1997) show that shear strengths of 200 to 2,000 Pa may be representative of DST wastes, with the upper end representing the more consolidated cohesive waste forms. Assuming a similar failure strain of 0.05 gives a shear modulus of 40,000 Pa. Higher shear strengths and lower shear failure strains will lead to higher shear moduli, and this may occur for some tank waste.

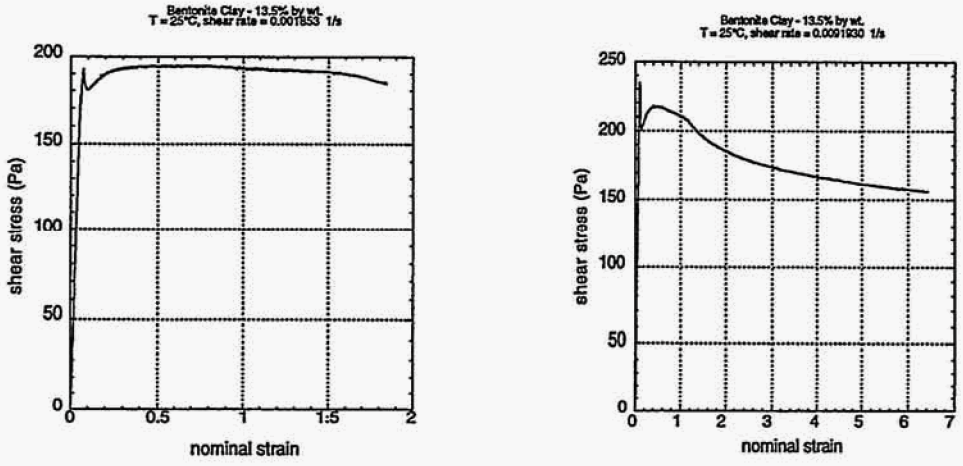

Figure 2.4. Shear Vane Test Results from Meyer et al. (1997; Figure 4.6.2)

The bulk modulus of waste (without gas bubbles) is probably similar to that of water, k = 2.069 GPa or 300 kip/in^2 and the Poisson's ratio is very close to 0.5. The extensional modulus and shear modulus can then be established from elastic relationships. Although the ANSYS® finite element code is limited to Poisson's ratios of about 0.499 or so within the isotropic material definition, one can avoid this limitation by using the orthotropic material model to define independent elastic constants.

Alderman et al. (1991) presents a detailed discussion of shear vane measurement techniques including the methodology and equations for calculating shear modulus from shear vane data. They also present test results of shear strength and modulus for bentonite gels that are in the same shear strength range as the waste tank sludges tested by Gauglitz and Aiken (1997). Figures 2.5 and 2.6 show the shear strength and modulus results for bentonite gels with volume fractions up to 0.12. These data were curve fit and converted from volume fraction to weight fraction (using density of bentonite = 2.6 g/cc and water = 1 g/cc) to allow plotting them with the Gauglitz and Aiken's data (see Figure 2.7). Assuming that shear moduli are consistent for a given weight fraction, this shows shear moduli up to about 14,000 Pa for Gauglitz's sample with shear strength of 2,660 Pa. This suggests a lower upper bound than the previous 40,000 Pa estimate. However, as mentioned above, shear moduli greater than 40,000 Pa may exist for some tank waste.

On the basis of the above information, the nominal upper bound for the waste shear modulus is 40,000 Pa. However, much stiffer materials were also evaluated to show the change in system dynamic response for materials outside the expected stiffness range. The Poisson's ratio for the waste was set to 0.49999 for all cases. The elastic material properties used in the analysis are shown in Table 2.1. Note that when the shear modulus is equal to 4,000, 22,000, or 40,000 Pa, the corresponding extensional modulus is greater than would result from using elastic relationships. This is a holdover to the time-history analyses reported in Rinker and Abatt (2008a, b) where the extensional modulus was set to be consistent with the bulk modulus of water, but the shear modulus was reduced to more closely simulate an inviscid fluid. For shear modulus values higher than 40,000 Pa, the values of the shear and extensional moduli are consistent with those defined by the elastic relationship.

In summary, the lowest value of waste shear modulus for this study was 4,000 Pa because that effectively reproduced the modal properties for an inviscid liquid according to Table 7-1 of Rinker and Abatt (2008a), so that there was no reason to consider lower values. The value of 40,000 Pa is believed to be an upper bound for at least a large portion of the DST waste. Higher values of shear modulus were studied to quantify the transition from liquid response to semi-solid response to solid response, but the highest value studied is several orders of magnitude higher than is expected for any DST waste.

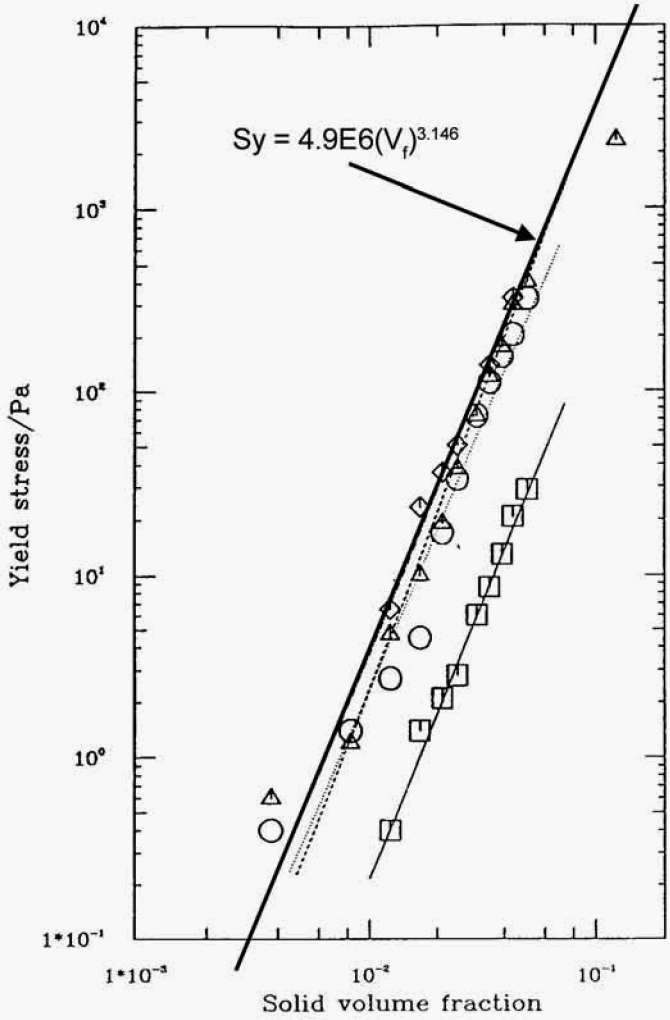

Fig. 9. Variation of τ_0 with solids volume fraction as a function of gelation time.

Figure 2.5. Yield Strength of Bentonite Gels as a Function of Volume Fraction and Gelation Time. Legend: □ and solid line, $t = 0$ h; ○ and dotted line, $t = 16$ h; Δ and dashed line, $t = 69$ h; ◊ and dot-dash line, $t = 120$ hr.

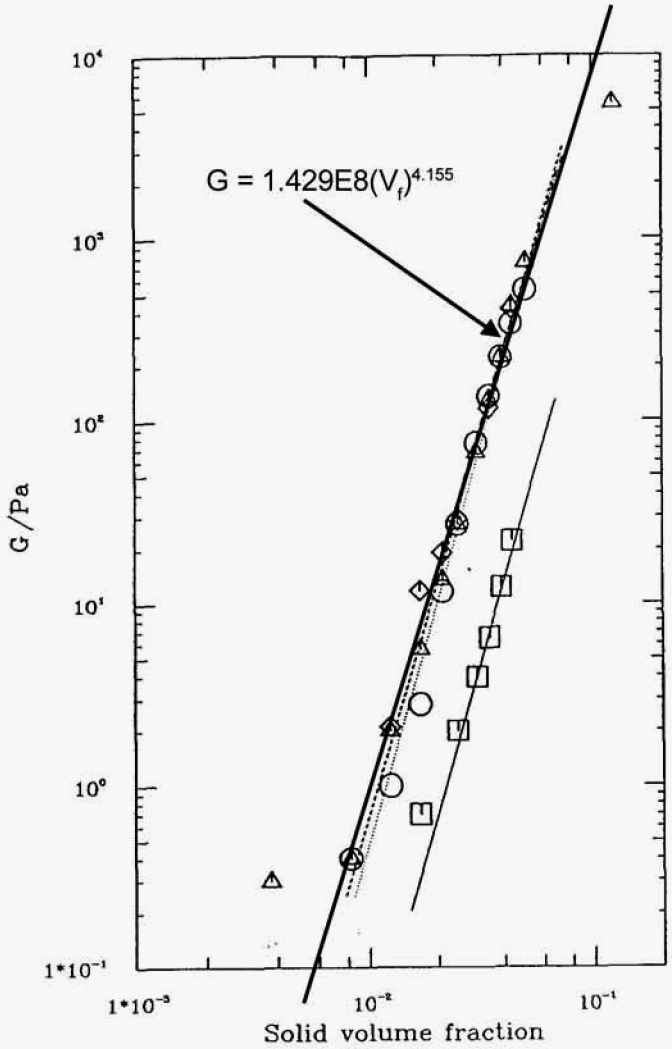

Fig. 10. Variation of G with solids volume fraction as a function of gelation time.

Figure 2.6. Shear Modulus of Bentonite Gels as a Function of Volume Fraction and Gelation Time. Legend: □ and solid line, t = 0 h; ○ and dotted line, t = 16 h; Δ and dashed line, t = 69 h; ◊ and dot-dash line, t = 120 hr.

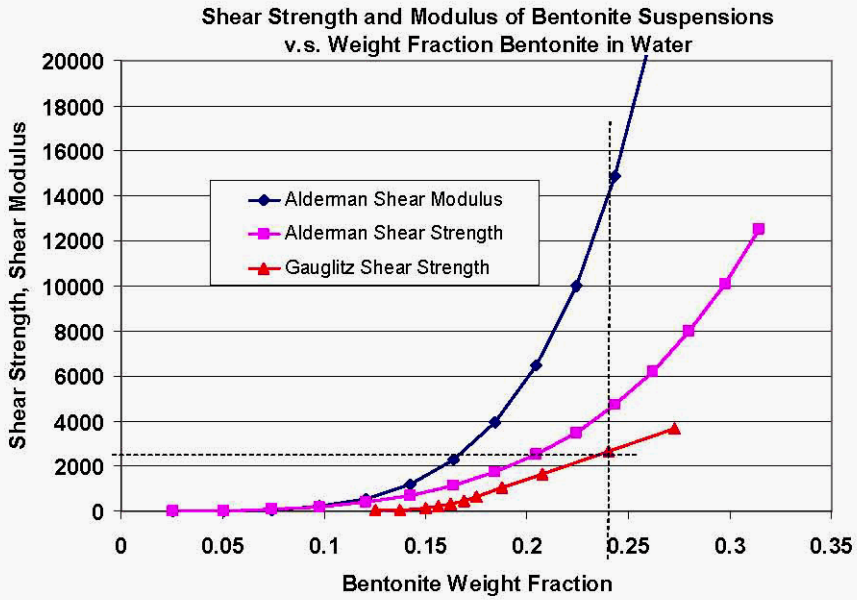

Figure 2.7. Comparison of Alderman and Gauglitz Bentonite Shear Strengths for Bentonite Gels with Common Weight Fractions

Table 2.1. Combinations of Linear Elastic Material Properties Used in the Analysis

Extensional Modulus (Pa)	Shear Modulus (Pa)	Representative Material
124,000	4,000	Room temperature peanut butter[(a)]
124,000	22,000	150% of the shear modulus of margarine spread at 6.5°C[(a)]
124,000	40,000	80% of the shear modulus of processed cheese spread at room temperature[(a)]
1.24×10^6	413,500	
1.24×10^7	4.135×10^6	
6.21×10^7	2.07×10^7	
1.24×10^8	4.135×10^7	Rubber
1.24×10^9	4.135×10^8	High density polyethylene (HDPE)
1.24×10^{10}	4.135×10^9	70% of the stiffness of lead

(a) Daubert et al. (1998)

2.3.1 Relative Flexibility of Tank Wall and Waste

Veletsos and Younan (1998) define a relative flexibility factor (d_w) that is a dimensionless measure of the tank wall flexibility. In that paper, the relative flexibility factor is used to illustrate how critical responses such as base shear depend on the relative flexibility of the tank and the contained material, and a relative flexibility factor of zero represents a rigid tank. Although the system analyzed in that paper is different than the one being considered here (for one thing, the top boundary condition is different), it is of some interest to calculate the relative flexibility factor for the current system. Equation 20 of Veletsos and Younan (1998) gives the relative flexibility factor as

$$d_w = \frac{1}{2}\frac{G_{waste}R}{G_{\tan k}t_{wall}}.$$

Given the tank radius of 450 inch, and an average wall thickness for the lower two-thirds of an AP tank of approximately 0.67 inch, the wall flexibility factor can be written as

$$d_w = 336\frac{G_{waste}}{G_{\tan k}}.$$

Given the shear modulus for the steel tank of 11.5×10^6 lbf/in^2, this can be further reduced to

$$d_w = 2.92\times10^{-5}G_{waste} \text{ (lbf, in, s)}$$

or

$$d_w = 4.25\times10^{-9}G_{waste} \text{ (N, m, s).}$$

For wastes with a shear modulus of 40,000 Pa or less, the resulting relative flexibility factor is:

$$d_w \le 1.7\times10^{-4}$$

This indicates that the DSTs are quite rigid relative to the contained waste. For the system considered in Veletsos and Younan (1998), and a tank height-to-radius ratio (H/R) of approximately unity (as is the case for the DSTs), this means that very little amplification (or de-amplification) of base shear relative to the rigid tank solution is expected.

Intentionally left blank.

3.0 Modal Properties of the Linearized System

Modal analyses were performed using both sliding and bonded contact conditions over a range of shear moduli from 4,000 to 4×10^9 Pa. Values lower than 4,000 Pa were not investigated because the modal response of an inviscid liquid was effectively reproduced with the value of 4,000 Pa as seen by comparing the results with those presented in Table 7-1 of Rinker and Abatt (2008a). Although the upper end of shear moduli for tank waste is uncertain, 40,000 Pa is believed to represent an upper bound for much of the tank waste. Modal analyses were performed for shear moduli several orders of magnitude higher than is expected for any tank waste in order to show the fundamental change in modal response for stiffer materials.

The primary reason that the modal properties of the system are of interest is because the global reaction forces on the primary tank, which are critical tank responses, can be estimated by forming products of the modal effective masses and the corresponding spectral accelerations (simplified response spectrum analysis). The following results show that when the waste shear modulus is less than 40,000 Pa, the impulsive mode is the dominant structural mode, and its effective mass is approximately 50% of the mass of the flexible portion of the system, namely that of the waste and the tank wall. This implies that the peak horizontal reaction force and, most likely, the peak overturning moment are expected to be nearly proportional to the spectral acceleration corresponding to the frequency of the impulsive mode.

3.1 Modal Results

For the range of shear moduli where the convective and impulsive modes are clearly identifiable, the convective mode shapes are shown. Although displacement plots of the impulsive modes are not shown, the impulsive mode is far more important than the convective mode in terms of contributing to the critical responses of the system because the accelerations associated with the convective modes are relatively low.

Also shown for each case are the effective modal masses and the cumulative mass fraction up to a specified natural frequency of the system. In these plots, the natural frequencies are shown on the horizontal axis. The effective modal masses are shown as vertical blue lines that are referenced to the primary vertical axis on the left. The cumulative modal mass fractions are shown with the magenta curves that are referenced to the secondary vertical axis on the right.

Typically there are between one and four dominant system frequencies. However, in many cases, there are numerous insignificant modes, and groups of closely-spaced modes near the dominant system frequencies. While some of these modes may be due to discretization error or other numerical approximations, many of these modes are expected to be "real" given that the waste was modeled as an elastic solid. As an example, the effective modal mass versus natural frequency for the sliding interface is shown in Figures 3.2, 3.8, 3.15, 3.20, 3.25, 3.26, 3.28, and 3.32 as the waste shear modulus varies from 4,000 Pa to 4.135×10^8 Pa. At the low end of waste stiffness, the system has two dominant natural frequencies representing the convective and impulsive modes. At the high end of waste stiffness considered, there is only one significant system mode (Figure 3.32). In between the two extremes the system transitions from liquid-like response to solid-like response. It is reasonable to expect that this transition will occur smoothly with an intermediate response such as shown in Figure 3.20. In other

words, many of the closely-spaced and less significant modes are expected to represent "real" system behavior, at least in the sense that the response is consistent with the modeling assumptions.

In ANSYS®, the reported cumulative mass fraction is normalized to the system mass that participates up to the cutoff frequency considered in the modal analysis rather than the total system mass. In the lateral direction parallel to the symmetry plane, the participating mass is at least 97% of the mass of the flexible portion of the system (mass of the waste and tank wall) in all cases. Thus, for the lateral directions, the reported mass fractions are effectively normalized to the system mass. In the vertical direction, the participating mass is approximately 2/3 of the flexible mass of the system up to the cutoff frequency. The natural frequency extractions were performed by specifying the number of frequencies to be extracted so that the cutoff frequency considered varies from case to case.

The focus of the analysis is on the response in the lateral direction parallel to the symmetry plane, but results shown for vertical direction are shown for the range of shear moduli believed to represent the tank waste. A summary of the modal properties in the horizontal (lateral direction parallel to the symmetry plane) direction is shown in Table 3.1.

The results show that when the shear modulus is less than or equal to 40,000 Pa, the system responds nearly the same as a liquid-filled tank, with convective and impulsive modes. When the shear modulus is greater than or equal to 4.135×10^7 Pa, the modal properties represent a tank containing a solid with a single dominant natural frequency. When the waste shear modulus is between 40,000 Pa and 4.135×10^7 Pa, the waste behaves as a semi-solid with multi-mode behavior.

Table 3.1. Dominant Natural Frequencies of Systems Examined and Effective Mass of the Associated Modes of Vibration Expressed as Ratios of the Mass of the Primary Tank and Contained Waste

Shear Modulus (Pa)	Natural Frequencies (Hz)		Modal Mass Ratios	
	Sliding Interface	Bonded Interface	Sliding Interface	Bonded Interface
4,000	0.19, 5.85	0.21, 5.86	0.3, 0.5	0.3, 0.5
22,000	0.22, 5.85	0.27, 5.8	0.3, 0.5	0.3, 0.5
40,000	0.24, 5.9	0.3, 5.7	0.3, 0.5	0.3, 0.5
413,500	0.76, 5.95	0.96, 6.0	0.1, 0.4	0.2, 0.35
4.135 × 106	Multiple between 2.4 and 8 Hz	Not calculated	Multiple significant between 2.4 and 8 Hz	Not calculated
2.07 × 107	4.9, 5.9, 7.8, and 8.2	Not calculated	0.48, 0.24, 0.03, 0.14	Not calculated
4.135 × 107	6.1	6.9	0.75	0.74
4.135 × 108	12.1	15.3	0.92	0.82
4.135 × 109	Not calculated	37.2	Not calculated	0.87
22,000a	Not calculated	4.7	Not calculated	0.95

(a) Capped boundary condition at waste surface.

3.1.1 Sliding Contact G=4,000 Pa

The results for modal analysis in the lateral direction parallel to the symmetry plane show that the significant frequencies are 0.19 Hz and 5.85 Hz, and the fundamental convective mode shape is shown in Figure 3.1. As shown in Figure 3.2, the cumulative effective mass increase between 5.6 Hz and 6 Hz is

approximately 50% – that is, approximately 50% of the flexible portion of the system mass is effective in the impulsive mode. Approximately 95% of the mass is participating by 6 Hz and 98% of the mass is participating below the cutoff frequency of 20.6 Hz.

In the vertical direction, approximately 75% of the participating mass is at the single dominant natural frequency of 5 Hz (see Figure 3.3).

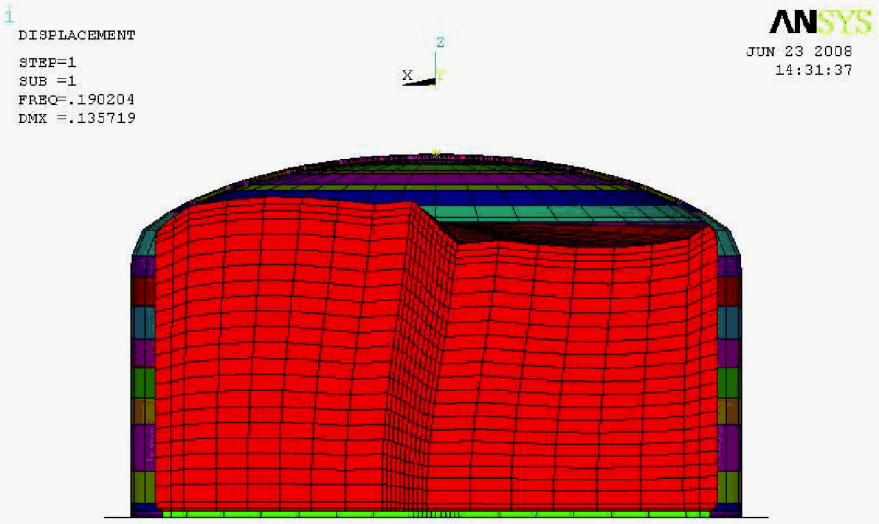

Figure 3.1. Fundamental Horizontal Convective Mode for Sliding Contact and Waste Shear Modulus of 4,000 Pa

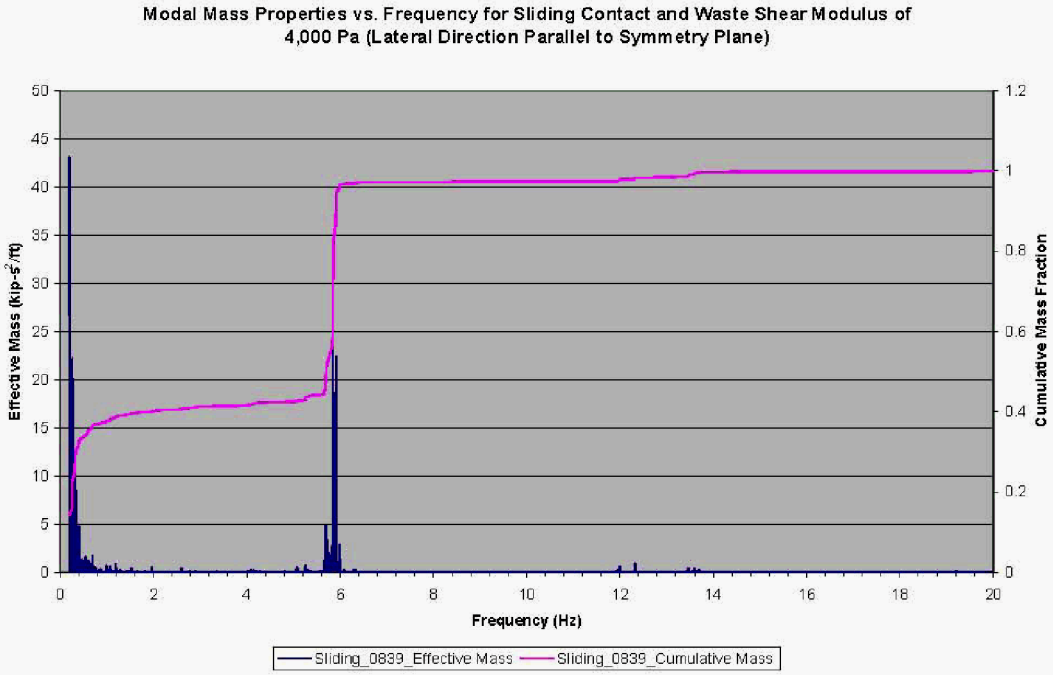

Figure 3.2. Natural Frequencies and Modal Masses for Sliding Contact and Waste Shear Modulus of 4,000 Pa (Lateral Direction Parallel to Symmetry Plane)

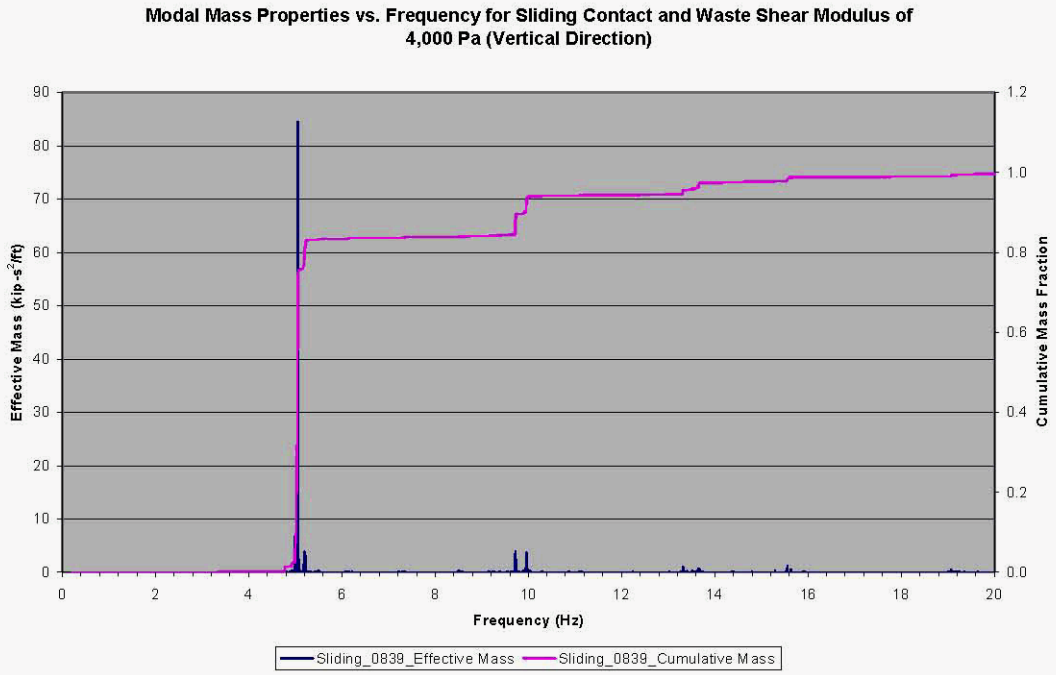

Figure 3.3. Natural Frequencies and Modal Masses for Sliding Contact and Waste Shear Modulus of 4,000 Pa (Vertical Direction)

3.1.2 Bonded Contact G=4,000 Pa

The results for modal analysis in the lateral direction parallel to the symmetry plane for bonded contact show that the significant frequencies are 0.21 Hz and 5.86 Hz and the convective mode shape is shown in Figure 3.4. As seen in Figure 3.5, the cumulative effective mass increase between 5.6 and 6 Hz is approximately 50%, that is, approximately 50% of mass is effective in the impulsive mode. Approximately 95% of the mass is participating by 6 Hz and essentially all of the mass is participating below the cutoff frequency of 25.3 Hz.

In the vertical direction, approximately 85% of the participating mass is at the dominant natural frequency of 5 Hz (see Figure 3.6).

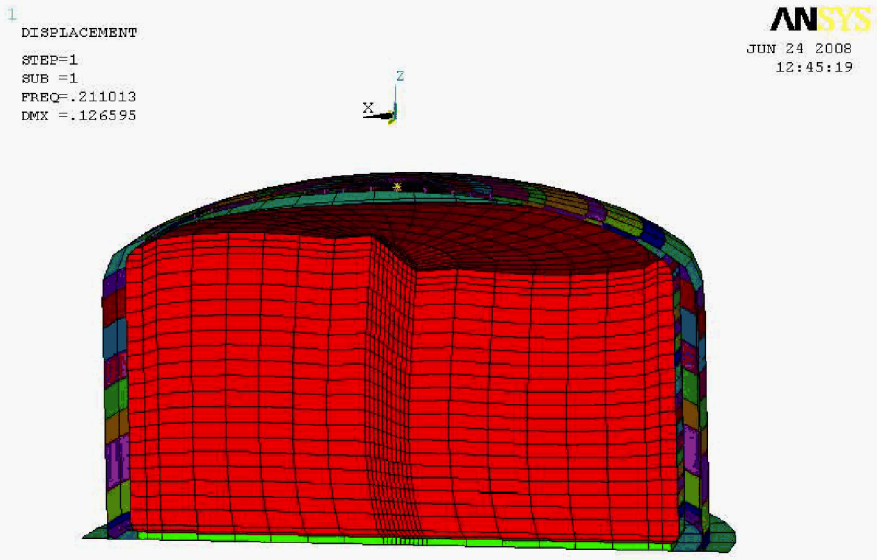

Figure 3.4. Fundamental Horizontal Convective Mode for Bonded Contact and G_{waste}=4,000 Pa

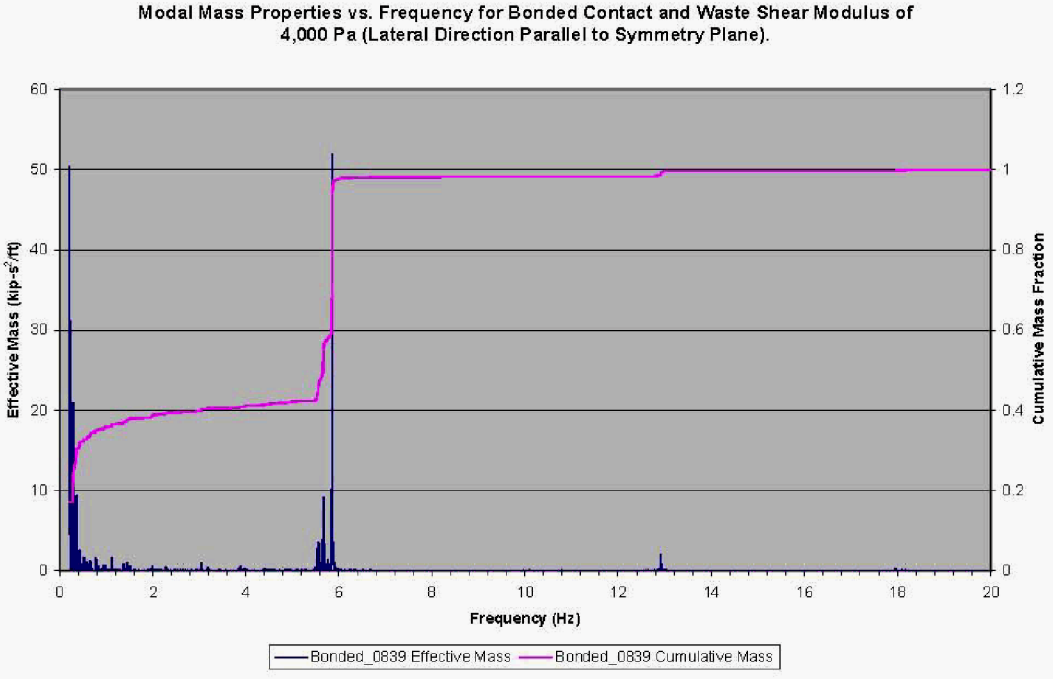

Figure 3.5. Natural Frequencies and Modal Masses for Bonded Contact and Waste Shear Modulus of 4,000 Pa (Lateral Direction Parallel to Symmetry Plane)

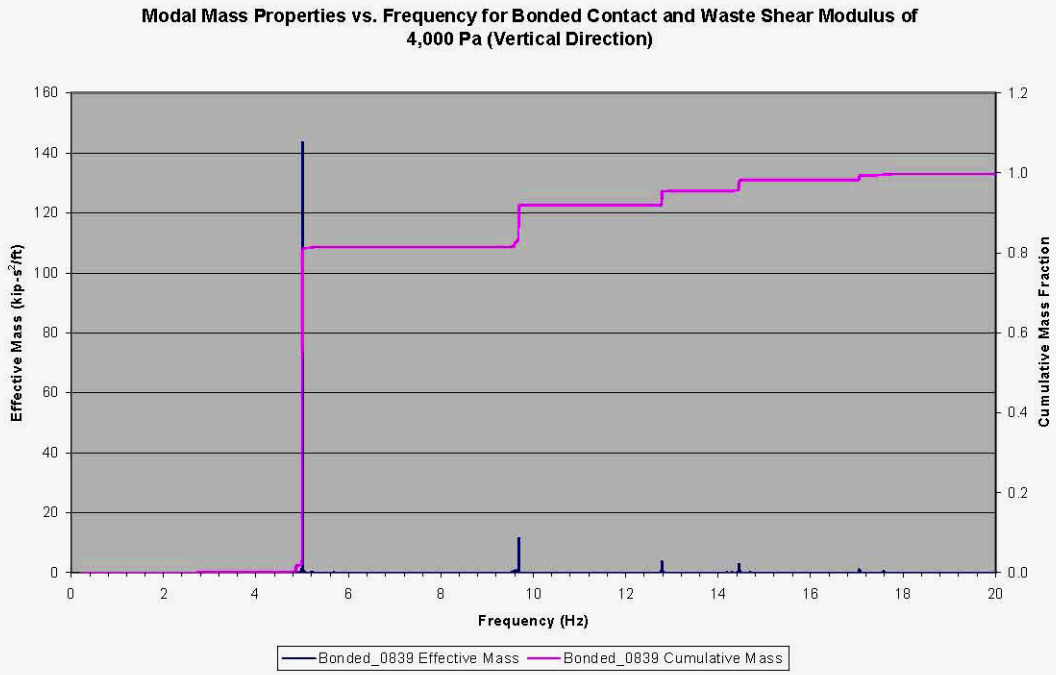

Figure 3.6. Natural Frequencies and Modal Masses for Bonded Contact and Waste Shear Modulus of 4,000 Pa (Vertical Direction)

3.1.3 Sliding Contact G=22,000 Pa

The results for modal analysis in the lateral direction parallel to the symmetry plane for sliding contact show that the significant frequencies are 0.22 Hz and 5.85 Hz, with the convective mode shape shown as Figure 3.7. According to Figure 3.8, the cumulative effective mass increase between 5.6 and 6 Hz is approximately 50%, that is, approximately 50% of mass is effective in the impulsive mode. Approximately 95% of the mass is participating by 6 Hz and essentially all of the mass is participating below the cutoff frequency of 21 Hz.

In the vertical direction, approximately 85% of the participating mass is at the dominant natural frequency of 5 Hz (see Figure 3.9).

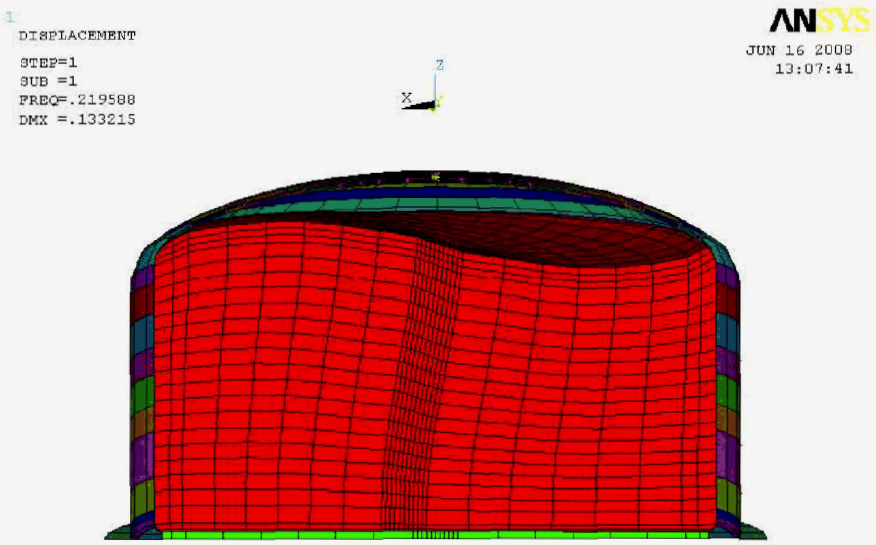

Figure 3.7. Fundamental Horizontal Convective Mode for Sliding Contact and G_{waste}=22,000 Pa

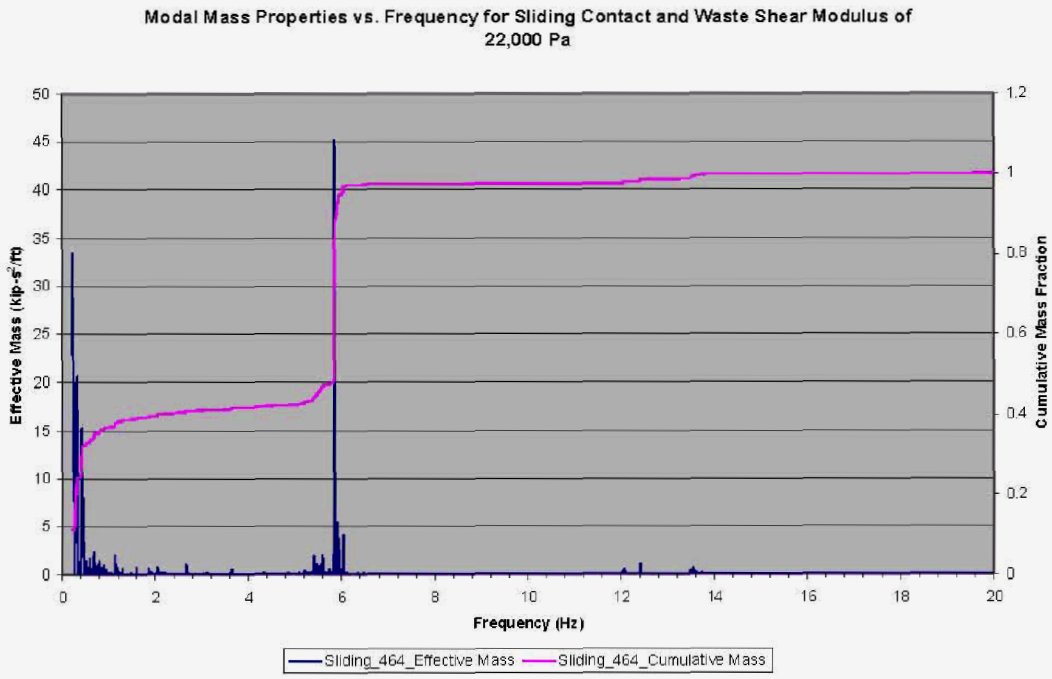

Figure 3.8. Natural Frequencies and Modal Masses for Sliding Contact and Waste Shear Modulus of 22,000 Pa (Lateral Direction Parallel to Symmetry Plane)

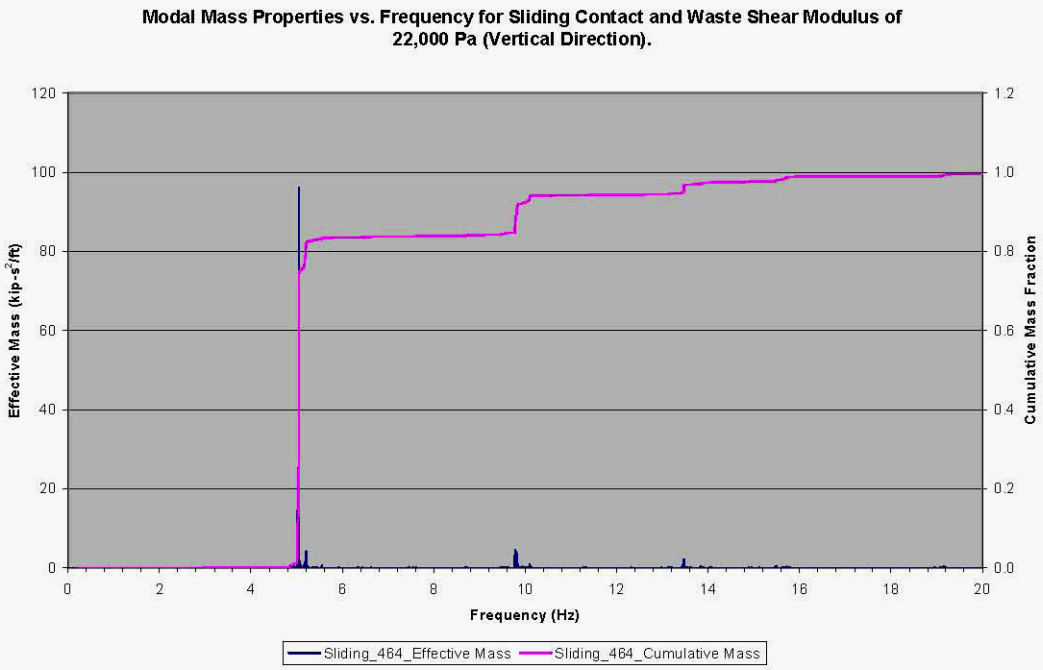

Figure 3.9. Natural Frequencies and Modal Masses for Sliding Contact and Waste Shear Modulus of 22,000 Pa (Vertical Direction)

3.1.4 Bonded Contact G=22,000 Pa

The results for modal analysis in the lateral direction parallel to the symmetry plane for bonded contact with a shear modulus of 22,000 Pa show that the significant natural frequencies are 0.27 Hz and approximately 5.8 Hz. As shown in Figure 3.10, the cumulative effective mass increase between 5.6 and 6 Hz is approximately 50%. Approximately 95% of the mass is participating by 6 Hz and essentially all of the mass is participating below the cutoff frequency of 25.5 Hz. In contrast to the sliding contact case, the impulsive frequency is not as well defined – instead, several significant natural frequencies occur in the range of 5.6 to 5.9 Hz.

In the vertical direction, more than 80% of the participating mass occurs at 5 Hz, with several other significant natural frequencies between 9 and 17 Hz (see Figure 3.11).

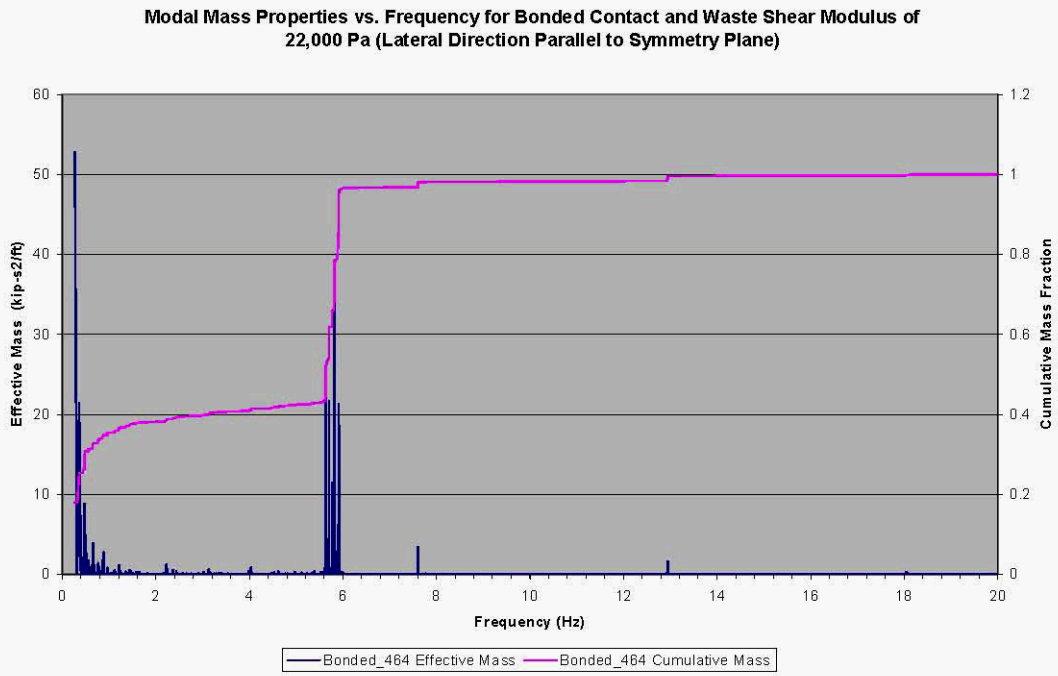

Figure 3.10. Natural Frequencies and Modal Masses for Bonded Contact and Waste Shear Modulus of 22,000 Pa (Lateral Direction Parallel to Symmetry Plane)

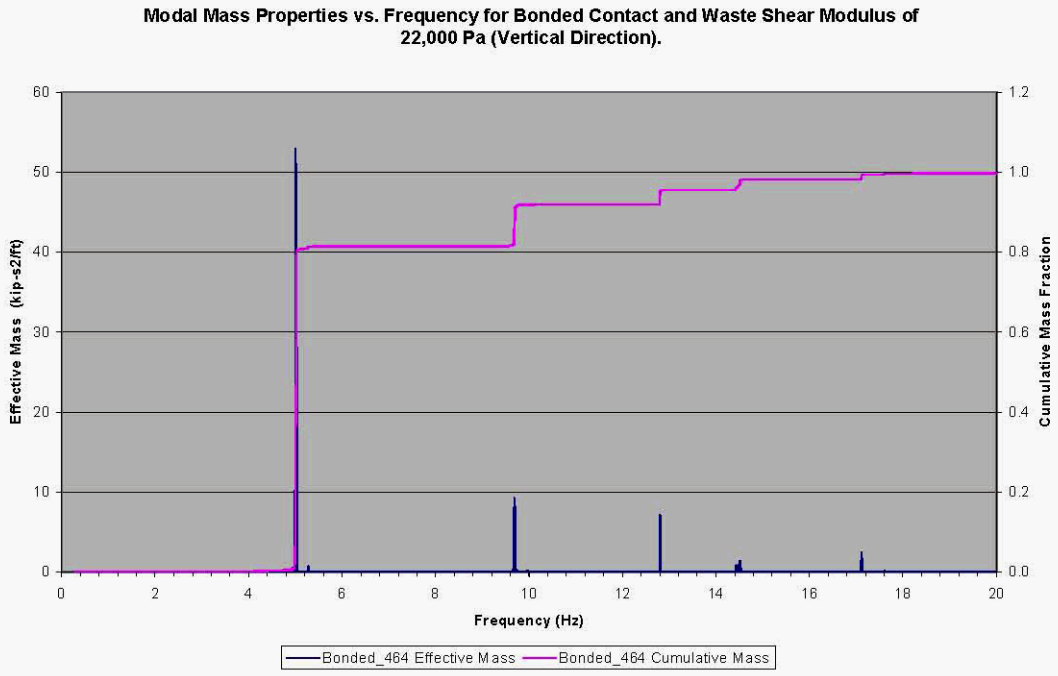

Figure 3.11. Natural Frequencies and Modal Masses for Bonded Contact and Waste Shear Modulus of 22,000 Pa (Vertical Direction)

3.1.5 Capped Bonded Contact G=22,000 Pa

Capped bonded contact refers to the bonded contact case in which the surface of the tank waste was prevented from moving in the vertical direction (capped) via a boundary condition on the surface nodes. The intent of this case was to force a 100% impulsive response and compare the peak reaction force from a time-history run to the corresponding case with a free surface where both the convective and impulsive modes are realized. The modal analysis will provide insight to the expected peak reaction force.

As shown in Figure 3.12, the fundamental horizontal mode is not a convective mode, as must be the case given the enforced boundary condition on the waste free surface. The dominant structural frequency occurs at approximately 4.7 Hz as seen in Figure 3.13, with approximately 95% of the mass participating in these few closely-spaced modes. From the point of modal analysis, probably the most important observation is the lowering of the dominant structural frequency from 5.8 Hz to 4.7 Hz, apparently due to the increase in participating mass at this frequency. The effect of the frequency shift on the peak horizontal reaction force and other critical responses depends on the seismic input.

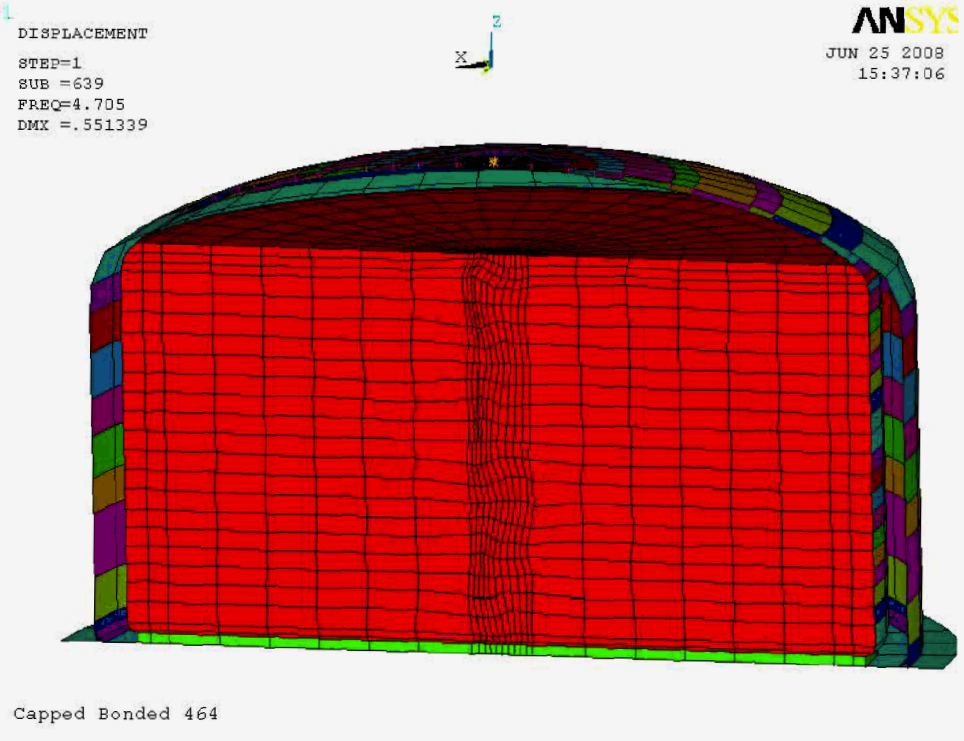

Figure 3.12. Fundamental Horizontal Mode Shape for Capped Bonded Contact and G_{waste}=22,000 Pa

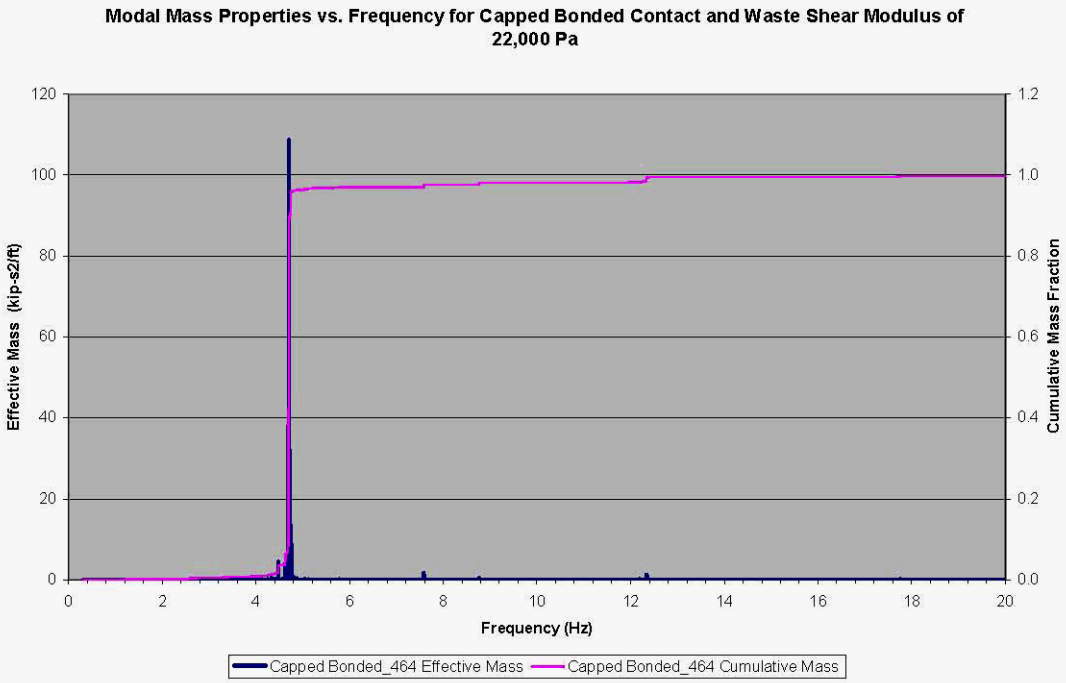

Figure 3.13. Natural Frequencies and Modal Masses for Capped Bonded Contact and Waste Shear Modulus of 22,000 Pa (Lateral Direction Parallel to Symmetry Plane)

3.1.6 Sliding Contact G=40,000 Pa

The results for modal analysis in the lateral direction parallel to the symmetry plane for sliding contact with a shear modulus of 40,000 Pa show that the significant frequencies are 0.24 Hz and approximately 5.9 Hz. The fundamental convective mode shape is shown as Figure 3.14. As shown in Figure 3.15, the cumulative effective mass increase between 5.6 and 6 Hz is approximately 50%, that is, approximately 50% of mass is effective in the impulsive mode. Approximately 95% of the mass is participating by 6 Hz and essentially all of the mass is participating below the cutoff frequency of 21.4 Hz. The impulsive frequency is not quite as well defined as in Figure 3.8 with the lower shear modulus of 22,000 Hz. As shown in Figure 3.16, more than 80% of the participating mass occurs at 5 Hz in the vertical direction.

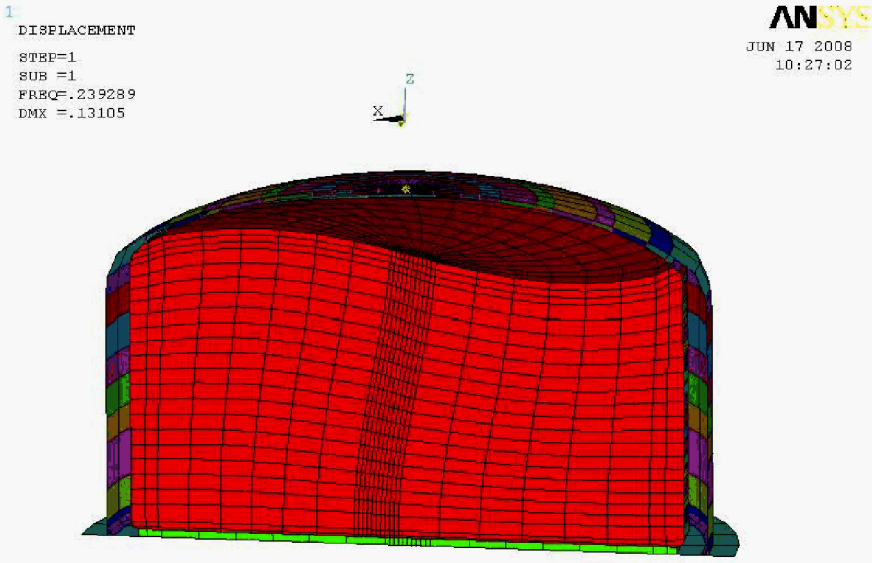

Figure 3.14. Fundamental Convective Mode for G_{waste}=40,000 Pa

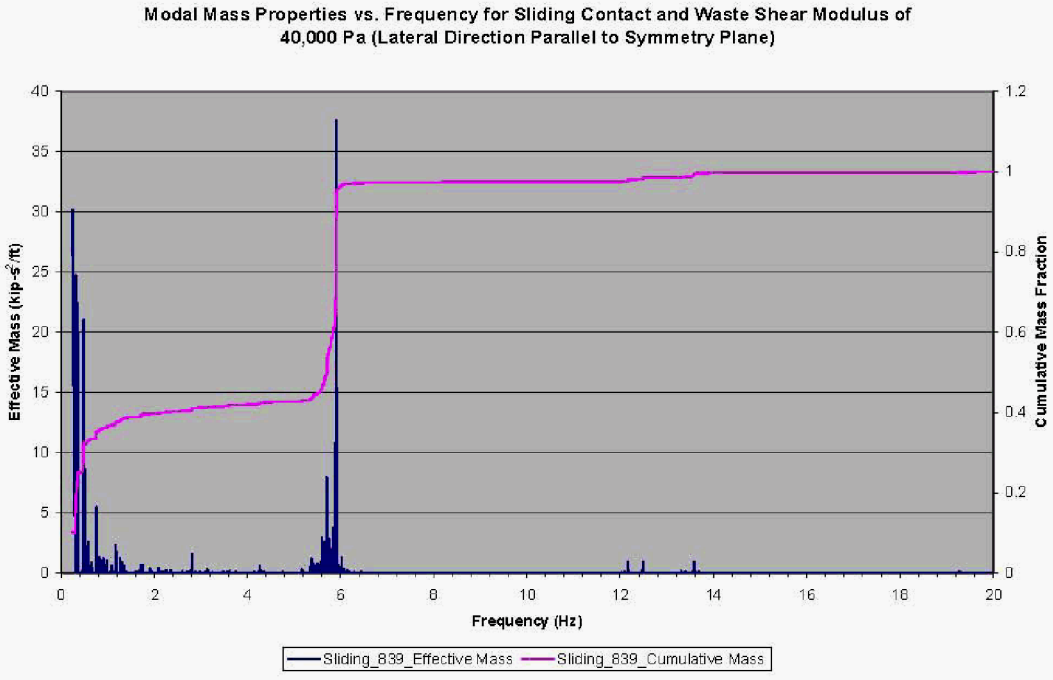

Figure 3.15. Natural Frequencies and Modal Masses for Sliding Contact and Waste Shear Modulus of 40,000 Pa (Lateral Direction Parallel to Symmetry Plane)

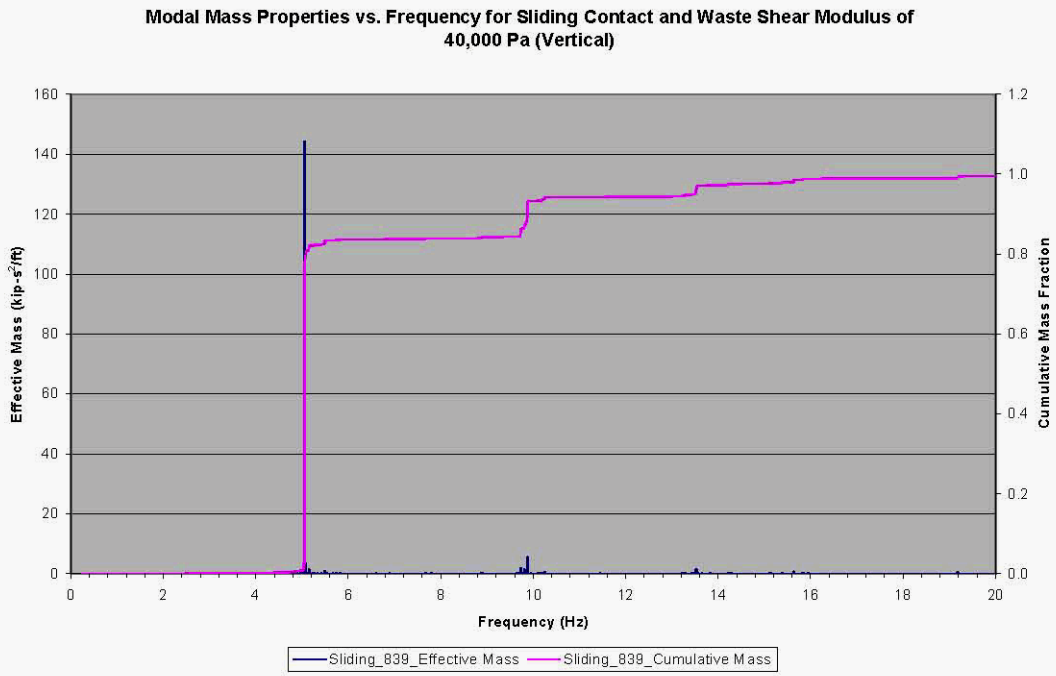

Figure 3.16. Natural Frequencies and Modal Masses for Sliding Contact and Waste Shear Modulus of 40,000 Pa (Vertical Direction)

3.1.7 Bonded Contact G=40,000 Pa

The results for modal analysis in the lateral direction parallel to the symmetry plane for bonded contact with a shear modulus of 40,000 Pa show that the significant frequencies are 0.3 Hz and approximately 5.7 Hz. As shown in Figure 3.17, the cumulative effective mass increase between 5.6 and 6 Hz is approximately 50%, that is, approximately 50% of mass is effective in the impulsive mode. Approximately 95% of the mass is participating by 6 Hz and essentially all of the mass is participating below the cutoff frequency of 25.8 Hz.

In the vertical direction, approximately 75% of the participating mass occurs at 5 Hz, with several other minor modes between 9 and 17 Hz (see Figure 3.18).

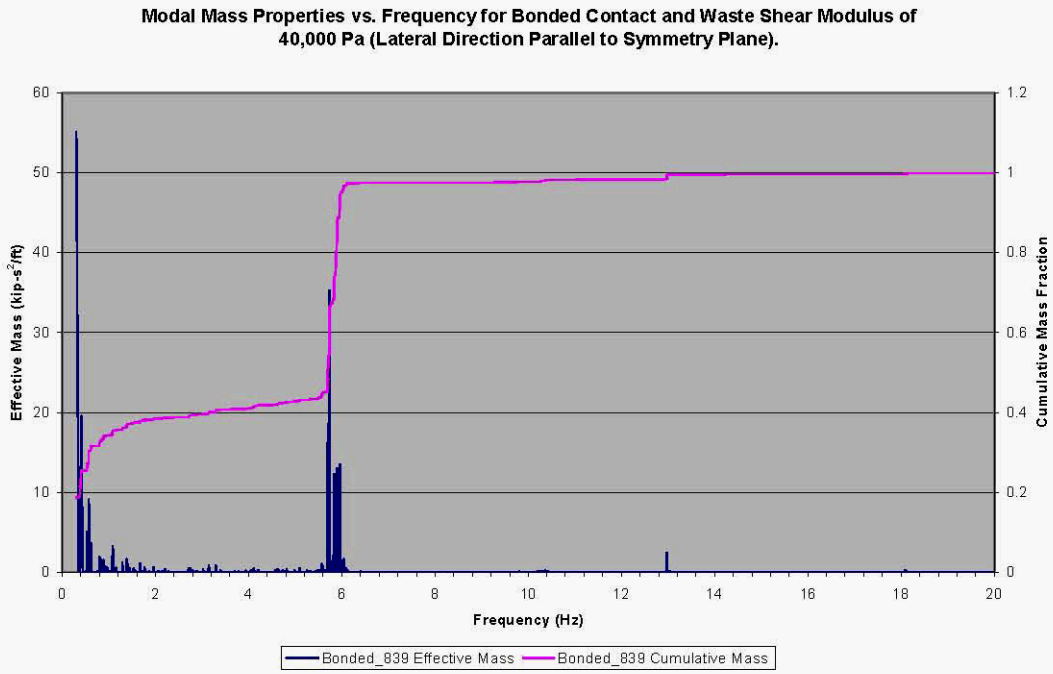

Figure 3.17. Natural Frequencies and Modal Masses for Bonded Contact and Waste Shear Modulus of 40,000 Pa (Lateral Direction Parallel to Symmetry Plane)

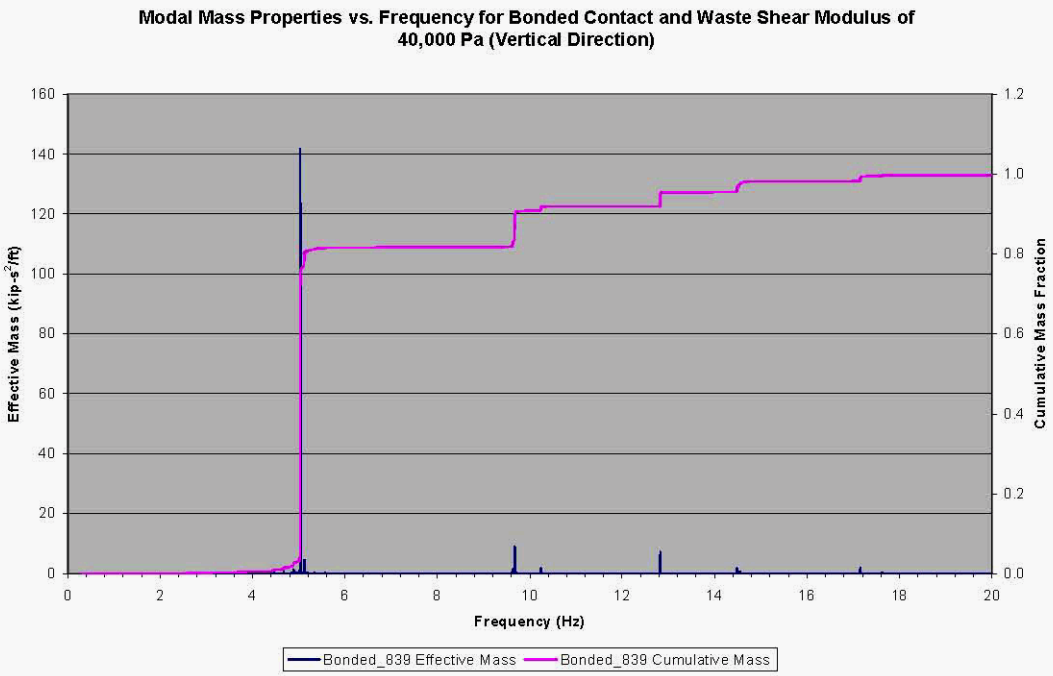

Figure 3.18. Natural Frequencies and Modal Masses for Bonded Contact and Waste Shear Modulus of 40,000 Pa (Vertical Direction)

3.1.8 Sliding Contact G=413,500 Pa

The results for modal analysis in the lateral direction parallel to the symmetry plane for sliding contact with a shear modulus of 413,500 Pa show that the significant frequencies are 0.76 Hz and approximately 5.95 Hz. The fundamental convective mode shape is shown as Figure 3.19. As shown in Figure 3.20, the cumulative effective mass increase between 5.5 and 6.1 Hz is approximately 45%, that is, approximately 45% of the mass is effective in the several closely-spaced modes near the dominant impulsive frequency. Approximately 95% of the mass is participating by 6.1 Hz and essentially all of the mass is participating below the cutoff frequency of 63.4 Hz.

In the vertical direction, approximately 60% of the participating mass occurs at 5.3 Hz, but, as shown in Figure 3.21, a single vertical frequency is not as well defined as is the case with more compliant tank contents.

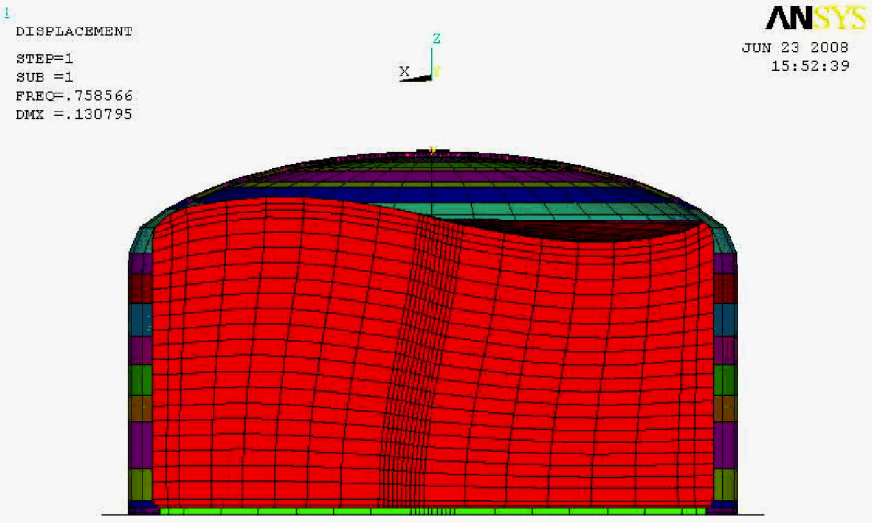

Figure 3.19. Fundamental Horizontal Convective Mode for G_{waste}=413,500 Pa with Sliding Contact

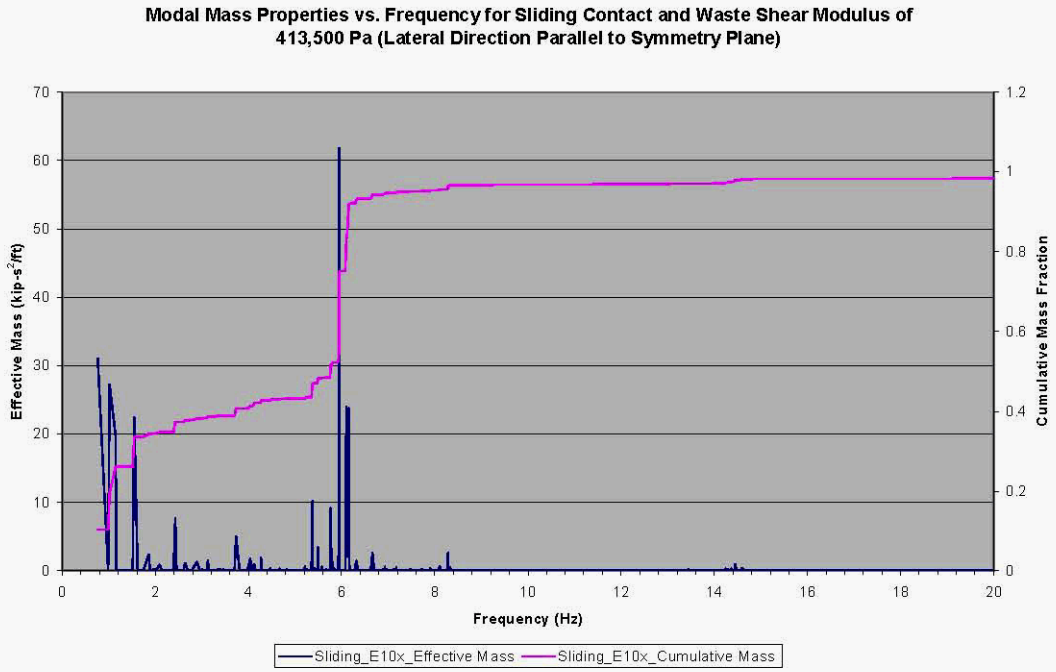

Figure 3.20. Natural Frequencies and Modal Masses for Sliding Contact and Waste Shear Modulus of 4.135×10^5 Pa (Lateral Direction Parallel to Symmetry Plane)

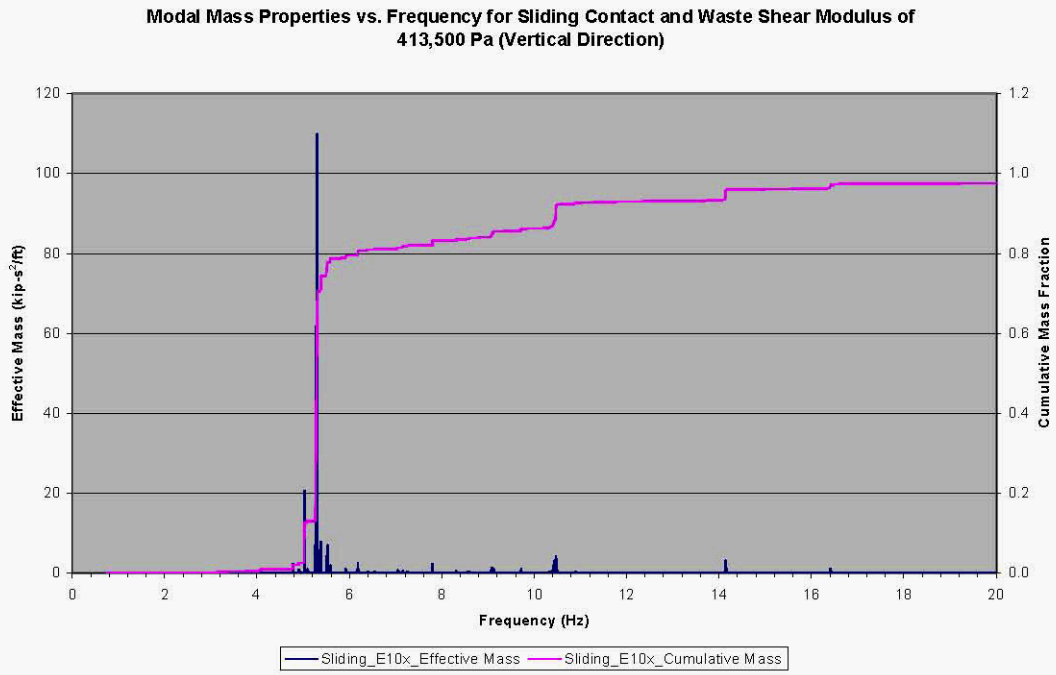

Figure 3.21. Natural Frequencies and Modal Masses for Sliding Contact and Waste Shear Modulus of 4.135×10^5 Pa (Vertical Direction)

3.1.9 Bonded Contact G=413,500 Pa

The results for modal analysis in the lateral direction parallel to the symmetry plane for bonded contact with a shear modulus of 413,500 Pa show that the significant frequencies are 0.96 Hz and approximately 6 Hz. The mode shape for the lower frequency is shown as Figure 3.22. There is a clear transition taking place in which numerous structural frequencies are distributed over a range as opposed to having isolated and clearly identifiable dominant frequencies. This is largely due to the increase in shear modulus, but it is also more pronounced for bonded contact than for sliding contact. As shown in Figure 3.23, the cumulative effective mass increase between 5.8 and 6.2 Hz is approximately 35%. Approximately 90% of the mass is participating by 6.5 Hz and essentially all of the mass is participating below the cutoff frequency of 57.6 Hz.

The modal analysis for the vertical direction (Figure 3.24) shows numerous closely-spaced modes near 5 Hz, with no single clearly dominant frequency (Figure 3.24).

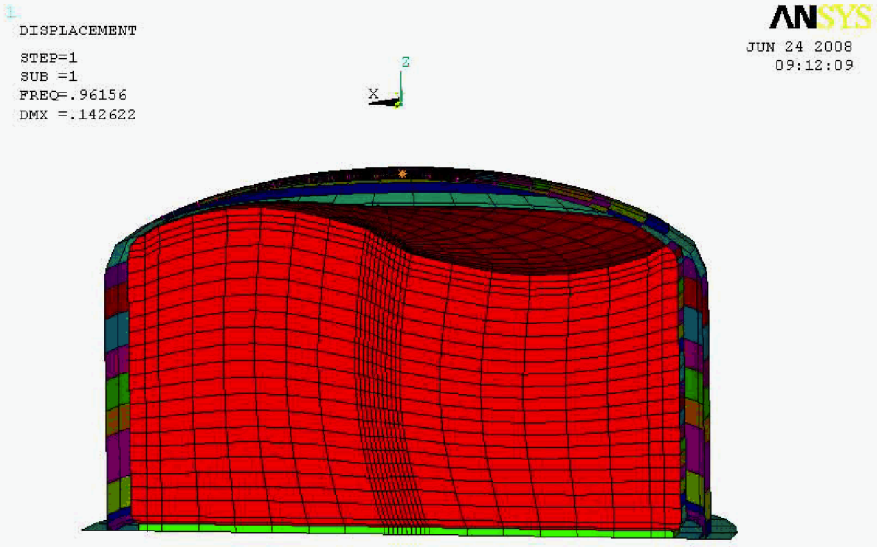

Figure 3.22. Fundamental Convective Mode for $G_{waste}=4.135 \times 10^5$ Pa with Bonded Contact

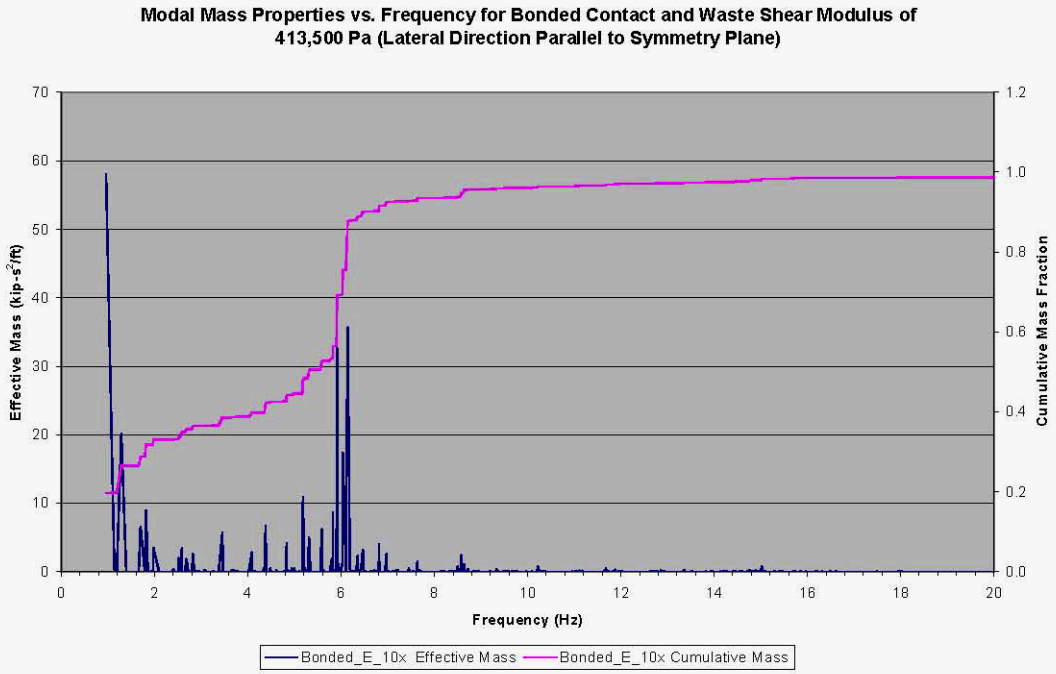

Figure 3.23. Natural Frequencies and Modal Masses for Bonded Contact and Waste Shear Modulus of 4.135×10^5 Pa (Lateral Direction Parallel to Symmetry Plane)

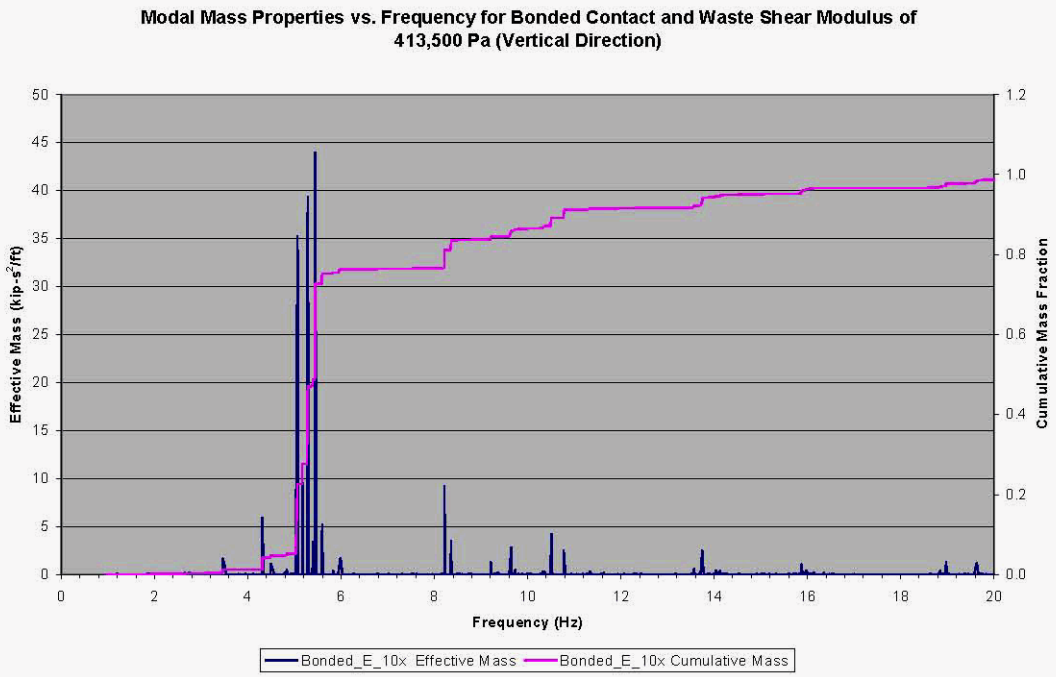

Figure 3.24. Natural Frequencies and Modal Masses for Bonded Contact and Waste Shear Modulus of 4.135×10^5 Pa (Vertical Direction)

3.1.10 Sliding Contact G=4.135 × 10^6 Pa

The results for modal analysis in the lateral direction parallel to the symmetry plane for sliding contact with a shear modulus of 4.135 × 10^6 Pa show that several significant frequencies occur between 2.4 and 8 Hz. The distinction between the "convective" and "impulsive" frequencies is blurred and the terminology is probably not meaningful.

As shown in Figure 3.25, approximately 95% of the mass is participating by 15 Hz and essentially all of the mass is participating below the cutoff frequency of 50.5 Hz.

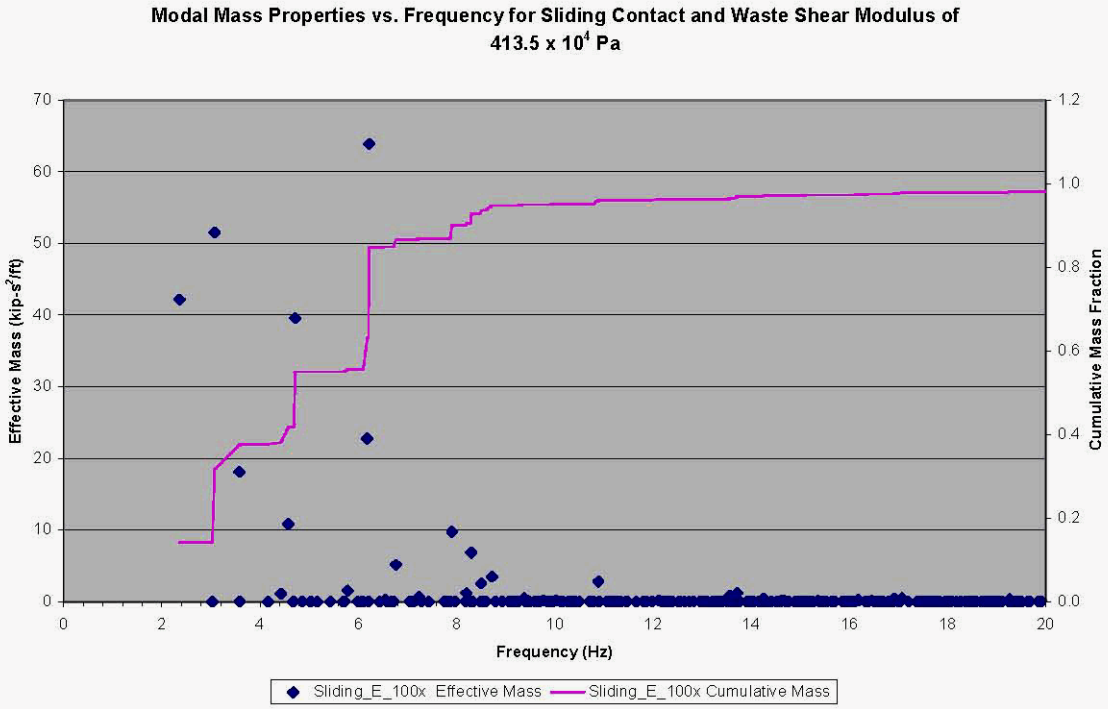

Figure 3.25. Natural Frequencies and Modal Masses for Sliding Contact and Waste Shear Modulus of 4.135 × 10^6 Pa (Lateral Direction Parallel to Symmetry Plane)

3.1.11 Sliding Contact G=2.07 × 10^7 Pa

The results for modal analysis in the lateral direction parallel to the symmetry plane for sliding contact with a shear modulus of 2.07 × 10^7 Pa shows four significant frequencies between 4.9 and 8.2 Hz (Figure 3.26). Approximately 90% of the mass is participating by 8 Hz and the transition from fluid-like to solid-like behavior is clearly evident.

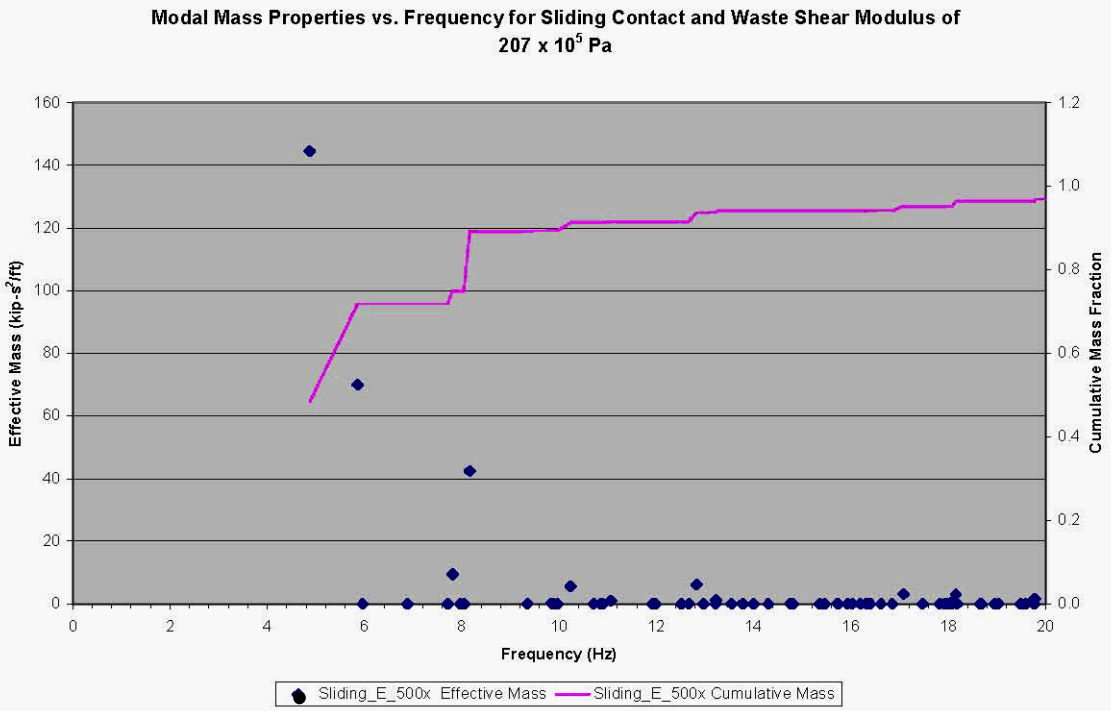

Figure 3.26. Natural Frequencies and Modal Masses for Sliding Contact and Waste Shear Modulus of 2.07×10^7 Pa (Lateral Direction Parallel to Symmetry Plane)

3.1.12 Sliding Contact G=4.135 × 10^7 Pa

In this case, the transition from fluid-like to solid-like behavior is nearly complete and the most significant structural frequency occurs at 6.1 Hz. The fundamental mode shape for this frequency is shown as Figure 3.27. Approximately 75% of the mass participates in this mode, but 90% mass participation does not occur until approximately 10 Hz (Figure 3.28). It is interesting to compare the difference in the fundamental convective mode shape shown in Figure 3.7 for a much lower shear modulus, and the fundamental mode shape shown in Figure 3.27. In the former plot, the first mode is purely convective, while in the latter plot, the flexing of the tank walls is inherent to the response.

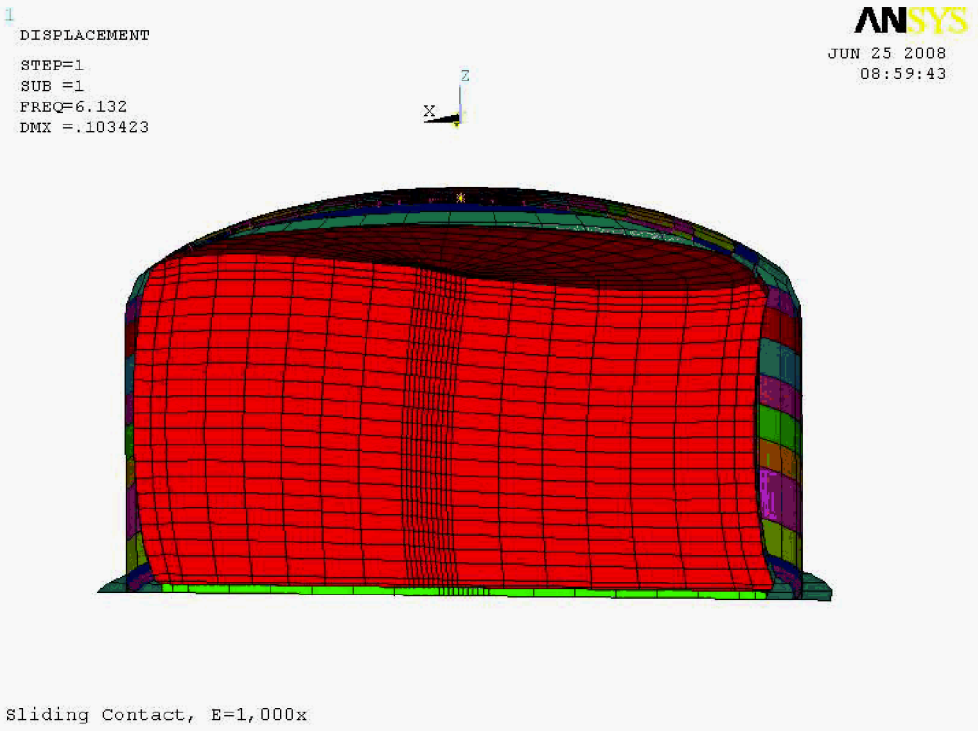

Figure 3.27. First Fundamental Mode for $G_{waste}=4.135 \times 10^7$ Pa with Sliding Contact

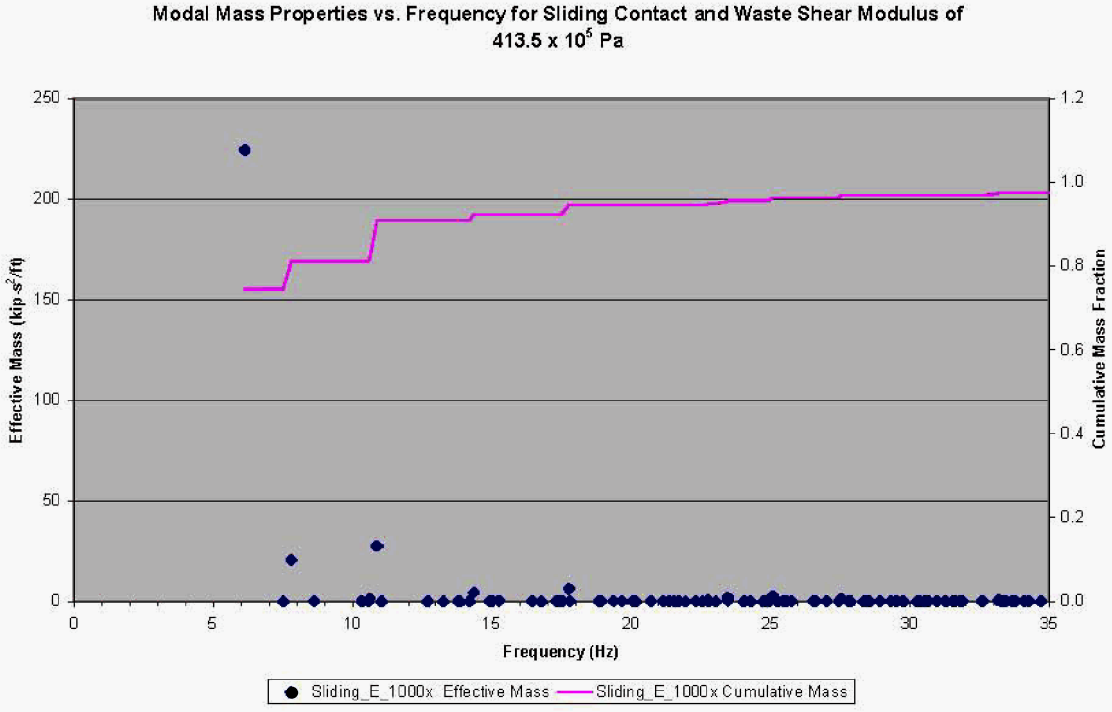

Figure 3.28. Natural Frequencies and Modal Masses for Sliding Contact and Waste Shear Modulus of 4.135×10^7 Pa (Lateral Direction Parallel to Symmetry Plane)

3.1.13 Bonded Contact G=4.135 x 10^7 Pa

This case is very similar to the case of sliding contact above except that the dominant structural frequency has increased from 6.1 Hz to 6.9 Hz. The fundamental mode shape is shown as Figure 3.29. Also, as shown in Figure 3.30 the threshold for 90% mass participation has increased from approximately 10 Hz up to approximately 20 Hz.

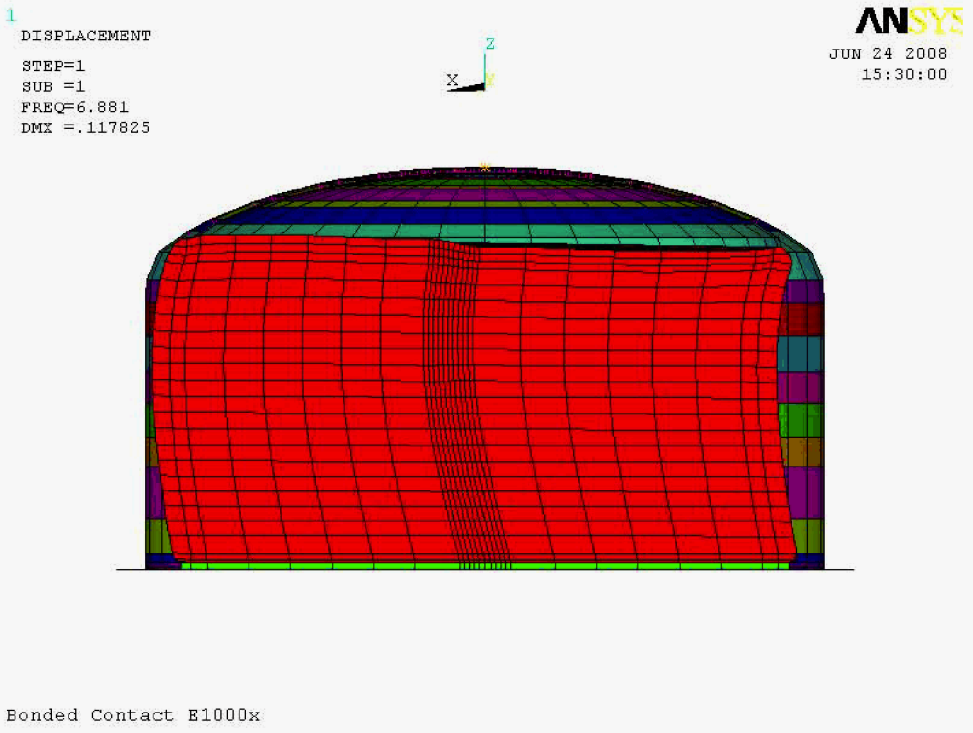

Figure 3.29. First Fundamental Mode for G_{waste}=4.135 × 10^7 Pa with Bonded Contact

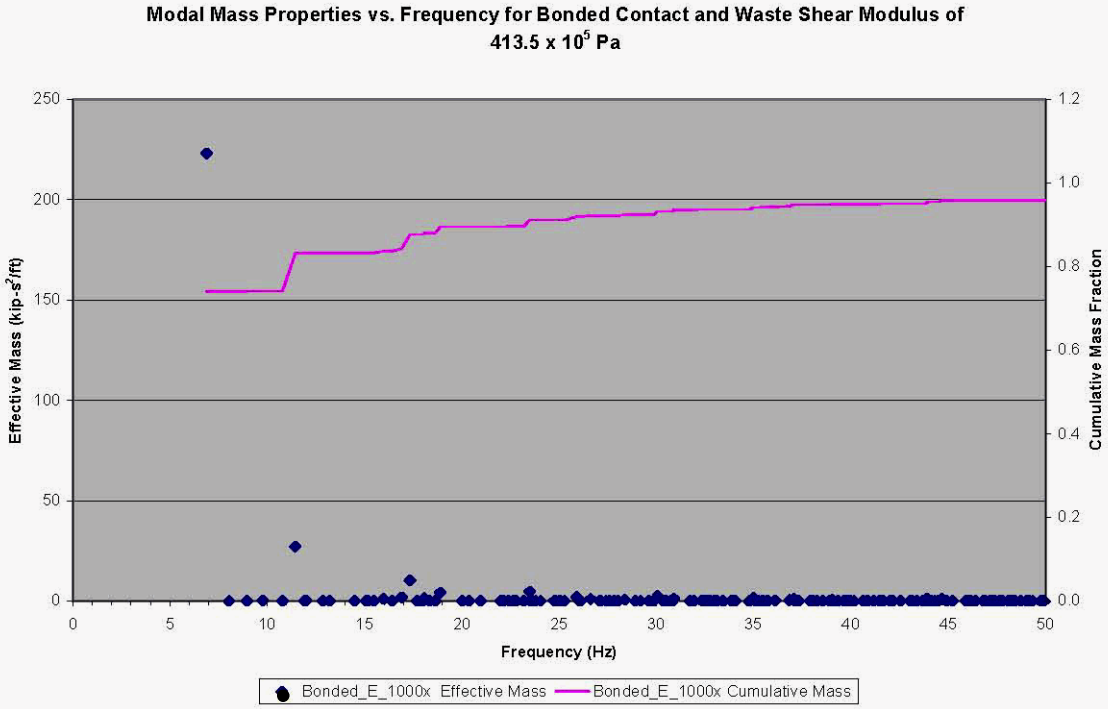

Figure 3.30. Natural Frequencies and Modal Masses for Bonded Contact and Waste Shear Modulus of 4.135×10^7 Pa (Lateral Direction Parallel to Symmetry Plane)

3.1.14 Sliding Contact G=4.135 × 10^8 Pa

In this case, the shear modulus is in the range of three to four orders of magnitude higher than expected for the tank waste and there is effectively a single significant structural frequency of 12.1 Hz. The associated mode shape is shown in Figure 3.31. Over 90% of the mass participates in this mode (see Figure 3.32).

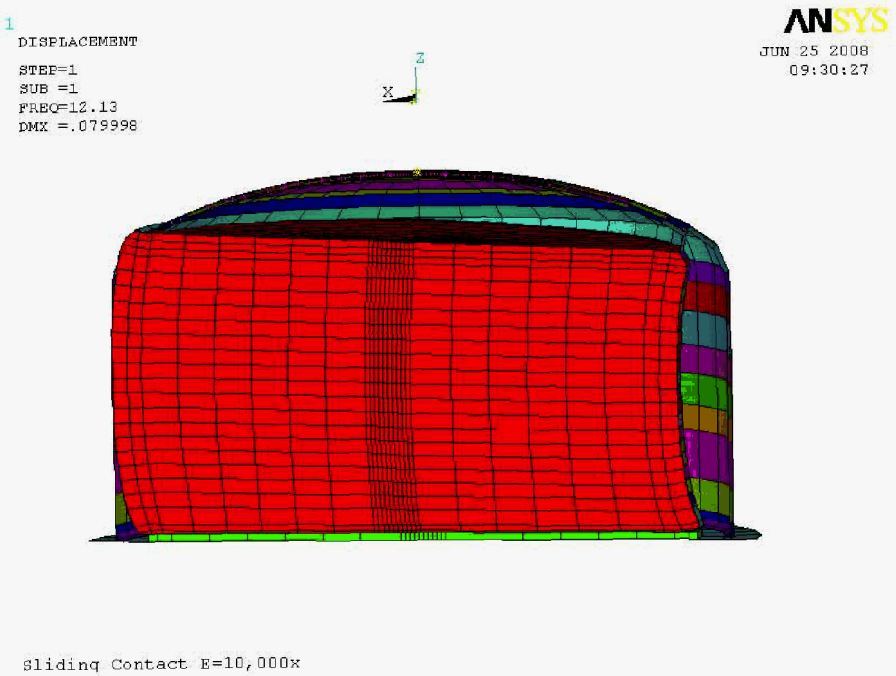

Figure 3.31. Single Significant Structural Mode Shape for Sliding Contact and Waste Shear Modulus of 4.135×10^8 Pa (Lateral Direction Parallel to Symmetry Plane)

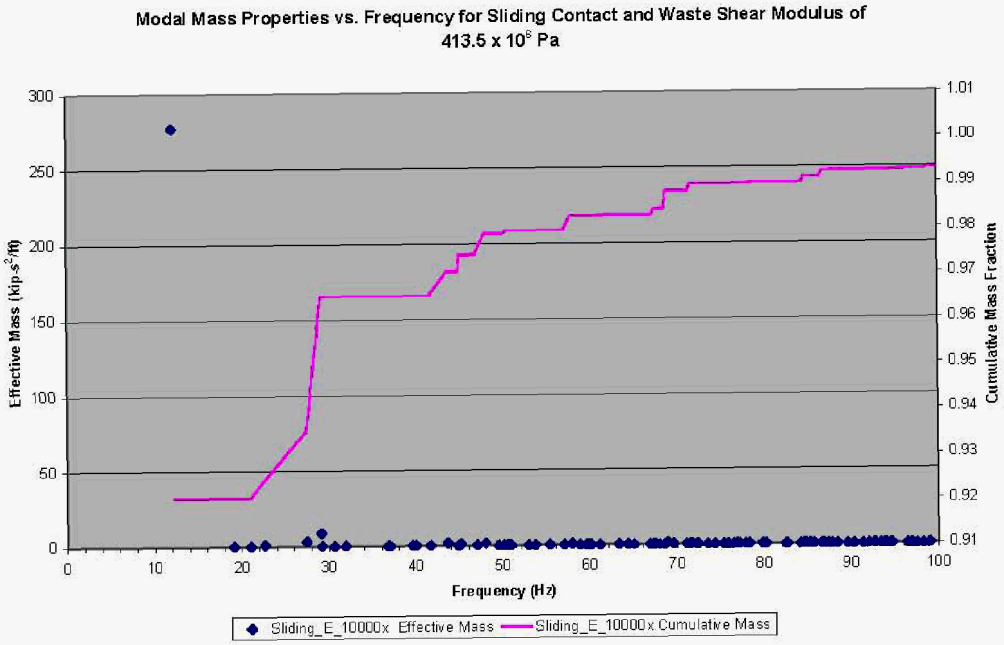

Figure 3.32. Natural Frequencies and Modal Masses for Sliding Contact and Waste Shear Modulus of 4.135×10^8 Pa (Lateral Direction Parallel to Symmetry Plane)

3.1.15 Bonded Contact G=4.135 x 10^8 Pa

With bonded contact, the structural frequency at this level of shear modulus increases to 15.3 Hz, and the associated mode shape is shown in Figure 3.33. As seen in Figure 3.34, slightly more than 80% of the mass participates in the first mode. With the bonded contact increasing the effective system stiffness, 90% mass participation does not occur until approximately 30 Hz.

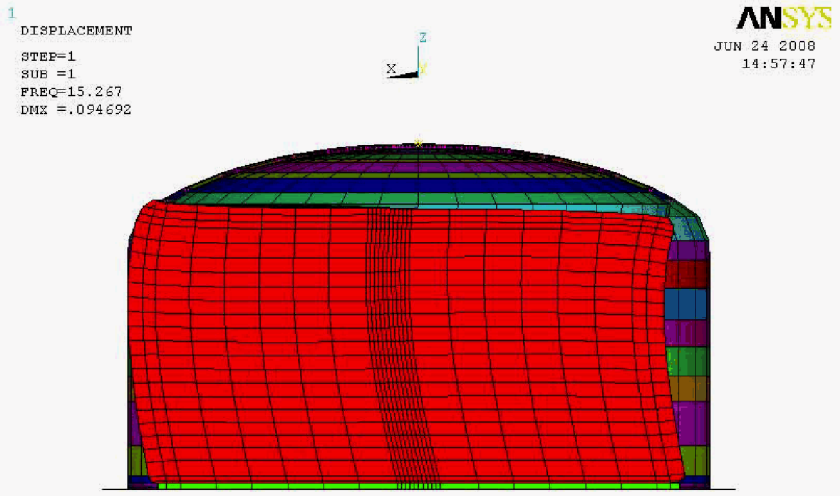

Figure 3.33. Single Significant Structural Mode Shape for Sliding Contact and Waste Shear Modulus of 4.135×10^8 Pa (Lateral Direction Parallel to Symmetry Plane)

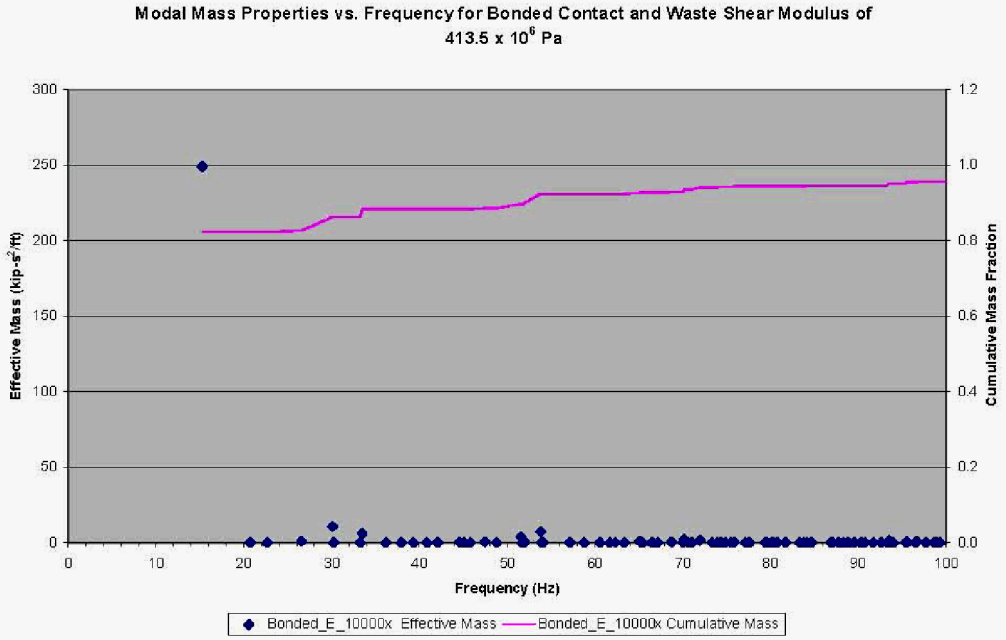

Figure 3.34. Natural Frequencies and Modal Masses for Bonded Contact and Waste Shear Modulus of 4.135×10^8 Pa (Lateral Direction Parallel to Symmetry Plane)

3.1.16 Bonded Contact G=4.135 x 10^9 Pa

With bonded contact at this level of material stiffness, the waste acts as an effectively rigid solid with a fundamental system frequency of 37.2 Hz. The associated mode shape is shown as Figure 3.35. As seen in Figure 3.36, 87% of the mass participates in the first mode, but 90% mass participation does not occur until approximately 95 Hz.

As a point of comparison, if the extensional modulus and shear modulus of the waste are increased to match the corresponding values for steel, approximately 93% of the mass participates in a fundamental mode at 71 Hz.

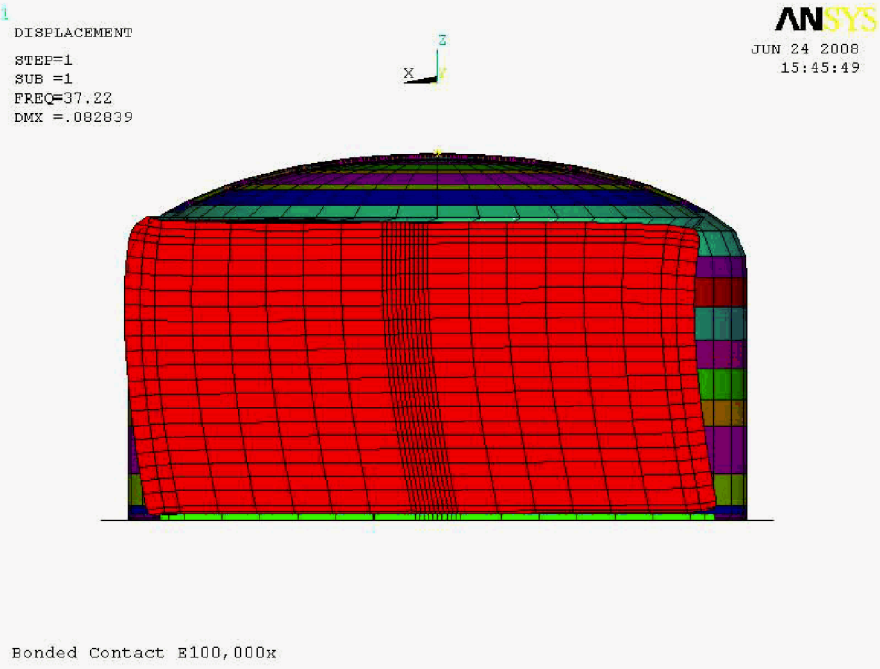

Figure 3.35. Single Significant Structural Mode Shape for Sliding Contact and Waste Shear Modulus of 4.135×10^8 Pa (Lateral Direction Parallel to Symmetry Plane)

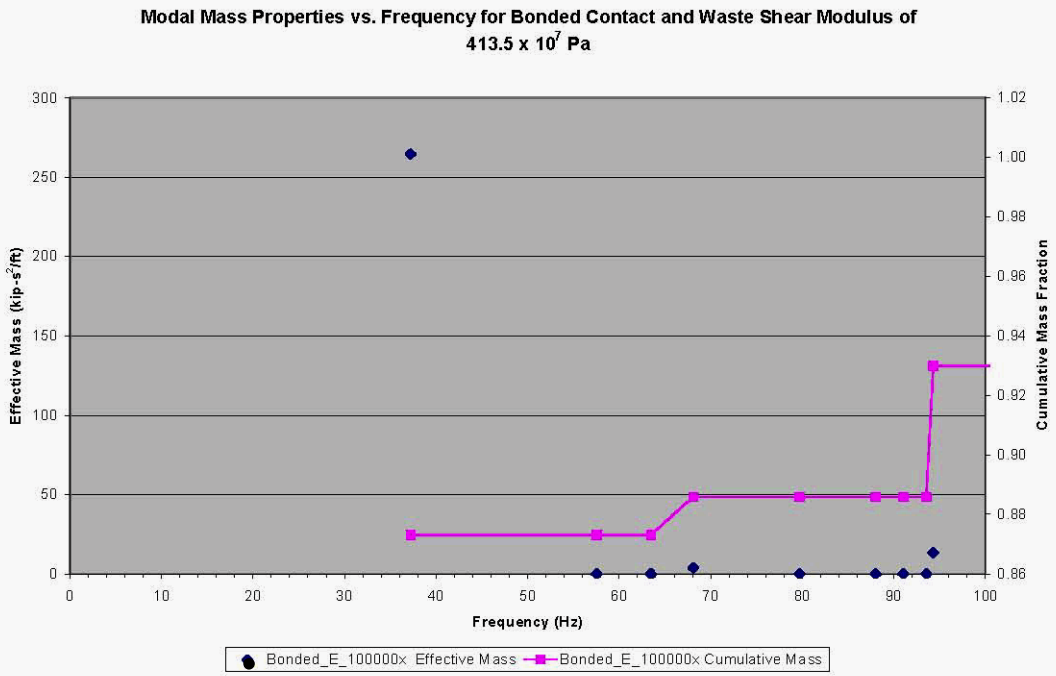

Figure 3.36. Natural Frequencies and Modal Masses for Bonded Contact and Waste Shear Modulus of 4.135×10^9 Pa (Lateral Direction Parallel to Symmetry Plane)

3.2 Comparisons of Modal Results

Figure 3.37 shows the dependence of the dominant convective and impulsive frequencies on the waste shear modulus for bonded and sliding contact conditions. The results emphasize that there is very little difference in impulsive frequency from 4,000 to 413,500 Pa waste shear modulus, although a single impulsive frequency becomes difficult to identify at 413,500 Pa shear modulus with bonded contact conditions as shown in Figure 3.23. The increase in the convective frequency from 0.2 to nearly 1 Hz, will tend to increase the peak horizontal reaction forces due to increased spectral accelerations for that mode, but the reactions will still be dominated by the impulsive response.

Figures 3.38 and 3.39 show the variation in the cumulative mass fraction distribution with waste shear modulus. The plots indicate graphically that there is little difference between the modal mass participation when the shear modulus ranges from 4,000 Pa to 40,000 Pa., but that a noticeable transition to more solid-like behavior occurs at higher values of the waste stiffness. Figures 3.40 and 3.41 show only the three curves for 4,000 Pa, 22,000 Pa, and 40,000 Pa to emphasize that the modal properties are very nearly the same when the waste shear modulus varies within this range.

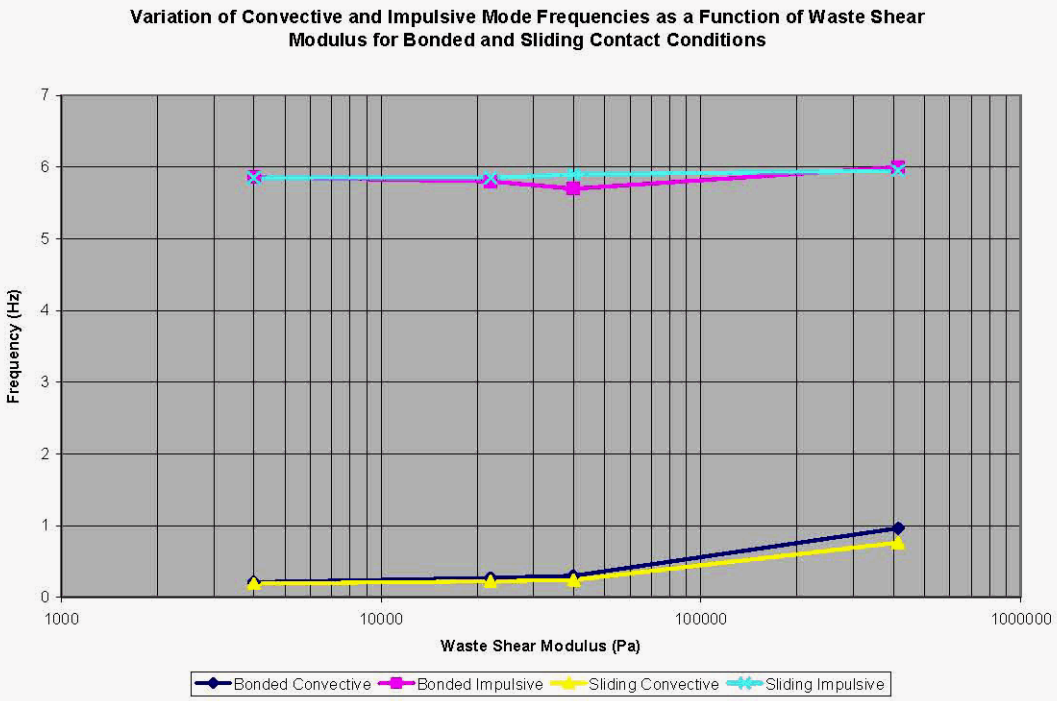

Figure 3.37. Variation of Modal Frequencies as a Function of Waste Shear Modulus for Bonded and Sliding Contact Conditions

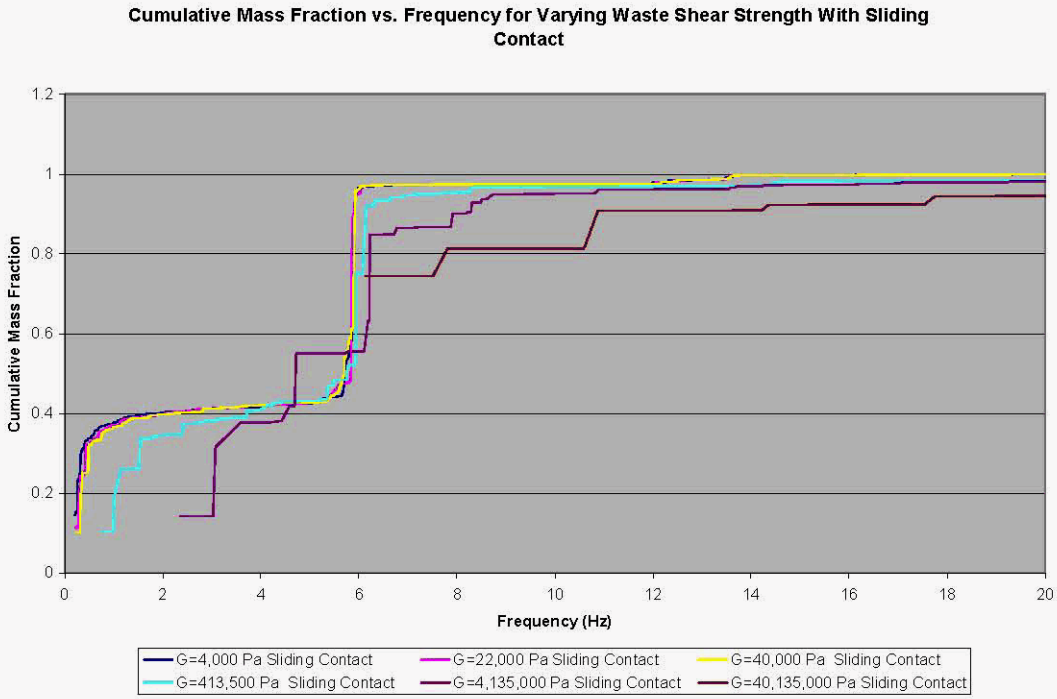

Figure 3.38. Variation of Cumulative Mass Fraction Distribution with Waste Shear Strength for Sliding Contact

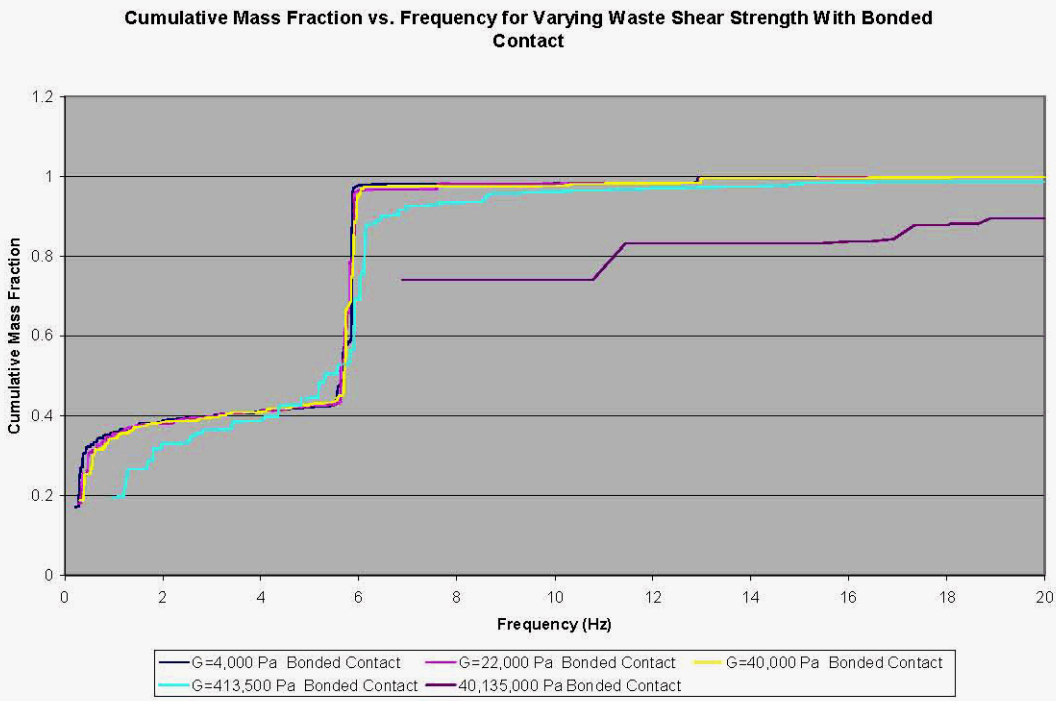

Figure 3.39. Variation of Cumulative Mass Fraction Distribution with Waste Shear Strength for Bonded Contact

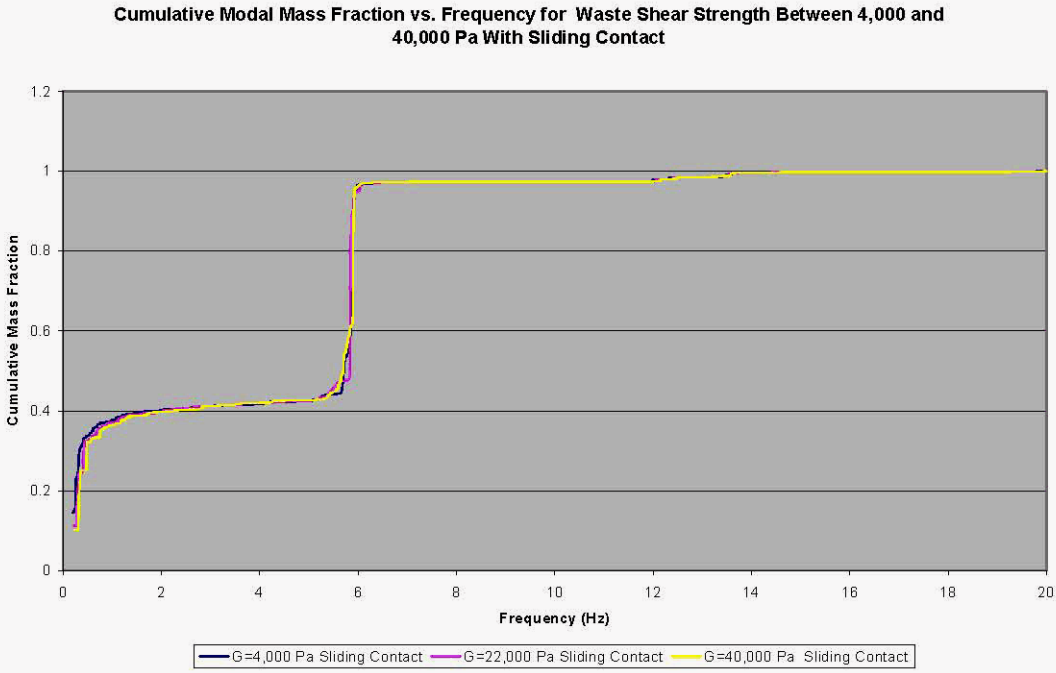

Figure 3.40. Cumulative Modal Mass Fraction vs. Natural Frequency for Waste Shear Strengths Between 4,000 and 40,000 Pa with Sliding Contact

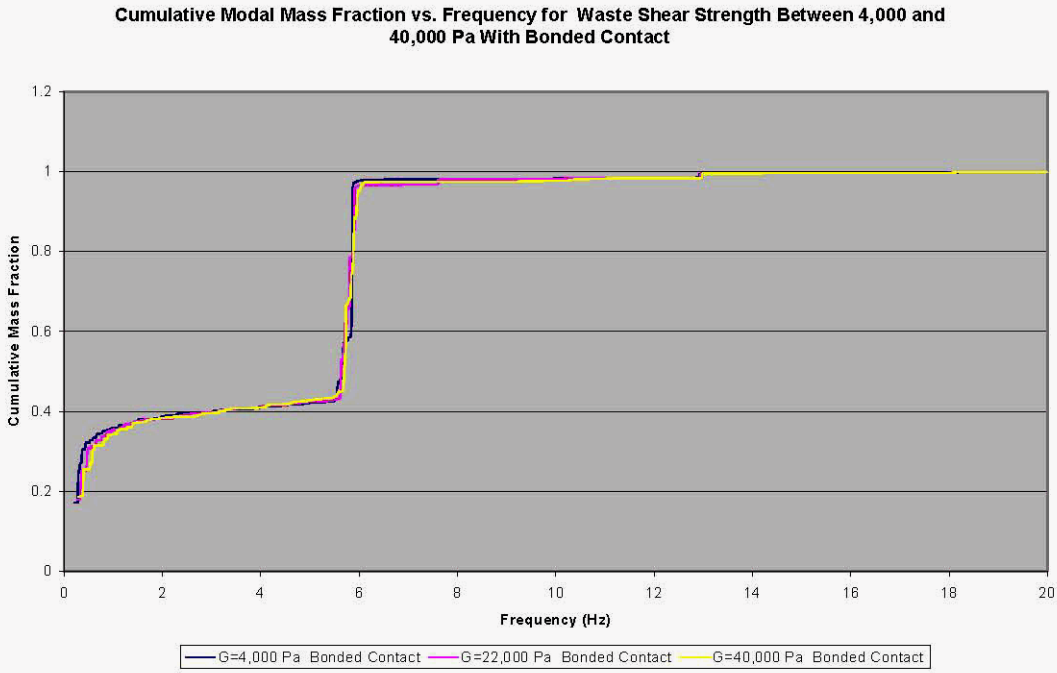

Figure 3.41. Cumulative Modal Mass Fraction vs. Natural Frequency for Waste Shear Strengths Between 4,000 and 40,000 Pa with Bonded Contact

Summaries of the cutoff frequencies and participating mass fractions for the lateral and vertical directions are shown in Table 3.2 and Table 3.3, respectively. The important point to note regarding Table 3.2 is that at least 97% of the mass of the flexible portion of the system participates in the modal analyses in the lateral direction. This means that there is effectively no difference between cumulative mass fractions for the lateral direction that are shown in the plots in this chapter (which are based on the total participating mass) and cumulative mass fractions based on the mass of the flexible portion of the system. In the vertical direction, the participating mass is approximately 2/3 of the flexible mass of the system up to the cutoff frequency.

Table 3.2. Cutoff Frequencies and Participating Modal Mass Fractions for Lateral Direction

Case Name (Shear Modulus)	Cutoff Frequency (Hz)	Sum of Effective Mass Up to Cutoff Frequency (kip-s^2/ft)	Mass of Flexible Portion of System for Half-Model (kip-s^2/ft)	Mass Participation Up to Cutoff Frequency (%)
Bonded_0839 (4,000 Pa)	25.3	294.282	303	97.1
Bonded_464 (22,000 Pa)	25.5	294.285	303	97.1
Bonded_839 (40,000 Pa)	25.8	294.291	303	97.1
Bonded_E10x (413,500 Pa)	57.6	295.408	303	97.5
Bonded_E1000x (4.135×10^7 Pa)	340.0	301.027	303	99.3
Bonded_E10000x (4.135×10^8 Pa)	912.2	302.740	303	99.9
Bonded_E100000x (4.135×10^9 Pa)	2671.3	302.996	303	100
Sliding_0839 (4,000 Pa)	20.6	297.935	303	98.3
Sliding_464 (22,000 Pa)	21.0	297.940	303	98.3
Sliding_839 (40,000 Pa)	21.4	297.951	303	98.3
Sliding_E10x (413,500 Pa)	63.4	299.275	303	98.8
Sliding_E100x (4.135×10^6 Pa)	50.5	296.718	303	97.9
Sliding_E500x (2.07×10^7 Pa)	59.7	298.245	303	98.4
Sliding_E1000x (4.135×10^7 Pa)	307.2	301.226	303	99.4
Sliding_E10000x (4.135×10^8 Pa)	234.8	301.116	303	99.4
Capped Bonded_464 (22,000 Pa)	27.35	293.858	303	97.0

Table 3.3. Cutoff Frequencies and Participating Modal Mass Fractions for Vertical Direction

Case Name (Shear Modulus)	Cutoff Frequency (Hz)	Sum of Effective Mass Up to Cutoff Frequency (kip-s^2/ft)	Mass Participation Up to Cutoff Frequency (%)	Breathing Mode Frequency (Hz)
Bonded_0839 (4,000 Pa)	25.3	208.503	69	5.0
Bonded_464 (22,000 Pa)	25.5	208.551	69	5.0
Bonded_839 (40,000 Pa)	25.8	208.599	69	5.0
Bonded_E10x (413,500 Pa)	57.6	203.421	67	Multiple significant frequencies from 5.0 to 5.6
Sliding_0839 (4,000 Pa)	20.6	208.745	69	5.0
Sliding_464 (22,000 Pa)	21.0	208.795	69	5.0
Sliding_839 (40,000 Pa)	21.4	208.822	69	5.0
Sliding_E10x (413,500 Pa)	63.4	205.082	68	5.3

4.0 Seismic Input

Two forms of seismic excitation were considered in this study. The first was seismic motion extracted from the global model of the DST described in Chapter 2 of Rinker and Abatt (2008a). The second was surface free-field motion for the Hanford Waste Treatment Plant (WTP) Site. Each time history is defined by 2,048 points at 0.01-second intervals over a total duration of 20.48 seconds.

In ANSYS® a large mass is required at the location of excitation to properly reproduce the seismic input. This mass was located at the apex of the concrete shell of the sub-model described in Chapter 2.0. The boundary conditions of the node at the apex are adjusted depending on the direction of excitation.

In each case, the same excitations were applied to all rigid elements simultaneously. That is, the top and bottom of the tank were excited together with the same seismic time history. The model configuration is the same as for the modal analyses. The model configuration is considered to be represented by the hinged top boundary condition discussed in BNL (1995) and shown in Figure 4.1.

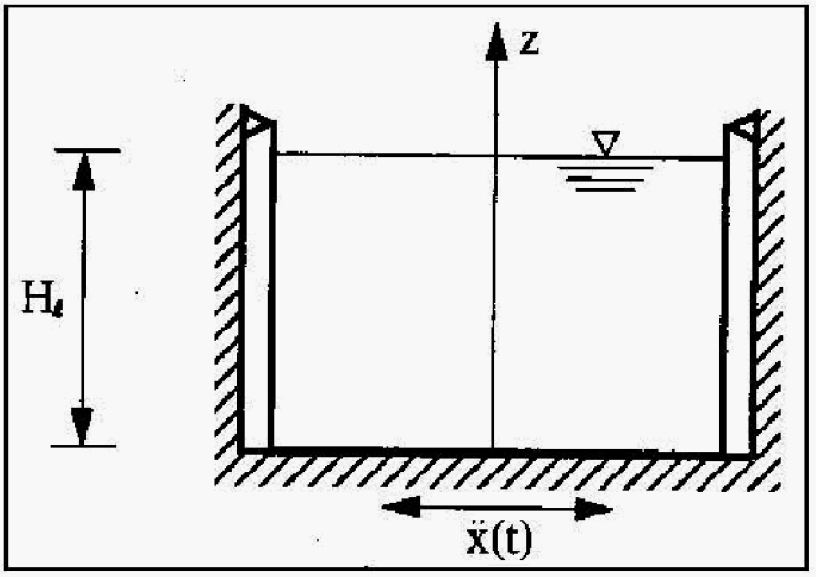

Figure 4.1. Tank with Hinged Top Boundary Condition per BNL (1995)

4.1 Seismic Motion Extracted from the Global DST Model

There are several choices for extracting in-structure motion from the global model of the DST. The global model was run with properties corresponding to lower-bound soil (LBS), best-estimate soil (BES), and upper-bound soil (UBS). Each case of soil properties will lead to different in-structure seismic motion. The in-structure seismic motion from the global model also depends, of course, on the point in the structure at which the motion is extracted. The in-structure motion used to excite the sub-model is foundation-level motion for the best-estimate soil case. Response spectra for the other two soil cases as well as for the best-estimate soil case at the dome apex are presented for comparison.

The global model described in Section 2.0 of Rinker and Abatt (2008a) was subjected to simultaneous horizontal and vertical input. The time history used as input to the sub-model was taken from node 495 in the concrete basemat of the global ANSYS® model as shown in Figure 4.2 and Figure 4.3. As shown in those figures, node 495 lies at the junction between the bottom of the concrete wall and the basemat 90° from the plane of horizontal excitation in the negative y-direction. Note that in Figure 4.2 and Figure 4.3, the tank wall elements near node 495 have been omitted from the plot for ease of visualization.

4.1.1 Foundation Response Spectrum Best-Estimate Soil, Best-Estimate Concrete (BES-BEC) Case

The horizontal acceleration, vertical acceleration, and the velocity and displacement time histories for horizontal and vertical input in the case of best-estimate soil, best-estimate concrete (BES-BEC) are shown in Figures 4.4, 4.5, 4.6, and 4.7, respectively. In all cases, the responses are extracted at node 495 on the basemat of the global model. The 4% damped response spectra for the horizontal and vertical time histories are shown in Figure 4.8, where the acceleration shown is the pseudo-acceleration.

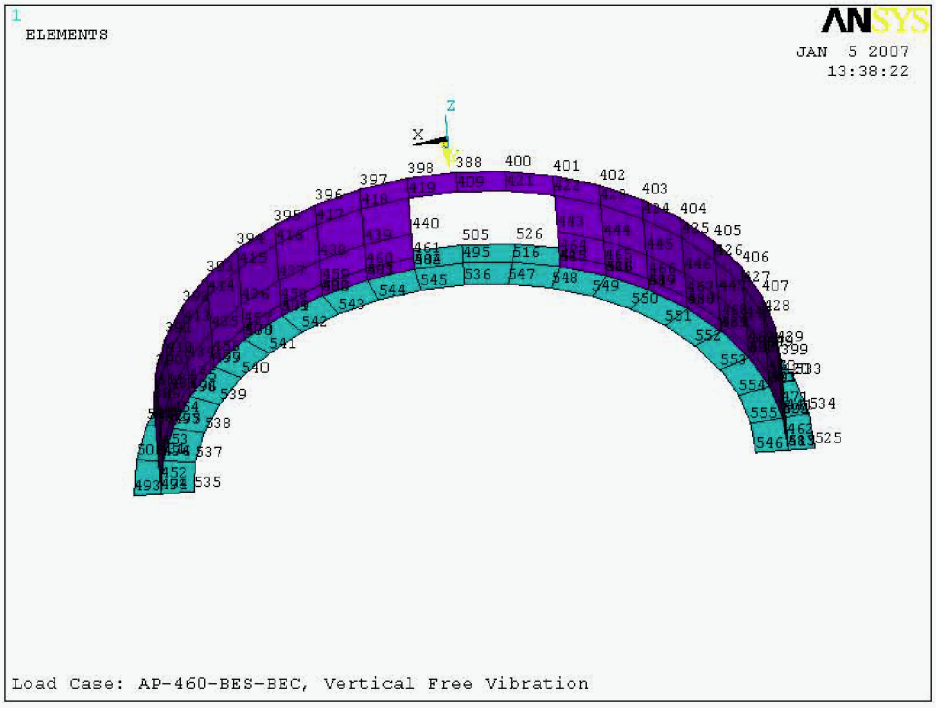

Figure 4.2. Plot of Location of Node 495 at Junction of Concrete Wall and Concrete Basemat from Global ANSYS® Model

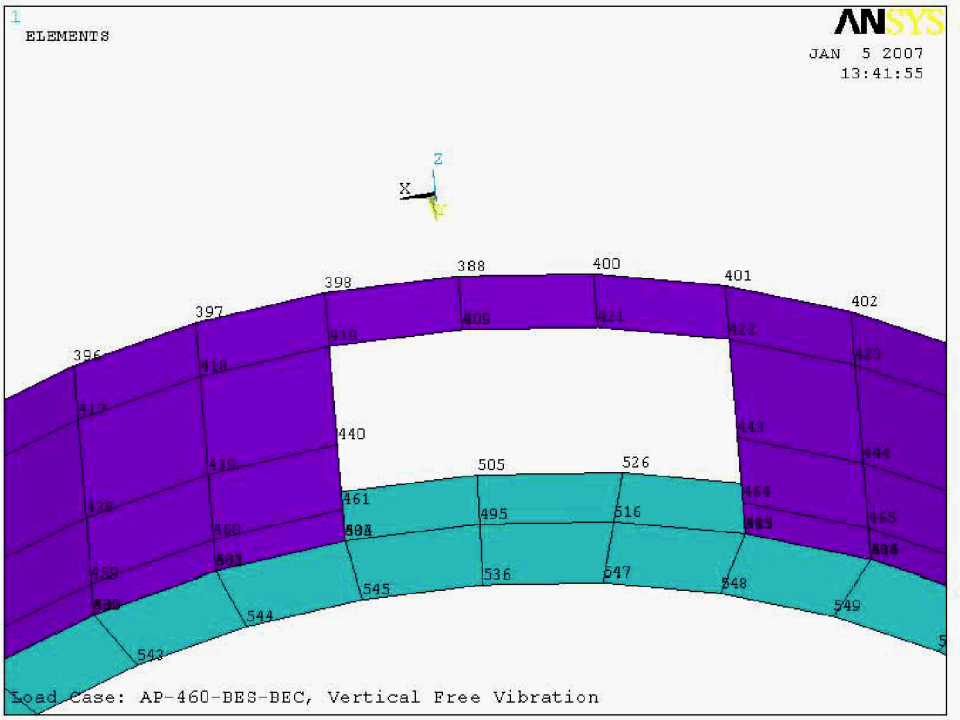

Figure 4.3. Detailed Plot of Location of Node 495 at Junction of Concrete Wall and Concrete Basemat from Global ANSYS® Model

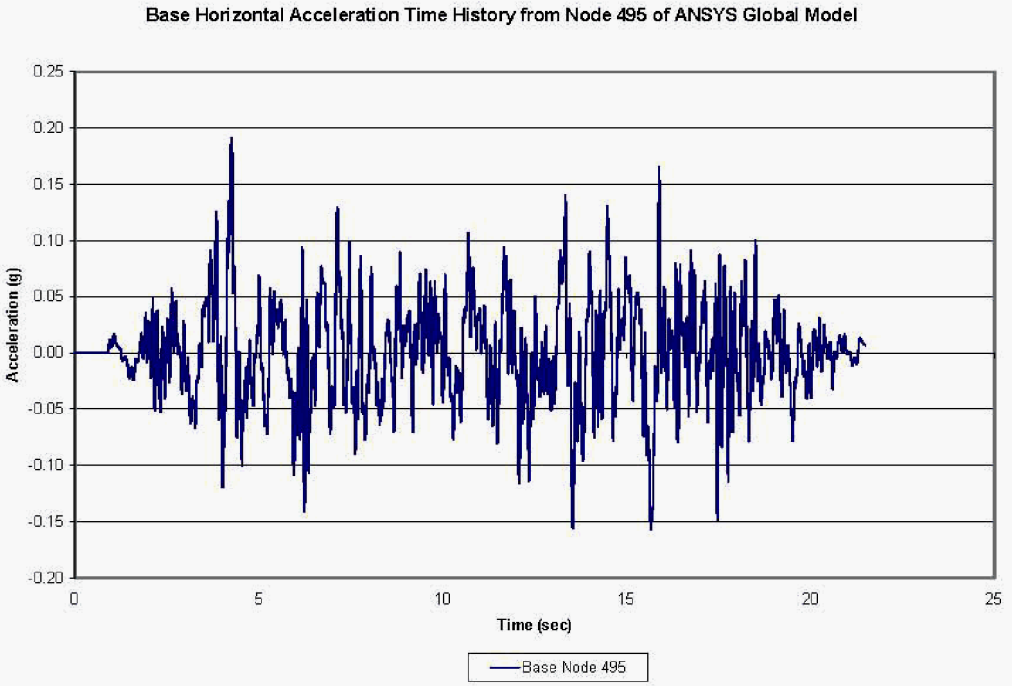

Figure 4.4. BES-BEC Horizontal Acceleration Time History from Basemat Node 495

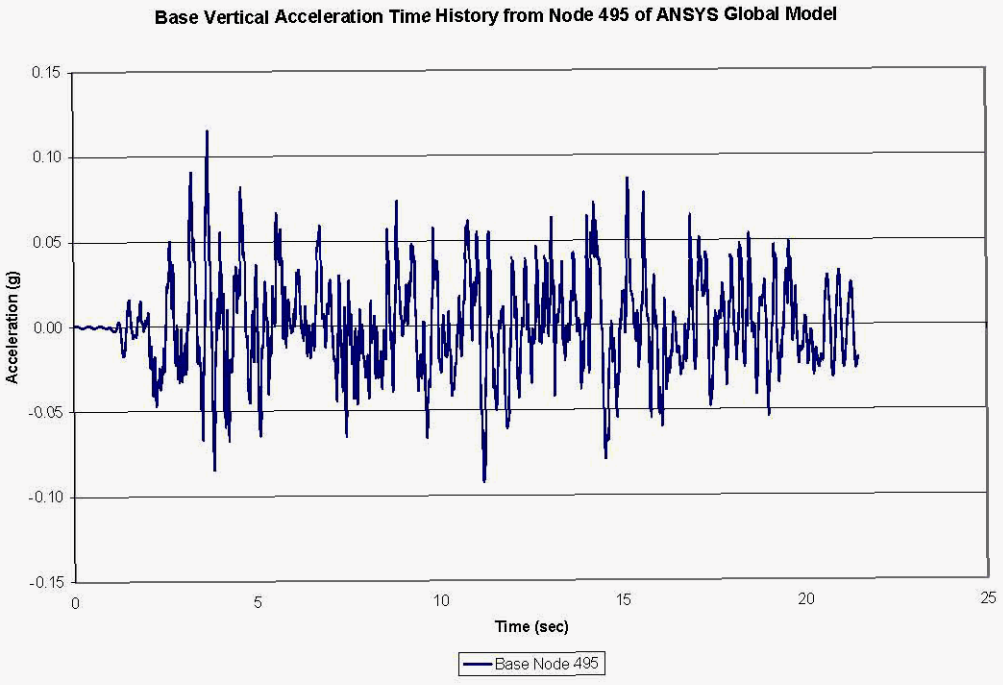

Figure 4.5. BES-BEC Vertical Acceleration Time History from Basemat Node 495

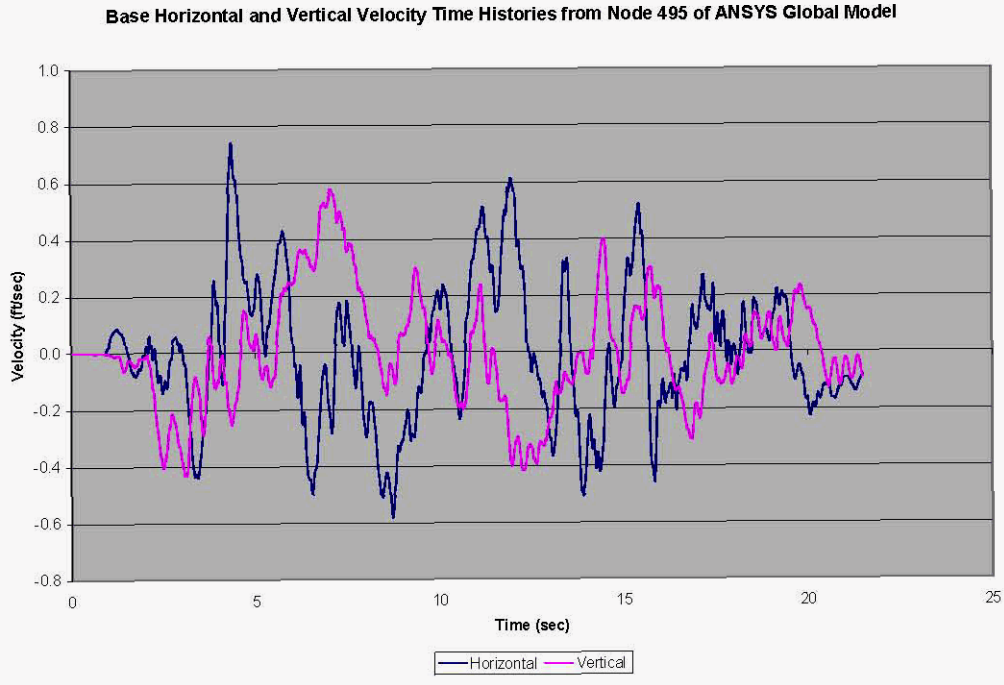

Figure 4.6. BES-BEC Horizontal and Vertical Velocity Time Histories from Basemat Node 495

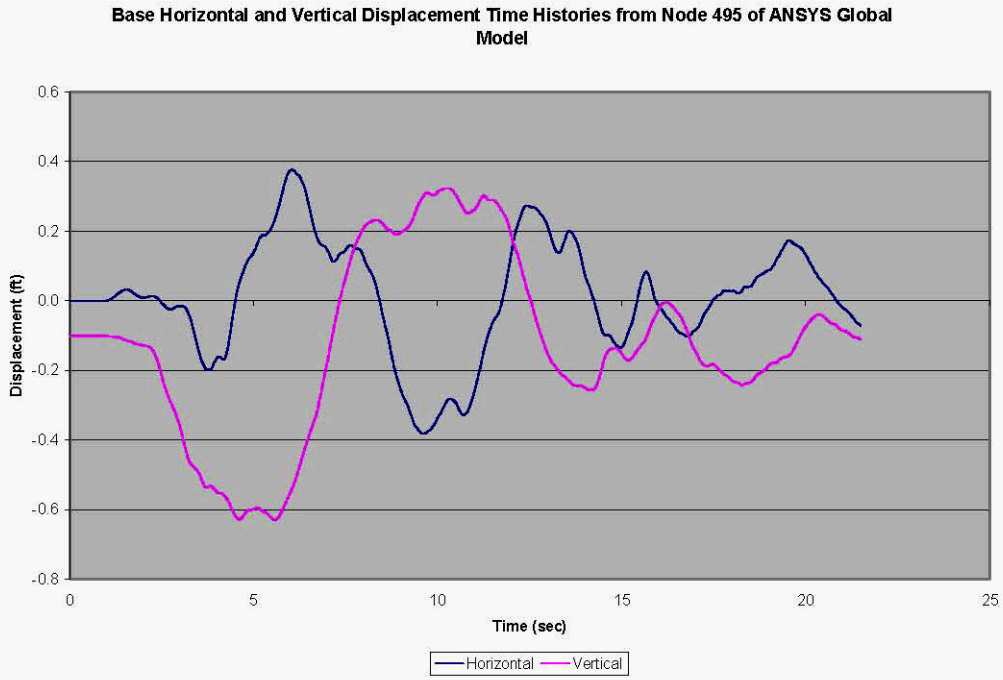

Figure 4.7. BES-BEC Horizontal and Vertical Displacement Time Histories from Basemat Node 495

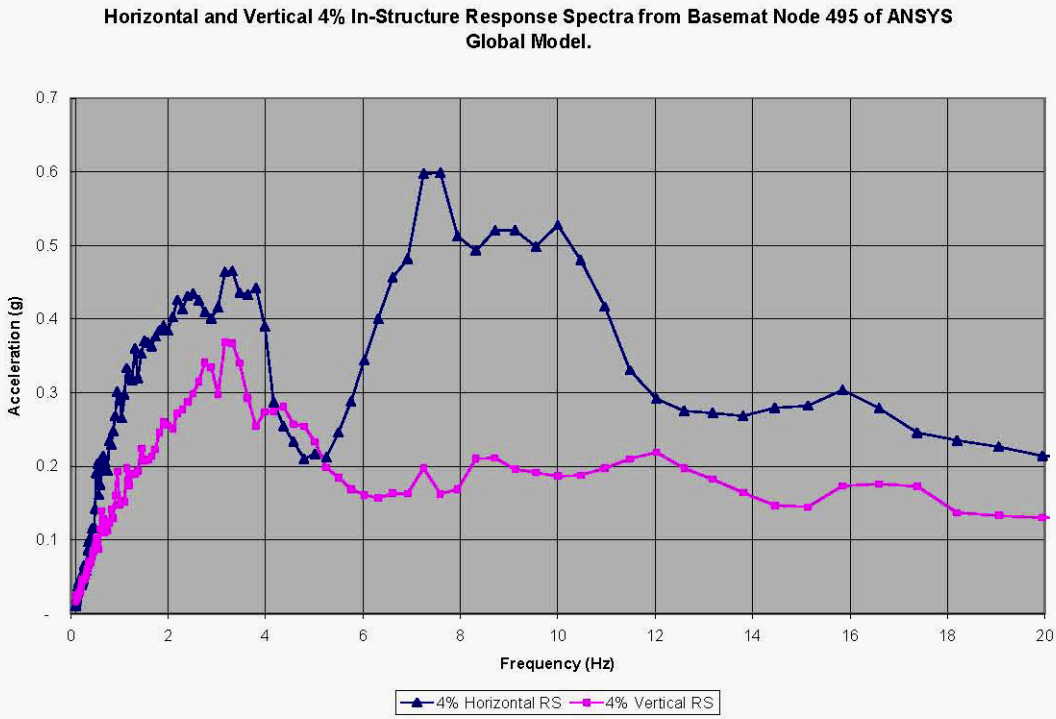

Figure 4.8. 4% Damped Response Spectra for Acceleration Time Histories Extracted from Basemat Node 495 of BES-BEC Global ANSYS® Model

4.1.2 Foundation Response Spectra for Lower-Bound Soil, Best-Estimate Concrete (LBS-BEC) and Upper-Bound Soil, Best-Estimate Concrete (UBS-BEC) Cases

The previous section presented seismic motions extracted from the tank basemat of the global model for the BES-BEC case when that model was excited with both horizontal and vertical input motions. Different soil conditions as well as input extracted from different locations on the tank structure will lead to different reaction forces from the sub-model. The 4% horizontal and vertical response spectra for the motion determined at basemat node 495 for the LBS and UBS cases are shown in Figures 4.9 and 4.10. As before, the spectra are in terms of the pseudo -acceleration. A comparison of the horizontal spectra for the lower-bound, best-estimate, and upper-bound soil cases in shown in Figure 4.11 along with the enveloping spectrum for the three cases. The corresponding vertical spectra are shown in Figure 4.12.

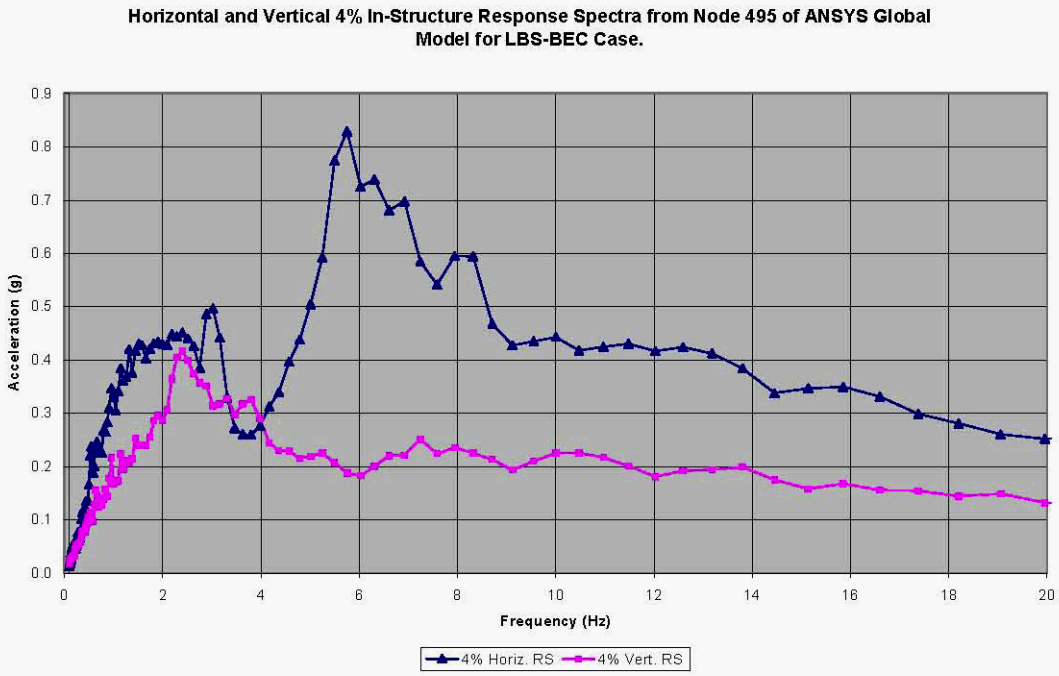

Figure 4.9. 4% Damped Response Spectra for Acceleration Time Histories Extracted from Basemat Node 495 of Lower-Bound Soil, Best-Estimate Concrete (LBS-BEC) Global ANSYS® Model

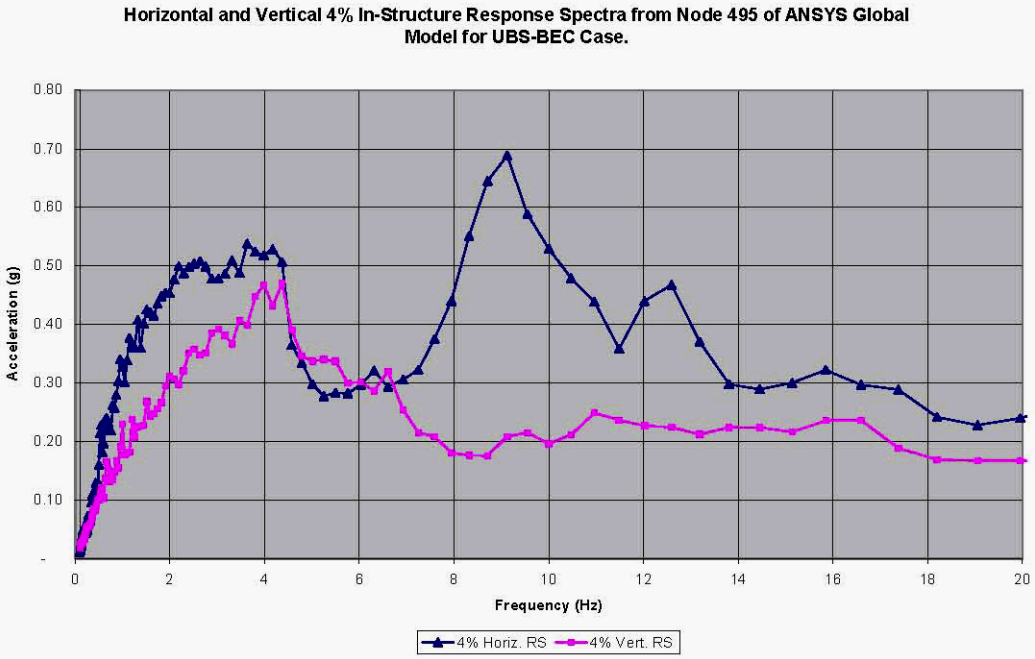

Figure 4.10. 4% Damped Response Spectra for Acceleration Time Histories Extracted from Basemat Node 495 of Upper-Bound Soil, Best-Estimate Concrete (UBS-BEC) Global ANSYS® Model

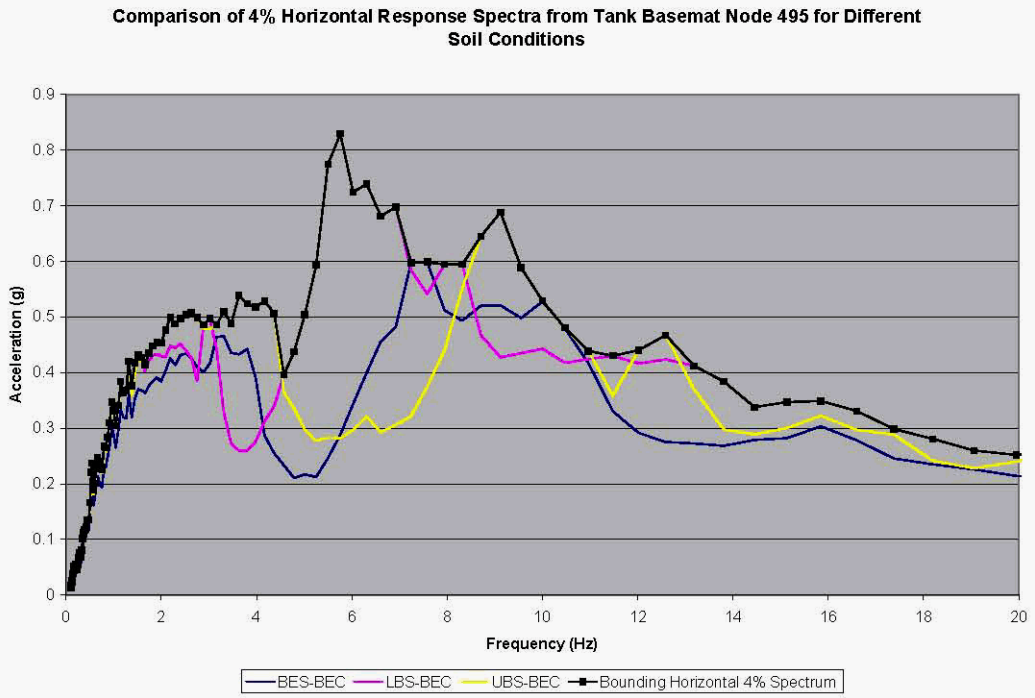

Figure 4.11. Comparison of 4% Damped Horizontal Response Spectra for LBS-BEC, BES-BEC, UBS-BEC Cases

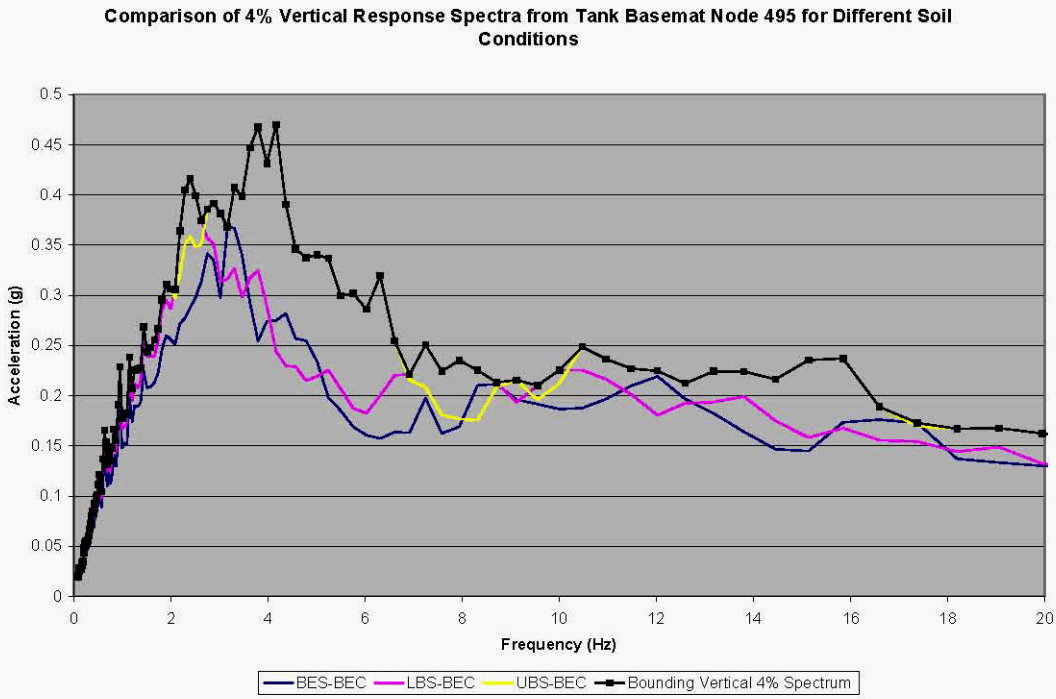

Figure 4.12. Comparison of 4% Damped Vertical Response Spectra for LBS-BEC, BES-BEC, UBS-BEC Cases

4.1.3 Dome Apex Spectrum for the BES-BEC Case

It was mentioned in the previous section that the motions extracted from different points on the tank structure will lead to different reaction forces when applied to the sub-model used in this study. A comparison of the tank basemat horizontal spectrum and the dome apex horizontal spectrum from the global model for the BES-BEC condition is shown as Figure 4.13. Clearly the differences in accelerations for frequencies in the range of 5 to 6 Hz are important and can have a dramatic effect on the tank demands. It has not been determined in this study which of the two spectra provides the better representation of the actual seismic input to a DST. Although the differences are less important for a comparative study of the effects of waste properties, they are important for determining true tank demands.

It should also be recognized that differences between in-structure response spectra (ISRS) at different points on the tank are handled naturally when performing a time-history analysis using the global model. That is, this issue is specific to using the tank sub-model, but it does not affect the results of the seismic analysis of record using the global model.

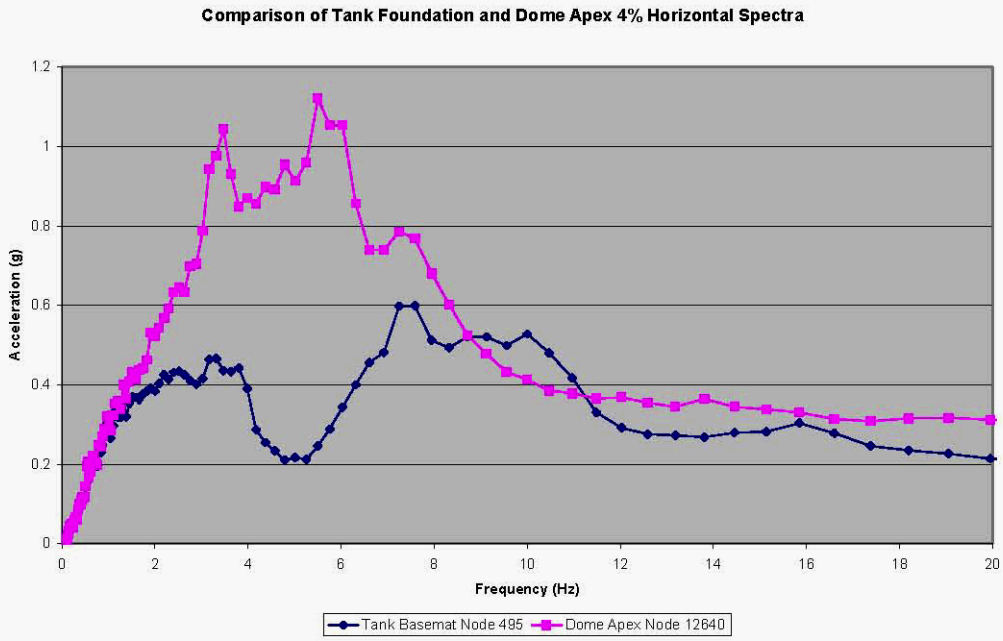

Figure 4.13. Comparison of Horizontal In-Structure Response Spectra from Basemat and Dome Apex of BES-BEC Global Model

4.2 Hanford Waste Treatment Plant Free-Field Surface Motion

The soil conditions used in the global model, the locations at which in-structure responses are extracted from the global model for use as input to the sub-model, and the waste properties used in the sub-model all affect the responses of the sub-model and it is instructive to estimate the relative sensitivity of the results to the different variables. The focus of this study is on the sensitivity of the sub-model response to the waste properties. One way to help isolate the effects of the waste properties on the sub-model response is to excite the sub-model using smooth input. As shown in Figure 4.13, the ISRS extracted from the basemat and dome apex have peaks and valleys that make it difficult to separate the changes in response due to waste properties from the changes in response due to varying seismic accelerations.

The representative excitation for the primary tank and waste system will be a combination of excitations at various locations on the supporting concrete vault. It is also reasonable to consider input to the sub-model that is a combination of basemat and dome apex excitation. A time history that is represented by a response spectrum that is the average of a basemat spectrum and a dome apex spectrum is a reasonable input to the sub-model and the averaging process may help to smooth out the peaks and valleys in the two individual spectra. A plot the basemat spectrum and dome apex spectrum along with the point-by-point average of the two is shown in Figure 4.14.

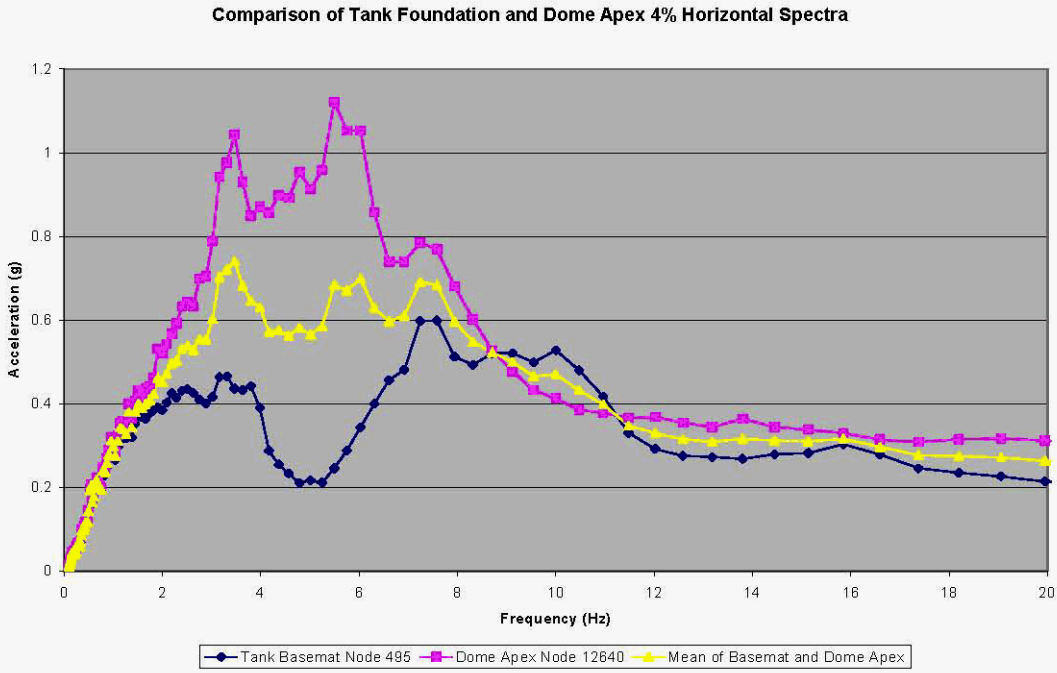

Figure 4.14. Comparison of Horizontal In-Structure Response Spectra from Basemat and Dome Apex of BES-BEC Global Model Showing the Average of the Basemat and Dome Spectra

The mean spectrum shown is somewhat smoother than the individual spectra, but it still shows undesirable variation in the important structural frequency range of 3 to 8 Hz.

The fourth curve shown in Figure 4.15 is the 4% damped horizontal response spectrum corresponding to a surface free-field time history developed for design at the Hanford Waste Treatment Plant (WTP). As seen in the plot, this spectrum provides a smoothed average of the basemat and dome spectra, at least up to approximately 10 Hz. Consequently, the corresponding time history is used for determining the sensitivity of the tank response to variations in waste properties.

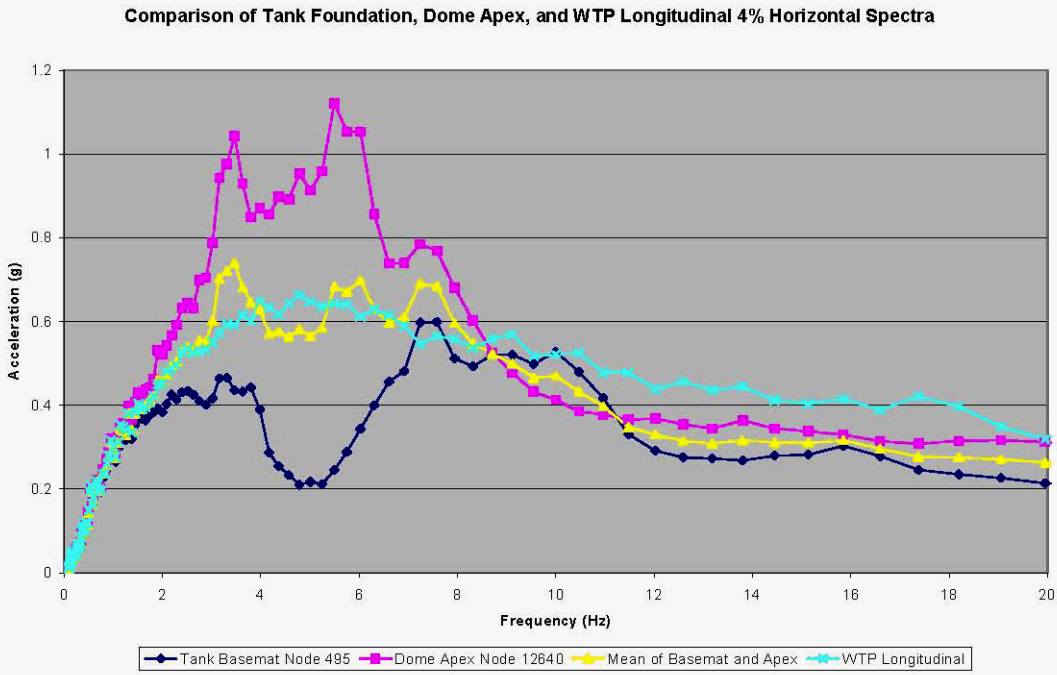

Figure 4.15. Comparison of Tank Foundation, Dome Apex, and WTP Longitudinal 4% Damped Response Spectra

Intentionally left blank.

5.0 Global Reaction Forces Estimated from Modal Analysis and Response Spectrum

The peak reaction forces can be approximated by determining the products of the effective masses and spectral accelerations for the dominant structural frequencies.

In cases where clearly identifiable convective and impulsive modes exist, the impulsive mode will be the dominant contributor to global reaction forces due to the relatively low spectral accelerations associated with the low-frequency convective mode. A lower bound single-term approximation to the peak reaction force (F_{peak}) can be expressed as

$$F_{peak} \cong (m_{eff})(SA),$$

where m_{eff} is the effective mass for the dominant structural frequency and SA is the associated spectral acceleration. A single-term approximation is not appropriate when multiple significant modes exist.

The above approximation amounts to a simplified single-term response spectrum analysis, but it is useful as a "quick and dirty" tool for estimating peak forces for different configurations based on modal results and input spectra. Differences between the above approximation and a time-history analysis are that a single damping value is assumed in the above approximation, not all modes are included in the above approximation, and missing mass is not accounted for in the above approximation. The latter point is insignificant for estimating the peak horizontal reaction force since almost all of the system mass participates in the horizontal direction below the modal cutoff frequencies.

Based on the damping characterization reported in Rinker and Abatt (2008b) for the AP Tank sub-model, the 4% spectral acceleration curves are used to estimate the peak reaction force. Reaction forces are estimated using both the basemat spectrum and the WTP spectrum shown in Figure 4.15. The estimated reaction forces are shown in Table 5.1.

One significant feature of the table is that the participating mass for the dominant structural mode is shown separately from the spectral acceleration. This provides insight into how much of the change in peak reaction force is due to a change in modal properties, and how much is due to a change in spectral acceleration.

As a point of comparison, the maximum horizontal reaction force from the BES-BEC global model of an AP Tank (using a waste shear modulus of 22,000 Pa and sliding interface conditions) excited with both horizontal and vertical motions as described in Rinker and Abatt (2008a) is 5,004 kips (when doubled to account for half-symmetry). This is more than the value of 3,025 kips estimated from the basemat spectral acceleration, but less than the value of 6,098 kips estimated from the WTP spectrum. This suggests that the driving motion for the primary tank lies between these two spectra.

Table 5.1. Estimated Peak Horizontal Reaction Forces

Case Name (Shear Modulus)	Dominant Frequency (Hz)	Percent Mass Participation in Dominant Mode	Effective Mass in Dominant Mode (kip-s^2/ft)	Spectral Acceleration in Dominant Mode from Figure 4.16 (g)		Estimated Peak Horizontal Reaction Force (kip)[a]	
				Basemat Spectrum	WTP Spectrum	Basemat Spectrum	WTP Spectrum
Bonded_464 (22,000 Pa)	5.8	50	151.5	0.29	0.635	2,824	6,184
Bonded_839 (40,000 Pa)	5.7	50	151.5	0.28	0.64	2,731	6,242
Bonded_E10 (413,500 Pa)	6.0	35	106.05	0.34	0.61	2,322	4,166
Capped Bonded_464 (22,000 Pa)	4.7	95	287.85	0.22	0.65	4,078	12,049
Sliding_0839 (4,000Pa)	5.85	50	151.5	0.31	0.625	3,025	6,098
Sliding_464 (22,000 Pa)	5.85	50	151.5	0.31	0.625	3,025	6,098
Sliding_839 (40,000 Pa)	5.9	50	151.5	0.32	0.62	3,123	6,050
Sliding_E10x) (413,500 Pa)	5.95	0.45	136.35	0.33	0.615	2,898	5,400

(a) Nominal reaction force doubled to account for half-symmetry model.

5.1 Interpretation of Critical Tank Responses in the Context of Modal Results

Critical responses of the system depend on the modal properties and the seismic input. So far, the report focused mostly on the modal properties because these are inherent to the system and are independent of the seismic input. The modal analysis has shown that if the shear modulus is less than 40,000 Pa, the natural frequencies of the system agree closely with the convective and impulsive frequencies of the equivalent liquid-containing system. For this effectively two-mode system, the global reactions are dominated by the impulsive response owing to the relatively small convective spectral accelerations.

It was shown that a lower bound approximation for the peak reaction force (F_{peak}) is given by

$$F_{peak} \cong (m_{eff})(SA),$$

where m_{eff} is the effective mass for the impulsive frequency and SA is the associated spectral acceleration.

Ground motion that is represented by a response spectrum that varies smoothly over the range of impulsive frequencies (or one that is constant over the range of impulsive frequencies, such as a design spectrum) will show that the peak force is nearly proportional to the effective mass in the dominant structural mode.

The modal properties of the system showed that approximately 50% of the system mass participated in the impulsive mode when the shear modulus was less than or equal to 40,000 Pa. Response spectrum analysis using a smooth spectrum as above would show that the peak forces remain fairly constant even if the impulsive frequency changes slightly due to varying waste properties.

Modal Mass Height and Overturning Moment

Given that the ratios of the waste height to the tank radius (H_l/R) and the waste height to the tank height (H_l/H_t) remain unchanged throughout this analysis, there is little reason to expect significant changes in the heights of the modal masses and overturning moments as the elastic constants of the waste are varied. If the height of the impulsive modal mass does not vary significantly, the overturning moment would be nearly proportional to the product of the effective mass in the impulsive mode and the spectral acceleration for the impulsive mode. For a spectrum that varies little over the range of expected impulsive frequencies, this is equivalent to saying that the overturning moment will be nearly proportional to the effective mass in the impulsive mode.

In the cases when the shear modulus does not exceed 40,000 Pa, the effective mass fractions for the impulsive mode remain close to 50%. In these cases, the overturning moment is expected to be nearly proportional to the spectral acceleration. If the spectral acceleration for the impulsive mode does not change substantially, it is reasonable to expect that the overturning moment will remain fairly constant. The variation of critical tank responses with waste properties is investigated more closely in Chapter 6.0.

Intentionally left blank.

6.0 Time-History Analyses

Time-history analyses were performed using both the time history extracted from basemat node 495 of the global model and the WTP surface free-field time history. Cases of bonded and general contact were considered for waste shear modulus values of 4,000, 22,000, 40,000, and 413,500 Pa. In contrast to the sliding interface condition enforced in the modal analysis, the interface with general contact provides not only for sliding, but also for opening and closing actions normal to the wall. However, this does not lead to a significant change in the behavior relative to that expected from the modal results.

Two critical structural responses for the system are the peak horizontal reaction force and the peak axial force in the tank wall near the lower knuckle. The peak horizontal reaction forces are reported in Section 6.1, and peak axial stresses in selected elements just above the tank lower knuckle are reported in Section 6.2. The axial force in the elements is simply the axial stress multiplied by the product of the element thickness and the element circumferential length.

$$F_{axial} = \sigma_{axial}(t \cdot l_{circumferential})$$

The axial stress that is reported is the mid-surface (membrane) stress. Moreover, the elements for which the axial stress is reported have the same dimensions, so that the axial stress is directly proportional to the axial force and the proportionality factor is the same for the elements considered. The axial stress in the lower wall of the tank provides information similar to that given by the overturning moment, but the stress is easier to extract from the model.

6.1 Hydrodynamic Forces

The peak horizontal reaction forces on the primary tank as predicted by the time-history simulations using the basemat and WTP time histories are shown in Table 6.1. Four of the five simulations using the basemat input were performed using the bonded interface condition, while all four of the simulations using the WTP input were performed using the general contact condition.

Table 6.1. Peak Horizontal Reaction Forces from Time-History Analyses

Shear Modulus (Pa)	Peak Horizontal Reaction Force for Basemat Time History (kip)[a]		Peak Horizontal Reaction Force for WTP Free-Field Surface Time History (kip)[a]	
	General Interface	Bonded Interface	General Interface	Bonded Interface
4,000			6,981	
22,000	3,294	3,136	6,921	
40,000		3,322	6,832	
413,500		3,728	5,751	
22,000[b]		4,103		

(a) Nominal reaction force doubled to account for half-symmetry model.
(b) Capped boundary condition at waste surface.

In the case of the basemat input, the results below show that the difference in reaction forces for the two interface conditions when the shear modulus is 22,000 Pa is minor as is the difference between the peak forces when the shear modulus increases from 22,000 Pa to 40,000 Pa for bonded contact. However, the peak force for bonded contact when the shear modulus is 413,500 Pa is significantly greater than the other cases (excluding the capped bonded contact case, which is shown as a benchmark). The discrepancy between the time-history prediction for this case and the single-term approximation shown in Table 5.1 is evidently due to the lack of accuracy of a single-term approximation when multiple significant modes are present.

In the case of the WTP input, the reaction forces for the shear modulus values of 4,000, 22,000, and 40,000 Pa are within 2% of each other. The peak reaction force at the higher shear modulus value of 413,500 Pa is approximately 20% lower. This is the opposite trend that was observed for bonded contact with the basemat input, but as both the interface condition and input motion have changed, it is difficult to make a direct comparison.

6.1.1 Comparison to Estimated Reaction Forces

Comparisons between the peak horizontal reaction forces from the time-history analyses and the values estimated Section 5.0 are shown in Tables 6.2 and 6.3. In all cases, the single-term approximation provides a lower-bound estimate as expected. With the capped bonded contact using the tank foundation input, the estimated peak reaction force is essentially the same as that computed from the time-history analysis, since the system is responding in a single mode. In contrast, the estimate for the case when the shear modulus is 413,500 Pa is poor, since this is a true multi-modal system.

In the cases using general contact, both the estimated and computed reaction forces show less variation than in the bonded contact cases. These results show that there is very little difference in the peak reaction forces for shear modulus values of 4,000, 22,000, and 40,000 Pa, but the peak reaction force drops by approximately 16% when the shear modulus is increased to 413,500 Pa.

Table 6.2. Comparison of Reaction Forces for Tank Foundation Input

Case Name (Shear Modulus)	Peak Reaction Force from Foundation Input	Estimated Reaction Force from Foundation Input	Ratio of Actual to Estimated Peak Reaction Forces	Comments
Sliding_464 (22,000 Pa)	3,294	3,025	1.09	Single-term estimate 9% low.
Bonded_464 (22,000 Pa)	3,136	2,824	1.11	Single-term estimate 11% low.
Bonded_839 (40,000 Pa)	3,322	2,731	1.22	Estimate based on impulsive frequency of 5.7 Hz, but several significant modes occur at 5.8-5.9 Hz, which correspond to higher spectral accelerations for the BES-BEC time history.
Bonded_E10 (413,500 Pa)	3,728	2,322	1.61	Multiple significant modes associated with higher waste stiffness make the single-mode approximate inappropriate.
Capped Bonded_464 (22,000 Pa)	4,103	4,078	1.01	Close estimate due to essentially single-mode response.

Table 6.3. Comparison of Reaction Forces for General Contact and WTP Input

Case Name (Shear Modulus)	Peak Reaction Force from WTP Input	Estimated Reaction Force from WTP Input	Ratio of Actual to Estimated Peak Reaction Forces	Comments
Sliding_0839 (4,000 Pa)	6,981	6,098	1.14	Single-term estimate 14% low.
Sliding_464 (22,000 Pa)	6,921	6,098	1.13	Single-term estimate 13% low.
Sliding_839 (40,000 Pa)	6,832	6,050	1.13	Single-term estimate 13% low.
Slidingd_E10x (413,500 Pa)	5,751	5,400	1.07	In contrast to the bonded contact with the foundation input, the higher stiffness in the sliding contact case with WTP input leads to lower reactions.

6.2 Axial Loads in the Primary Tank Wall

Axial (vertical) stresses are reported for two selected elements just above the lower knuckle of the primary tank. The four cases examined are for general contact with the waste shear modulus set to 4,000, 22,000, 40,000, and 413,500 Pa. All results are for runs that used the WTP free-field surface time history as input. As mentioned is Section 4.2, the use of a seismic motion with a smooth, nearly constant response spectrum in the frequency range dominating the response helps to isolate the effects of the waste properties on the sub-model response from the effects of the seismic input.

The locations of the elements for which axial stresses are reported are shown in Figures 6.1 and 6.2. The vertical location of the elements for which axial stresses will be reported is shown in Figure 6.1 as the dark blue row just above the lower knuckle elements. The corresponding element numbers are shown in Figure 6.2, beginning with element number 1342 and increasing sequentially around the tank in 20 slices of 9-degrees each through element number 1361.

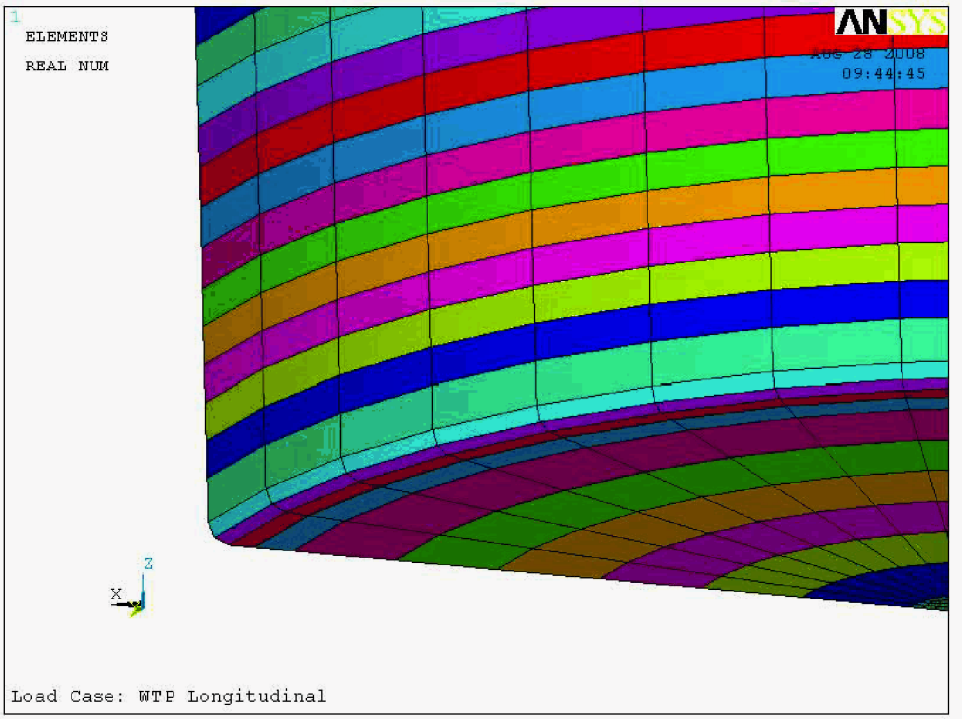

Figure 6.1. Elements of the Primary Tank in the Vicinity of the Lower Knuckle Colored by Real Constant Value

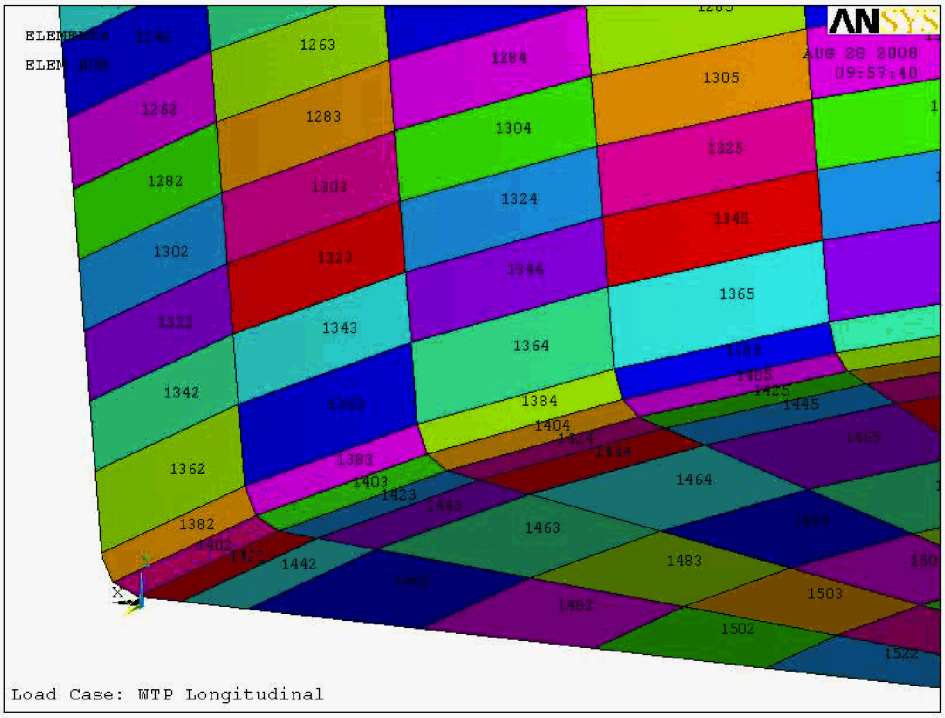

Figure 6.2. Selected Elements of the Primary Tank in the Vicinity of the Lower Knuckle Showing Element Numbers

The membrane stresses for elements 1342 through 1361 for gravity-only loading with a shear modulus of 4,000 Pa are shown below (units are kip/ft^2). The results show that the membrane stress is nearly constant around the tank circumference with an average value of approximately 42 kip/ft^2 (292 lbf/in^2) under gravity loading.

```
PRINT ELEMENT TABLE ITEMS PER ELEMENT

***** POST1 ELEMENT TABLE LISTING *****

  STAT     CURRENT
  ELEM     SZ
  1342    41.149
  1343    41.273
  1344    41.444
  1345    41.541
  1346    41.483
  1347    41.467
  1348    41.661
  1349    41.993
  1350    42.081
  1351    42.086
  1352    42.208
  1353    42.428
  1354    42.729
  1355    42.916
  1356    42.922
  1357    42.809
  1358    42.983
  1359    43.240
  1360    43.239
  1361    43.117
```

```
MINIMUM VALUES
ELEM       1342
VALUE    41.149

MAXIMUM VALUES
ELEM       1359
VALUE    43.240
```

The following results are for combined gravity and seismic loading for element numbers 1342 and 1361, which are the two elements adjacent to the symmetry plane at angular locations of 0-degrees and 180-degrees, respectively.

Waste Shear Modulus (G)=4,000 Pa

Post26 Summary of Variable Extreme Values							
Vari	**Type**	**Identifiers**	**Name**	**Minimum**	**At Time**	**Maximum**	**At Time**
2	ESOL	1342 S Y	sy1342-m	-52.12	103.2	146.0	103.1
21	ESOL	1361 S Y	sy1361-m	-62.20	103.1	136.3	103.2

Waste Shear Modulus (G)=22,000 Pa

Post26 Summary of Variable Extreme Values							
Vari	**Type**	**Identifiers**	**Name**	**Minimum**	**At Time**	**Maximum**	**At Time**
2	ESOL	1342 S Y	sy1342-m	-51.27	103.2	144.9	103.1
21	ESOL	1361 S Y	sy1361-m	-59.89	103.1	134.3	103.2

Waste Shear Modulus (G)=40,000 Pa

Post26 Summary of Variable Extreme Values							
Vari	**Type**	**Identifiers**	**Name**	**Minimum**	**At Time**	**Maximum**	**At Time**
2	ESOL	1342 S Y	sy1342-m	-51.11	103.2	143.5	103.1
21	ESOL	1361 S Y	sy1361-m	-58.17	103.1	134.3	103.2

Waste Shear Modulus (G)=413,500 Pa

Post26 Summary of Variable Extreme Values							
Vari	**Type**	**Identifiers**	**Name**	**Minimum**	**At Time**	**Maximum**	**At Time**
2	ESOL	1342 S Y	sy1342-m	-42.43	115.2	137.2	106.9
21	ESOL	1361 S Y	sy1361-m	-49.76	106.9	128.6	115.2

The previous results are summarized in Table 6.4 and plotted in Figure 6.3. The results from the dynamic evaluation show that the maximum and minimum axial stress remains nearly constant when the shear modulus varies between 4,000 and 40,000 Pa. At the higher shear stiffness of 413,500 Pa, the maximum and minimum axial stress magnitudes decrease by approximately 5%.

Table 6.4. Summary of Axial Membrane Stress in Primary Tank Lower Wall for Gravity Plus Seismic Loading

Shear Modulus (Pa)	Element Number		Element Angular Location (degrees)		Minimum Axial Stress (kip/ft^2)		Maximum Axial Stress (kip/ft^2)	
4,000	1342	1361	9	180	-52.1	-62.2	146.0	136.3
22,000	1342	1361	9	180	-51.3	-59.9	144.9	134.3
40,000	1342	1361	9	180	-51.1	-58.2	143.5	134.5
413,500	1342	1361	9	180	-42.2	-49.8	137.2	128.6

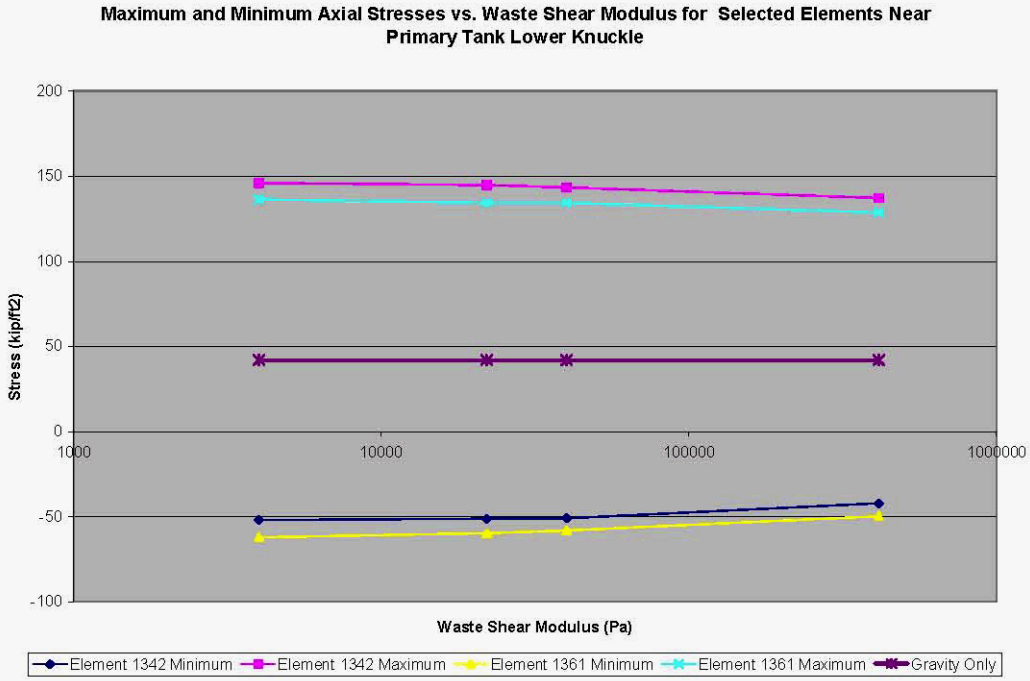

Figure 6.3. Variation of Axial Membrane Stress in Selected Elements of the Primary Tank Lower Wall as a Function of Waste Shear Modulus for General Contact Conditions

Intentionally left blank.

7.0 References

Alderman NJ, GH Meeten and JD Sherwood. 1991. "Vane Rheometry of Bentonite Gels." *Journal of Non-Newtonian Fluid Mechanics* **39**(3):291-310.

BNL. 1995. *Seismic Design and Evaluation Guidelines for the Department of Energy High-Level Liquid Storage Tanks and Appurtenances*. Report No. 52361. Engineering Research and Applications Division, Department of Advanced Technology, Brookhaven National Laboratory, Associated Universities, Inc., Upton, New York.

Daubert CR, JA Tkachuk and VD Truong. 1998. "Quantitative Measurement of Food Spreadability Using the Vane Method." *Journal of Texture Studies* **29**(4):427-435.

Deibler JE, KI Johnson, SP Pilli, MW Rinker, FG Abatt and NK Karri. 2008a. *Hanford Double-Shell Tank Thermal and Seismic Project – Increased Liquid Level Analysis for 241 AP Tank Farms*. RPP-RPT-32237, Rev. 1. Pacific Northwest National Laboratory, Richland, Washington.

Deibler JE, MW Rinker, KI Johnson, FG Abatt, NK Karri, SP Pilli and KL Stoops. 2008b. *Hanford Double-Shell Tank Thermal and Seismic Project – Summary of Combined Thermal and Operating Loads With Seismic Analysis*. RPP-RPT-28968, Rev. 1. Pacific Northwest National Laboratory, Richland, Washington.

Gauglitz PA and JT Aikin. 1997. *Waste Behavior During Horizontal Extrusion Effect of Waste Strength for Bentonite and Kaolin/Ludox Simulants and Strength Estimates for Wastes from Hanford Waste Tanks, 241-SY-103, AW-101, AN-103, and S-102*. PNNL-11706. Pacific Northwest National Laboratory, Richland, Washington.

Kennedy RP and AS Veletsos. 2005. *Comments and Recommendations Concerning Seismic Evaluation of Hanford Double-Shell Tanks*. RPK Structural Mechanics Consulting, Escondido, California and Rice University, Houston, Texas.

Kennedy RP and AS Veletsos. 2006. *Further Comments and Recommendations Concerning Seismic Evaluation of Hanford Double-Shell Tanks*. RPK Structural Mechanics Consulting, Escondido, California and Rice University, Houston, Texas.

Kennedy RP and AS Veletsos. 2007. *Comments Regarding Seismic Evaluation of Hanford Double-Shell Tanks and Effect of Increased Liquid Level in 241-AP Tank Farms*. RPK Structural Mechanics Consulting, Escondido, California and Rice University, Houston, Texas.

Meyer PA, ME Brewster, SA Bryan, G Chen, LR Pederson, CW Stewart and G Terrones. 1997. *Gas Retention and Release Behavior in Hanford Double-Shell Waste Tanks*. PNNL-11536, Rev. 1. Pacific Northwest National Laboratory, Richland, Washington.

Rinker MW and FG Abatt. 2008a. *ANSYS Seismic Analysis of Hanford Double-Shell Tank*. RPP-RPT-28966, Rev. 1. Pacific Northwest National Laboratory, Richland, Washington.

Rinker MW and FG Abatt. 2008b. *Hanford Double Shell Tank Thermal and Seismic Project – Seismic Analysis of Increased Liquid Level for 241-AP Tank Farms*. RPP-RPT-32239, Rev. 1. Pacific Northwest National Laboratory, Richland, Washington.

Veletsos AS and AH Younan. 1998. "Dynamics of Solid-Containing Tanks. II: Flexible Tank." *J. Struct. Eng.* **124**(1):62-70.

Intentionally left blank.

Pacific Northwest
NATIONAL LABORATORY

U.S. DEPARTMENT OF
ENERGY

902 Battelle Boulevard
P.O. Box 999
Richland, WA 99352
1-888-375-PNNL (7665)
www.pnl.gov